Modulation of the Brain's Hyaluronan-Based Extracellular Matrix in Mouse Models of Epilepsy

Thesis for the degree

doctor rerum naturalium (Dr. rer. nat.)

approved by the Faculty of Natural Sciences of Otto von Guericke University Magdeburg

by MSc. Armand Blondiaux,

born on 18th September 1992 in Poitiers (France)

Examiner : apl. Prof. Constanze Seidenbecher

Prof. Dr. Andreas Faissner

submitted on 27th May 2021

defended on 16th December 2021

Summary

Epilepsy is a common brain disorder which is characterised by recurrent electrographic seizures that affect the brain and the behaviour of patients. In order to better understand the pathophysiology underlying the epileptic phenotype, several animal models have been developed. A genetic model of epilepsy, a mouse mutant for the pre-synaptic active zone protein Bassoon, is known to develop seizures early in life while expressing a truncated version of Bassoon (Bsn1). Other lines of Bassoon mutants with constitutive mutations (Bgt & Bsn3) or conditional mutations in inhibitory (B2I) or excitatory neurons (B2E) are also available, but their epileptic phenotype is yet unevaluated.

Seizures modify the morphology as well as the electrophysiology of neuronal networks, and they do so by acting on neuronal plasticity, cell migration, neurogenesis and synaptic activity. Among these various mechanisms, there are overlaps with the functions of the brain extracellular matrix (ECM), and more precisely the hyaluronic acid (HA)-based ECM which became recently a new research focus in mechanistic epilepsy research. Indeed, the ability of the brain ECM to regulate cell migration in early life as well as its control of synaptic plasticity in the mature brain and its more recently discovered ability to affect adult neurogenesis concerns processes in the central nervous system that are affected in epilepsy. Moreover, the dynamic meshwork of proteoglycans, chondroitin sulphate (CS), glycoproteins and HA that form the brain ECM undergoes a series of changes in epilepsy patients as well as in animal models. In the classical model of kainic acid (KA) injection, the peri-neuronal nets, a dense ECM structure around the inhibitory interneurons, are digested following seizures. Furthermore, some ECM components characteristic for the mature brain are down-regulated, while ECM molecules typically found in a juvenile brain are up-regulated. In the KA model, a change in the synaptic density of hippocampal neurons was reported, concomitant with the digestion of the proteoglycan Brevican.

Based on previous findings in chemically induced models of epilepsy, I hypothesise that the state of the ECM is reflected in the severity and the strength of the seizures observed in long-lasting epilepsy. I evaluated this possible link in the different lines of Bassoon mutants. As a reference to established models, I also evaluated the reconstruction of the ECM in the KA-treated animals one and four weeks after injection.

In order to evaluate the epileptic phenotype of the 5 different lines of Bassoon mutants, the EEG was recorded and the brains of the recorded animals were collected for the quantification of ECM components afterwards. I have used semi-quantitative Western Blot analyses, immunohistochemistry and proteomics and could show that the mutants for Bassoon, with the exception of the B2E line, systematically develop seizures and an epileptic phenotype in early-life that continues into adulthood, where they display more frequent seizures than the KA model. These seizures are concomitant with changes to the HA-based ECM in the brain. Notably there is a strong decrease in the amount of Brevican in the Bsn3 line, the one with the strongest epileptic phenotype. The B2I line is distinct

from the others with an increase in Aggrecan, similar to the one week post KA injection model.

Overall, among the Bassoon mutants, the amount of Brevican negatively correlates with the frequency of seizures, reinforcing the idea of a link between the ECM state and the epileptic phenotype. Applying immunohistochemistry to brain slices, I evaluated whether specific modifications of the ECM would occur in the hippocampus, a region known to be strongly affected in epilepsy. The ECM patterns were different between Bsn3 mutants and KA-injected animals, with the dentate gyrus of Bassoon mutants having high levels of WFA-positive CS whereas the WFA label accumulated in the CA1 sub-region of the hippocampus of KA-injected animals, suggesting CS was being digested.

Taken together, the results of this thesis provide new information about the HA-based ECM in epilepsy, both for the KA model and for a new model of early-onset generalised epilepsy: the Bassoon mutants. In the Bassoon mutants, the ECM changes could be at the origin of several previously described phenotypes such as the increase in neurogenesis or modifications to the function of mossy fibres. These phenotypes are likely to be the cause of seizures as they are observed in other models of epilepsy, notably the KA-injected animals. Thus, it appears that the HA-based ECM could be a target for alleviating seizures through the regulation of other cell or network modifications happening in epilepsy.

Zusammenfassung

Epilepsie ist eine häufig auftretende neurologische Erkrankung, die durch wiederkehrende elektrografische Anfälle gekennzeichnet ist und sowohl die Hirnfunktion als auch das Verhalten der betroffenen Patienten erheblich beeinträchtigt. Um die Pathophysiologie, die dem epileptischen Geschehen zugrunde liegt, besser zu verstehen, wurden verschiedene Tiermodelle entwickelt. Ein genetisches Epilepsie-Modell , eine Mausmutante für das präsynaptisch aktive Zonen-Protein Bassoon (*Bsn1*), die eine abnorm verkürzte Version von Bassoon exprimiert, entwickelt früh im Leben epileptische Anfälle. Andere konstitutive Bassoon-Mutanten (Bgt und Bsn3) oder konditionale Mutanten mit Bassoon-Defizienz in inhibitorischen (B2I) oder exzitatorischen Neuronen (B2E) sind ebenfalls verfügbar, aber ihr epileptischer Phänotyp war bisher nicht charakterisiert.

Epileptische Anfälle verändern sowohl die Morphologie als auch die Elektrophysiologie neuronaler Netzwerke, indem sie auf neuronale Plastizität, Zellmigration, Neurogenese und synaptische Aktivität einwirken. Beeinträchtigt ist dabei auch die extrazelluläre Matrix (EZM) des Gehirns, genauer gesagt die von Hyaluronsäure (HA) als Grundgerüst organisierte EZM, die in letzter Zeit zu einem neuen Forschungsschwerpunkt in der mechanistischen Epilepsieforschung geworden ist. In der Tat kontrolliert die EZM im sich entwickelnden Gehirn unter anderem die Migration von Neuronen und im reifen Gehirn die synaptische Plastizität, aber auch, wie erst kürzlich entdeckt, die Neurogenese – Prozesse im zentralen Nervensystem, die vom Epilepsiegeschehen wesentlich betroffen sind. Darüber hinaus erfährt das dynamische Geflecht aus Proteoglykanen, Chondroitinsulfat, Glykoproteinen und HA, das die EZM des Gehirns bildet, sowohl bei Epilepsiepatienten als auch im Tiermodell eine Reihe von Veränderungen. Im klassischen Modell der Kainsäure-Injektion (Kainat-Modell) werden die perineuronalen Netze, eine dichte ECM-Struktur um inhibitorische Interneuronen, nach Anfällen strukturell beeinträchtigt. Außerdem werden einige ECM-Komponenten, die für das reife Gehirn charakteristisch sind, herunterreguliert, während ECM-Moleküle, die typischerweise in einem juvenilen Gehirn zu finden sind, hochreguliert werden. Im Kainat-Modell wurde eine Veränderung der synaptischen Dichte von Hippocampus-Neuronen berichtet, die mit dem Abbau des Proteoglykans Brevican einhergeht.

Basierend auf früheren Befunden in chemisch induzierten Epilepsiemodellen stellte ich die Hypothese auf, dass sich die Komposition der ECM in der Schwere der Anfälle widerspiegelt, die bei chronischem Status epilepticus beobachtet werden. Ich habe diesen möglichen Zusammenhang in den verschiedenen Linien der Bassoon-Mutanten untersucht. Als Referenz dazu untersuchte ich Veränderungen der ECM in Kainat-behandelten Tieren eine und vier Wochen nach der Injektion.

Um den epileptischen Phänotyp der 5 einbezogenen Bassoon-Mutanten zu studieren, wurden Langzeit-EEGs aufgezeichnet und die Gehirne der Tiere für eine anschließende Quantifizierung der ECM-Komponenten entnommen. Mittels semiquantitativer Western-Blot-Analysen, Immunhistochemie und Proteom-Untersuchungen konnte ich zeigen, dass

die Mutanten für Bassoon, mit Ausnahme der B2E-Linie, systematisch Anfälle und einen epileptischen Phänotyp bereits im frühen Lebensalter entwickeln, der sich bis ins Erwachsenenalter fortsetzt, wo sie häufiger Anfälle zeigen als die Kainat-Modell-Tiere. Diese Anfälle gehen einher mit Veränderungen in der HA-basierten EZM des Gehirns. Bemerkenswert ist eine starke Abnahme der Brevican-Menge in der Bsn3-Linie, der Linie mit dem stärksten epileptischen Phänotyp. Die B2I-Linie unterscheidet sich von den anderen durch die Erhöhung der Aggrecan-Immunreaktivität, was eher den Veränderungen im Kainat-Modell ähnelt.

Insgesamt korreliert bei den Bassoon-Mutanten die Menge an Brevican negativ mit der Häufigkeit der Anfälle, was die Idee eines Zusammenhangs zwischen ECM-Zustand und epileptischem Phänotyp untermauert. Mittels Immunhistochemie an Hirnschnitten untersuchte ich, ob spezifische Modifikationen der EZM im Hippocampus auftreten, einer Region, von der bekannt ist, dass sie vom Epilepsiegeschehen stark betroffen ist. Die EZM-Struktur unterschied sich zwischen Bsn3-Mutanten und Kainat-injizierten Tieren deutlich, wobei der Gyrus dentatus der Bsn3-Mutanten hohe WFA-positive Chondroitinsulfat-Konzentrationen aufwies, während sich das WFA-Signal in der CA1-Region des Hippocampus der Kainat-Tiere anreicherte.

Insgesamt liefern die Ergebnisse dieser Arbeit neue Informationen über Veränderungen der HA-basierten EZM bei Epilepsie, sowohl für das Kainat-Modell als auch für ein neues Modell der früh einsetzenden generalisierten Epilepsie: die Bassoon-Mutanten. In den Bassoon-Mutanten könnten die EZM-Veränderungen die Ursache für mehrere zuvor beschriebene Phänotypen sein, wie die Zunahme der Neurogenese oder Modifikationen in der Funktion der Moosfasern. Solche Veränderungen sind vermutlich die Ursache für die Anfälle oder tragen zumindest dazu bei. Somit scheint es möglich, dass die HA-basierte ECM ein therapeutisches Target für die Linderung von Anfällen sein könnte, etwa durch Gegensteuern gegen Zell- oder Netzwerkmodifikationen, die bei Epilepsie auftreten.

Abbreviations

ADAMTS	A disintegrin and metalloproteinase with thrombospondin motifs
AMPA	α-amino-3-hydroxy-5-methyl-4-isoxazolepropionic acid
ANOVA	Analysis of variance
BDNF	Brain-derived neurotrophic factor
CAZ	Cytomatrix at the active zone
ChABC	Chondroitinase ABC
cKO	conditional knock-out
CS	Chondroitin-sulphate
DG	Dentate gyrus
ECM	Extracellular matrix
ECS	Extracellular space
EEG	Electroencephalogram
E/I	Excitation/Inhibition
GABA	γ-aminobutyric acid
GalNAc	N-acetyl galactosamine
GAG	Glycosaminoglycan
GlcA	Glucuronic acid
HA	Hyaluronic acid
HAPLN	Hyaluronan and proteoglycan link protein
HAS	Hyaluronic acid synthase
HYP	Hypersynchronous
ILAE	International league against epilepsy
KA	Kainic acid
KO	Knock-out
LTP	Long-term potentiation
LVF	Low-voltage fast
MMP	Matrix metalloproteinase
MTLE	Mesial temporal lobe epilepsy
NMDA	N-methyl D-aspartate

PAGE	Polyacrylamide gel electrophoresis
PBS	Phosphate buffer saline
PG	Proteoglycan
PNN	Perineuronal net
PTR	Proteoglycan tandem repeat
PVDF	Polyvinylidene fluoride
SDS	Sodium dodecyl sulphate
TBS	Tris buffer saline
TCE	2,2,2-Trichloroethanol
TLE	Temporal lobe epilepsy
TnC	Tenascin-C
TnR	Tenascin-R
WFA	Wisteria Floribunda agglutinin
WT	Wild-type

Table of Contents

I Introduction....3
I.1 - Epilepsy: definition and properties....3
I.1.a. - The epileptic brain....5
I.1.b. - Epileptic seizures....7
I.1.c. - Models of epilepsy in laboratory animals....9
I.2 - Bassoon mutants as epileptic animals....11
I.3 - The brain extracellular matrix in epilepsy....14
I.3.a. - Specificities of the brain extracellular matrix....14
I.3.b. - Structures and functions of the hyaluronan-based ECM....16
I.3.c. - Proteolysis of the ECM and matricryptins, the ECM as a signal....19
II Aims of the study....20
III Material and Methods....21
III.1 - Animal housing and mutant genetic details....21
III.2 - Solutions and buffers....22
III.3 - Antibodies....22
III.4 - Surgery and electrode implantation....23
III.5 - Kainic acid injection....23
III.6 - EEG recording, analysis and seizure counting....24
III.7 - Seizure onset classification....25
III.8 - Perfusion and extraction of the brain....25
III.9 - Preparation of brain slices for immunohistochemistry....25
III.10 - Immunohistochemistry....25
III.11 - Microscopy and image analysis....26
III.12 - Subcellular fractionation of the brain....26
III.13 - SDS PAGE gel preparation....27
III.14 - SDS-PAGE, Western Blot & Immunoblot detection....27
III.15 - Sample preparation for proteomics....29
III.16 - Mass spectrometry data acquisition....29
III.17 - Mass spectrometry data analysis....30
III.18 - Survival analysis....30
III.19 - Statistical analysis....30
IV Results....32
IV.1 - Spontaneous deaths in Bassoon mutants suggest an early-onset epilepsy....32

IV.2 - All investigated models display epileptic seizures....34
IV.3 - The Bsn3 line has the most severe epileptic phenotype....36
IV.4 - Diverse seizure onsets for diverse epilepsy models....38
IV.5 - Differential regulation of the ECM between epilepsy models....39
IV.5.a. - Brevican amounts are consistently lower in the Bsn3 line....41
IV.5.b. - Increase in soluble Aggrecan in the B2I and KA1wk animals....44
IV.5.c. - The Bgt line has higher levels of the 90kDa Neurocan fragment....45
IV.6 - Brevican levels negatively correlates with seizure properties in the Bassoon lines…46
IV.7 - ECM component amounts are co-regulated differently in KA and Bassoon epilepsy models....52
IV.7.a. - Correlation of the full-length Brevican with its cleaved fragment....52
IV.7.b. - Opposite correlation between full-length Brevican and 130kDa Neurocan between Bassoon and KA-injected groups....52
IV.7.c. - Tenascins and HAPLNs correlate with different ECM components in the Bassoon and KA-injected groups....52
IV.8 - The membrane fractions of Bsn3 and B2I mouse hippocampi contains increased CD44 levels....55
IV.9 - Higher expression of ECM markers in the dentate gyrus of the Bsn3 mutants....56
IV.10 - The hippocampus of KA1wk mice shows WFA aggregates....59
V Discussion....62
V.1 - Epilepsy in the Bassoon mutant lines in comparison to a classical model....62
V.1.a. - Severity of the epileptic phenotype in Bassoon mutants....62
V.1.b. - The epileptic phenotype of Bassoon mutants is more severe than the one from KA-induced epilepsy....64
V.1.c. - Speculation on the origin of the epilepsy in Bassoon mutants....64
V.2 - Changes to the extracellular matrix in epilepsy....65
V.2.a. - A link between Brevican and epileptic phenotypes....66
V.2.b. - A role for other lecticans in the epileptic phenotype....67
V.2.c. - ECM correlations as hints to co-regulations and ECM structure....68
V.2.d. - Changes to the ECM cell receptor in the epileptic animals....69
V.3 - Changes to the hippocampal ECM in Basson and KA-injected epilepsy models....69
VI Conclusion and outlooks....72
VII References....74

I Introduction

I.1 - Epilepsy: definition and properties

The International League Against Epilepsy (ILAE) describes the disorder as follows: “a transient occurrence of signs and/or symptoms due to abnormal excessive or synchronous neuronal activity in the brain” (ILAE, 2014a).

Epilepsy is a term that encompasses a wide range of brain disorders with different origins and consequences. All patients suffering from epilepsy share one main phenotype: recurrent seizures. Currently, the clinicians and researchers define seizures in two ways: through a behavioural approach and through an electrophysiological one. Starting with the behavioural approach, at the onset of an epileptic seizure, one can observe a sudden behavioural arrest in the patient’s movements. Underlying the behavioural aspect is the abnormal electrophysiology of the epileptic brain. In fact, an uncontrolled electrical activity arises from an increased excitation or lower inhibition, leading to bursts of neuronal activity. Many hypotheses agree on an imbalance between excitatory and inhibitory circuits to explain the onset of seizures (for a review, see Staley, 2015).

Epilepsy is classified into different categories, all based on the description of the seizures that accompany the disorder (Scheffer et al., 2017). The seizures may be generalised and thus affect the whole brain, or they affect only a part of the brain, therefore called focal seizures (Figure 1). The epilepsy itself (i.e. the disorder as a whole rather than the single seizures) is then described as generalised or focal, based on the type of seizures observed. In the classification of the epilepsy type, if both focal and generalised seizures appear in the patient, then the epilepsy is considered a hybrid of focal and generalised type (Figure 1, Scheffer et al., 2017). To further the description of the epilepsy, the classification describes in parallel the aetiology of the disorder. Epilepsy can appear at any age, arising for a range of different reasons. In the adult and senior population, epilepsy is often the consequence of a primary injury such as a stroke or a shock during an accident. The physical changes brought to the brain by the injury lead to the formation of an epileptic network. Although the mechanisms are not completely understood, a handful of laboratories have investigated the changes following traumatic brain injury or ischaemia and how it reaches an epileptic state (for a thorough review, refer to Fordington & Manford, 2020).

In my thesis, however, I focused on the cases with a different aetiology, where a traumatic injury was not the starting point of the epileptic phenotype. Indeed, it happens quite often that the origin of the disorder cannot be exactly set nor linked to a specific event. In such cases, the first seizure is considered to be the starting point.

Finally, the classification makes a major distinction between non-motor seizures, where the patients stop their behaviour and do not engage in any further movement, and the motor seizures where the movements are uncontrolled following the onset of the seizure. Moreover, one can distinguish several types of motor seizures: tonic (with muscle contraction), clonic (with repetitive movements) and tonic-clonic events. In this last category lies the strongest type of seizures.

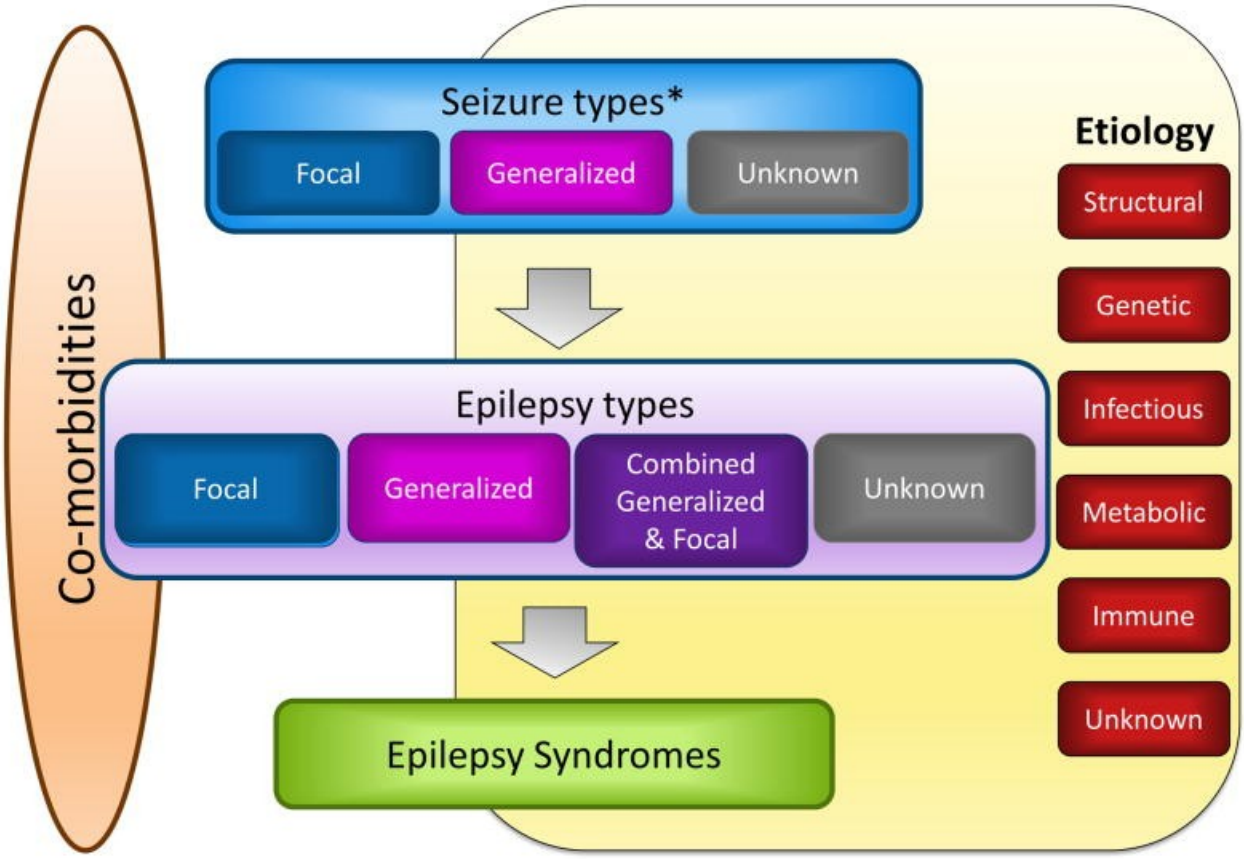

Figure 1: Framework of the classification of seizures (top) and epilepsy (middle and bottom) according to the International League Against Epilepsy (from Scheffer et al., 2017). The seizures are divided into focal and generalised. Based on the observed seizure types, the nature of the epilepsy is deduced. Further information, such as the aetiology and the co-morbidities, can lead to the classification of the phenotype into one of the well-known epilepsy syndrome (e.g. Dravet syndrome, Rett syndrome, childhood absence epilepsy). (*) this classification concerns only the onset of the seizure.

As it turns out, we are currently only able to classify the epilepsy into different categories based on the observation of the seizures. There are not yet any classifications based on the actual cellular dysregulation in the brain that lead to the epileptic phenotype. The dysfunctions are difficult to observe in living organisms (even more so in humans) and still little is known about the underlying mechanisms that distinguish one epilepsy type from another. Thus the description of epilepsy relies mostly on the observation of the consequences of the disorder but not the disorder itself.

In parallel to the seizures, there are often other pathological consequences. Along with seizures come increased mortality, cognitive deficits, depression and also a co-morbidity in about 50% of the epilepsy cases, with developmental disorders such as autism or hyperactivity appearing alongside the seizures (Keezer et al.,2016). Here also, the ILAE considers these as part of the disorder as they include the following words in their description of epilepsy: “[with] enduring predisposition of the brain to generate epileptic seizures, with neurobiological, cognitive, psychological and social consequences” (ILAE, 2014a).

Some forms of epilepsy lead to an increased risk of sudden unexplained death, a death not directly linked to a seizure but rather to the epilepsy condition itself. This is a major life expectancy risk for epileptic persons, alongside *status epilepticus*. In humans, *status epilepticus* is defined as a seizure that lasts longer than five minutes, potentially reaching the heart or preventing proper breathing (ILAE, 2014b). The sudden unexplained death, on the other hand, is simply defined as a spontaneous death that cannot be linked to a seizure (Devinsky et al., 2016).

Currently, more than half of the epilepsy cases receive an adequate medication. Noteworthy, our current treatments are targeting the seizures which are the apparent part of the disorder; however, this means that there are no drugs actually against epilepsy, only against the seizures (reviewed by Johnson & Kaminski, 2019). This reveals a lack of understanding of the mechanisms involved in the epileptic brain. In fact, about 30% of the epileptic patients are resistant to all known treatments and despite years of research on epilepsy, little has actually been brought to the table in terms of new treatments (Abramovici & Bagic, 2016). To add to the people unable to find a treatment, the ILAE also reports a long time period after diagnosis to actually control the seizures. Here also, there has not been much progress to improve the life and comfort of the people affected by the disorder (Chen et al., 2017).

I.1.a. - The epileptic brain

It is difficult to decipher whether changes observed in the epileptic brain are a cause or a consequence of the epilepsy. In any case, the changes that are described below have an underlying common point: they rely on brain plasticity mechanisms (Jarero-Basulto et al., 2018). Of importance is the fact that some modifications may be compensatory mechanisms used by the brain to bring back its activity to physiological levels; nevertheless, the fact that seizures appear proves that the brain is unable to establish its activity balance back to a physiological state.

To begin with, epilepsy induces changes in glia. At least, there is reactive astrogliosis in response to the brain damage caused by the seizures. Most likely this is not a primary cause for epilepsy (Devinsky et al., 2013), however, there are some evidences that astrogliosis participates in the epileptic phenotype and a recent study challenges that

point of view by triggering seizure only by genetically engineering a mouse strain with activated astrocytes (Robel et al., 2015). This is not surprising as glia cells, especially astrocytes, are involved in the homeostasis of neurotransmitters and ions in the brain, both of which are major actors of neurotransmission and therefore can cause seizures in case a dysregulation happens.

Concerning neurons and their networks, they are also disrupted in several regions of the brain such as the entorhinal cortex, the striatum and the hippocampus (Kumar & Buckmaster, 2006, Jarero-Basulto et al., 2018, Thom, 2014). The latter has been at the centre of the attention for many years when it comes to epilepsy. Many observations converge onto the hippocampus as it is a more plastic region of the brain and this makes it more vulnerable to changes following the activity bursts of seizures. Among the most studied changes are mossy fibre sprouting, a more complex dendritic tree in some neurons, and granule cell dispersion (Jarero-Basulto et al., 2018, Thom, 2014).

To detail a bit more this picture, mossy fibre sprouting affects the hippocampus granule cells. In fact, these cells from the Dentate Gyrus (DG) project their axons to the CA3 region in normal conditions. Instead, the DG axons of epileptic brains develop recurring collaterals into the inner molecular layer of the DG itself (Okazaki et al., 1999). Thus, the granule cells could create an excitatory feedback loop leading to seizures (Scharfman et al., 2003). This hypothesis has not been verified and since not all epileptic patients present with mossy fibre sprouting (it appears in about 30 to 40% of the cases), the consensus is that it is a consequence of epilepsy rather than an actual cause (Heng et al., 2013).

Along the mossy fibre sprouting, dendritic trees in the epileptic hippocampus grow much bigger (Zhang et al, 2009). This could be due to a decline in inhibition, which seems to affect the proper growth of the hippocampal neurons' dentritic tree (Gupta et al., 2019). If the number of interneurons is more often lower in epilepsy cases than in healthy counterparts, there is however a compensatory mechanism and therefore interneurons in epileptic brains have a dendritic tree that spans much more area (Zhang et al., 2009). The interneurons seem to be a priority target in epilepsy and the disorder alters their function or leads to their disappearance in a reliable way from one case to another.

The matter of the granular cell layer dispersion is an interesting one. Instead of forming a dense layer in the dentate gyrus, granule cells tend to disperse much more in the epileptic hippocampus (Houser, 1990). The ectopic granule cells play a role in the epilepsy and its genesis. In and of itself, neurogenesis in the hippocampus is not pathological, the DG being one of the regions were adult neurogenesis happens throughout life. Nevertheless, epilepsy bends the rules and alters the neurogenesis to create new epileptic networks (Danzer, 2019). As one can suspect, this is also the result of a pathological plasticity. Indeed, cell migration is an important part of the development and new cell generation.

Epilepsy, however, affects the migration of the *de novo* cells and therefore they are not properly integrated into the granular cell layer.

Recently, there has been more and more evidence that the extracellular matrix (ECM) affects the physiology of the brain and the neuronal networks. As a part of plasticity mechanisms, the ECM also plays a role in epilepsy (reviewed in Dityatev, 2010). For example, its ability to regulate the extracellular space prevents the spread of excitation from one neighbouring cell to another (Arranz et al., 2014), and changes to the extracellular space volume can lead to seizures. The ECM also affects the excitability of Parvalbumin interneurons, with the deletion of Brevican, a core ECM protein, leading to higher excitability in the interneurons (Favuzzi et al., 2017). Interestingly, the levels of Brevican are lower in patients, suggesting that the interneurons would have a higher activity (Favuzzi et al., 2017), which is probably a compensatory mechanism similar to the extension of dendritic trees (Zhang et al., 2009).

At the synaptic level, glutamatergic signalling is the most obvious target, being the number one excitatory input in the brain. It turns out that seizures change the level of expression of different subtypes of metabotropic and subunits of ionotropic glutamate receptors (Umpierre et al., 2019, Zubareva et al., 2018). Umpierre and colleagues (2019) showed that the metabotropic receptor mGluR5 reappears in astrocytes in temporal lobe epilepsy (TLE) and affects the glutamate reuptake at the synapse during high frequency activity, thus increasing the risk of seizure. On the other hand, ionotropic receptors are at the core of neurotransmission and the shift to a higher expression of GluA2 in epilepsy changes the signal sent by the glutamate and increase its depolarising power as GluA2 is a subunit of the AMPA receptor known to be more permissive to Ca^{2+} ions (Russo et al., 2013; reviewed in Barker-Haliski & White, 2015).

The second suspect is γ-Aminobutyric acid (GABA), the main inhibitory neurotransmitter. Generally, GABAergic transmission alleviates the seizures and an impairment of the GABAergic transmission leads to seizures (Yang et al., 2021). However, there are some cases where GABA can actually participate in seizure genesis. A first way is with the GABAergic signalling enforcing a general synchrony within the network. This hypothesis relies (not exclusively) on the effects of the $GABA_B$ receptor, able to change the resting potential of the cell membrane upon long-lasting activation (Trevelyan et al., 2015). The other hypothesis involves a reversed Cl^- gradient between cell and extracellular space, therefore leading to excitatory GABAergic signals as is already the case in juvenile brains (Trevelyan et al., 2015). This gradient reversal does not need to be sustained, even a transient reversal – or a precisely localised one – could be enough to trigger a seizure.

I.1.b. - Epileptic seizures

The best way to study seizures is to record the electrical brain activity. Until now, electroencephalography (EEG) is the most convenient technology for this thanks to its fast

recording rate. While in human patients it is used primarily for diagnostic purposes, it is also a research tool in animal models.

When it comes to the study of seizures, the most studied part of the signal is the onset. Both basic scientists and clinicians have seen time and time again that the switch from a normal brain activity to an ictal activity (the seizure) is similar from one seizure to another. Although there is a complex range of onsets (Perucca et al., 2014), the epilepsy community currently recognises two major types. The first category is the “low voltage fast frequency” (LVF). Here, a single spike is seen at the start of the seizure. Following that spike, the EEG pattern flattens and slowly rises again, with a high frequency activity (Figure 2A). The second type of onset is related to hippocampal damage and focal epilepsy. It is described as “hypersynchronous” (HYP) pattern as there are repeated high-amplitude spikes at the onset of the seizure due to an inhibitory network failure (Köhling et al., 2016, Figure 2B).

Current hypotheses about the different onsets attach different neuronal origins to each. Indeed, some studies prove that GABAergic signalling is an essential part of the LVF onset (Elahian et al., 2018). The use of picrotoxin (a $GABA_A$ antagonist) leads to HYP seizures whereas an optogenetic approach to stimulate specifically either Parvalbumin- or Somatostatin-positive interneurons leads to LVF seizures (reviewed in Avoli et al., 2015). Therefore, based on the EEG pattern, one can deduce part of the physiology behind the origin of the seizures.

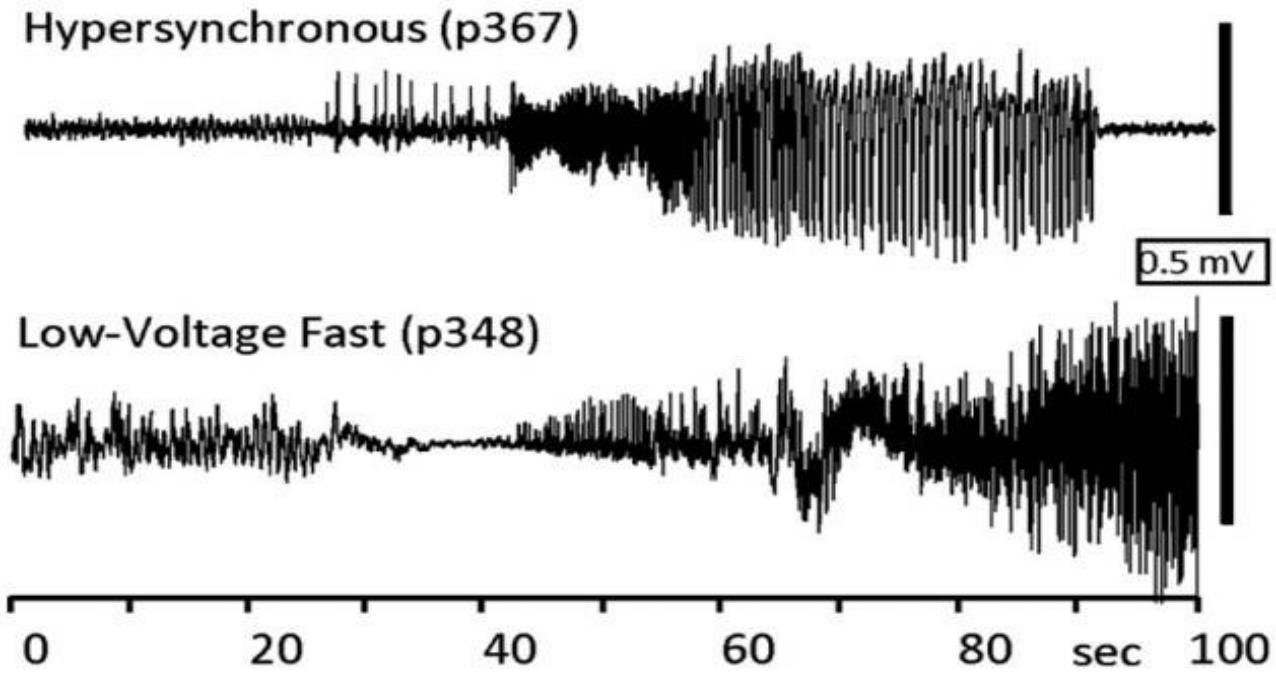

Figure 2: Examples of Hypersynchronous (top) and Low-Voltage Fast (bottom) onsets of seizures. From Li et al., 2019.

Following the onset, seizures develop into the “tonic” phase where there is sustained oscillatory activity of high amplitude before going in the “clonic” phase with regular bursts of activity. In most cases, the EEG flattens and there is a much smaller activity after a seizure, this phenomenon is called “post-ictal depression”. These phases do not see as much attention although adequate analysis may inform about the type of seizure and further help their detection.

I.1.c. - Models of epilepsy in laboratory animals

There are many different animal models available to study epilepsy, with mainly three approaches: chemically induced, electrically induced or genetic epilepsy (for a thorough review of the different models, see Löscher, 2017).

The chemically-induced epilepsy models consist in the injection of a chemical into the organism or directly into the brain. This injection changes the neural network and its activity leading to seizures in the end. There are different chemicals in use for such protocol, often to provoke a dire seizure (the *status epilepticus*) but it can also be used in kindling models (where sub-threshold doses are applied regularly until the animal becomes epileptic). These two methods, kindling and *status epilepticus* induction, are similar in electrically induced epilepsy. The most common mesial temporal lobe epilepsy (MTLE) model is a chemically induced model based on a single injection of kainic acid (KA), an activator of the kainate receptor subtype of the glutamatergic receptor family (Bouilleret et al., 1999).

Despite the usefulness of these induced models, they are currently regarded with more criticism in the clinical and translational research environment (Löscher, 2017). Indeed the lack of new treatment, especially for refractory epilepsy, could be due to the limited amount of models in use and the fact that they reproduce an epileptic phenotype for which we already have an efficient treatment rather than a refractory epilepsy.

Over the years, another way to provoke seizures in laboratory animals got more attention: the use of genetic manipulation to create a strain of animals more susceptible to pro-convulsant treatment or affected by some form of epilepsy as proven by recurrent seizures. Concerning these models, they are generally models of generalised seizures that are less used for drug discovery. There are several types of protein that, when deleted or modified, can lead to an epileptic phenotype (Löscher, 2017).

Ion channels are generally good targets, such as the Na^+ channel sub-unit SCN1a which is mutated in the Dravet syndrom. Indeed, ion channels have a direct impact on the excitability of the neurons and on neurotransmission, their mutations or deletions can thus affect the overall brain activity state (for a review, see Wei et al., 2017).

Among the various other gene targets whose mutation lead to epileptic phenotypes, many affect the synaptic functions. For example, it is known that the synaptic cleft protein LGI1

is an important activity regulator as its deletion leads to the apparition of seizures in mice (Chabrol et al., 2010). Animals heterozygous for the synaptic vesicle protein SV2A are more prone to seizures, even though they do not spontaneously develop an epileptic phenotype (Kaminski et al., 2009). SV2a is involved in the fusion and release of neurotransmitter vesicles at the synaptic membrane. Another protein that is involved in the cycle of synaptic vesicle is the Bassoon protein. It seems that this pre-synaptic scaffolding protein is an activity regulator as its homozygous deletion also leads to uncontrolled seizures (Altrock et al., 2003).

I.2 - Bassoon mutants as epileptic animals

Bassoon is a protein located at the pre-synapse, more precisely at the cytomatrix at the active zone (CAZ), the site where vesicles dock and fuse to liberate the neurotransmitters into the synaptic cleft (Südhof, 2012). It acts primarily as a scaffold protein through its multiple interaction domains and thus ensures the physical proximity of synaptic proteins and their functional interactions (tom Dieck et al., 1998, Dresbach et al., 2003, Mukherjee et al., 2010; reviewed in Gundelfinger et al., 2016).

In order to identify the functions of Bassoon at the synapse, several mouse lines have been generated with different mutations in the Bassoon gene. In the first one, $Bsn^{\Delta Ex4/5}$ (referred to as **Bsn1**), the exons 4 and 5 of the gene were replaced by a lacZ-Neomycin cassette, thus leading to the expression of a truncated version of Bassoon (Altrock et al., 2003, Figure 3A). In the Bsn1 mutants, the truncated Bassoon gene product is not targeted specifically to the synapse, concomitant with some excitatory synapses not being active. Despite this lack of some excitatory input, there is an epileptic phenotype with strong generalised seizures, the cause of a ~50% mortality by 6 months of age in these mice (Altrock et al., 2003).

Following up on those findings, Ghiglieri and colleagues (2009) found that the neurons in the striatum of the Bsn1 animals had an altered plasticity and neuronal morphology; noteworthy is the presence of more Parvalbumin interneurons in the mutants, a phenotype opposite to the one generally found in the KA model (Zhang et al., 2009). Despite this increase in interneuron numbers, they still develop more complex dendritic trees (Ghiglieri et al., 2009), a phenotype similar to the one observed in the KA model (Zhang et al., 2009). Another study showed similar morphological and functional changes in the hippocampus; the morphological changes were resistant to anti-epileptic treatment with Valproate, whereas the functional alterations were rescued (Sgobio et al., 2010). Furthermore, it seems like some synapses are unable to properly mature in the Bassoon mutants (Lanore et al., 2010). Taken together these studies suggest that morphological changes in the brain of the Bsn1 animals are independent from the epilepsy and happen before the onset of seizures, while the functional changes most likely arise from the epileptic phenotype.

The origin of the Bassoon mutant epileptic phenotype is yet unclear, however, there are several changes that have been observed over time in the Bsn1 mutants and other Bassoon lines that could underlie such a phenotype. A striking parallel is the involvement of Brain-Derived Neurotrophic Factor (BDNF) and its receptor, TrkB, in the epileptic phenotype of Bsn1 animals (Ghiglieri et al., 2010), quite similar to the mechanism observed in many other epilepsy models (reviewed in McNamara et al., 2012). In the Bsn1 animals, BDNF accumulates at the pre-synapse (Dieni et al., 2012), an increase in its expression that is also seen in other epilepsy models and even in patients (McNamara et al., 2012). The increase in BDNF levels in the Bassoon mutants could explain the epileptic phenotype as BDNF is known to increase the neuronal excitability (Messaoudi et al., 1998), but it may also be the reason for an increased brain volume in the Bassoon mutants (Angenstein et al., 2008). This increase in volume, however, is in contrast to the usual observation made in epilepsy where all brain structures are consistently shrunk (Whelan et al., 2020).

Further Bassoon mutants were created with a gene-trap strategy between introns 1 & 2 of the *Bsn* gene (a mutant line referred to as **Bgt,** Figure 3A). This Bgt mutant, just like Bsn1, has a slower speed of vesicle reloading at the synapse (Hallermann et al., 2010), which leads to a decrease in sustained activity in neurons but does not affect the synaptic response otherwise (Mendoza-Schulz et al., 2014). This decreased sustained activity in the Bgt mutants may be due to the lack of the Ca^{2+} voltage-gated channel $Ca_V2.1$ at the synapse, involved in the Ca^{2+} influx leading to vesicle fusion with the membrane (Davydova et al., 2014). Alongside this, Bgt mutants also display a reduced level of Arc expression in the DG, a hallmark of a lower activity (Dieni et al., 2015).

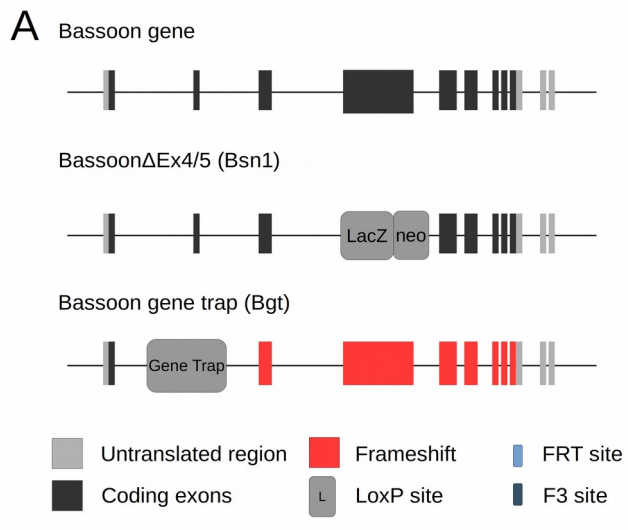

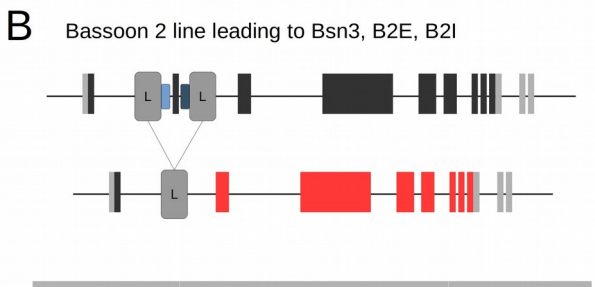

Line name	Targeted cells	Cre-driver
Bsn3	All cells	CMV-Cre
B2E	Excitatory forebrain neurons	Emx-Cre
B2I	Inhibitory interneurons	Dlx5/6-Cre

Figure 3: Representation of the Bassoon gene and its modifications to give rise to the different Bassoon lines. (A) Representation of the Bassoon gene and the genetic engineering leading to the Bsn1 and Bgt lines. (B) Representation of the Bassoon gene with LoxP sites framing exon 2, as in the Bsn2 line, which gives rise to the Bsn3, B2E and B2I lines once crossed with the adapted Cre-driver lines stated in the table.

In hindsight, the findings about the Bassoon lines seem paradoxical, linking the higher activity of an epileptic phenotype with several functional changes that mark a lower activity overall. Hence, the mechanisms involved in the epilepsy of the Bassoon lines must be more diverse than a simple increased excitation to lead to a systemic alteration of the excitation/inhibition (E/I) balance.

Several hypotheses can be made concerning the origin of the epilepsy in the Bassoon mutants, however, no study to this date has unveiled the causes behind the phenotype. Considering the early onset of seizures observed in Bsn1 (Ghiglieri et al., 2009), it could be that the brain development is affected. This hypothesis is relevant as Bassoon is expressed at the synapse during development (Zhai et al., 2000). Its appearance in the inhibitory growth cones before the excitatory ones is also an argument toward a differential function in the development of the inhibitory and excitatory network that could lead to the altered E/I balance (Zhai et al., 2000). In the adult brain of the Bsn1 mutants, the increased brain size has been linked to a highly increased adult neurogenesis (Heyden et al., 2011), an abnormal generation of new neurons that could trigger an epileptic phenotype.

More recently, new Bassoon lines have been generated, although not yet tested for any epileptic phenotype. The use of LoxP sites around exon 2 of the *Bsn* gene (an animal line referred to as **Bsn2**) can be used to generate knock-outs (KOs) in specific cell types when crossed with an appropriate conditional Cre mouse line (Figure 3B and III.1). This has given rise to a full KO line (hereby called **Bsn3**), a conditional KO (cKO) of the *Bsn* gene in excitatory neurons (called **B2E**) and finally a cKO in inhibitory neurons (called **B2I**). Out of these three lines, the B2E is characterised by morphological similarities with the Bsn1 line: increased brain volume and more complex dendritic trees in the DG (Annamneedi et al., 2018). Moreover, the cells of the DG do not mature properly in the B2E line, causing an increase in the excitability of the network, which reinforces the hypothesis of a possible developmental origin to the epilepsy in Bassoon mutant lines.

I.3 - The brain extracellular matrix in epilepsy

As already stated, it appears that a modified ECM is an integral part of the epileptic phenotype (Dityatev, 2010). One main function of the brain ECM is to organise and regulate the properties of the extracellular space (ECS). As the ECS changes, so do the properties of the cells around. As a matter of fact, Arranz and colleagues (2014) have shown that simply modifying the hyaluronan (HA) in the ECS leads to changes in the neuronal network activity. By genetically removing each HA synthase (HAS), they have shown that they could affect the length of the HA and thus the ECS volume, which in turn caused seizures.

Moreover, overall changes in the ECM of both epilepsy models and patients are the subject of many reports. Studies in post-mortem brains from patients showed an increase

in the HA content of epileptic brains compared to healthy ones (Perosa et al., 2002). Similarly, an increase in chondroitin-sulphate (CS), a major sugar chain of the ECM, was observed in the brain of epileptic rats (Naffah-Mazzacorrati et al., 1999). In parallel, research in Ihara's epileptic rat (a model of spontaneous epilepsy) lead to the discovery of ECM changes even before the onset of the first seizure. More precisely, an increase in Neurocan expression a few days before the first seizures (Kurazono et al., 2001).

Changes around the epileptic phenotype also affect the peri-neuronal nets (PNNs) and peri-synaptic ECM. For example, in the KA epilepsy model, several experiments confirmed that the PNNs are degraded (McRae et al., 2012) due to the action of matrix metallo-proteases (MMPs) (Rankin-Gee et al., 2015). One study on the KA model found that the proteolytic cleavage of Brevican following the seizures was concomitant with a loss of synapses in the hippocampus (Yuan et al., 2002).

Nevertheless, studies are focused on a few models of epilepsy, generally chemically induced, and often observe changes following the first seizures but more rarely after a long-lasting epilepsy.

I.3.a. - Specificities of the brain extracellular matrix

Contrary to the ECM of other organs, the brain ECM is not composed of the classical collagens and fibronectins. One needs to distinguish the neuropil ECM from the basal membrane, which separates the brain parenchyma from the blood vessels and the cerebral ventricles. This basal membrane has a specific ECM composition (reviewed in Reed et al., 2019) which is quite different from the one observed in the neuropil and around synapses (reviewed in Krishnaswamy et al., 2019).

The ECM in the brain extends in the entire interstitial space between the cells, which represents up to 20% of the brain volume (Ruoslathi, 1996). HA polymers occupy most of the space and serve as a backbone for the remainder of the ECM components. HA is a chain composed of disaccharides elongated directly into the ECS from the cell membrane by the HASs. In vertebrates, there are three known variants for the HASs, namely HAS1, HAS2 and HAS3 (Itano & Kumata, 2002). All three of the HASs elongate the HA chain by adding alternatively glucuronic acid and N-acetylglucosamide to the polymer. The length of the chain depends on the synthase, with HAS3 producing shorter fragments than the other two isoforms (Itano et al., 1999). The length of the HA chains actually favours some specific type of communication in between the cells and, for example, short (<500kDa) and long (>500kDa) HA fragments regulate differentially the immune response of glia (Chistyakov et al., 2019).

In its role as a backbone, HA links a range of glycoproteins and proteoglycans which are produced by both neurons and glia cells (Krishnaswamy et al., 2019, Zhang et al., 2014). There are several families of proteoglycans (PGs) present in the brain, all defined by the

glycosaminoglycan (GAG) chain that is attached to their core: heparan-sulphate PG, keratan-sulphate PG and last but not least, the most present and major constituents of the brain ECM, the CSPG (chondroitin-sulphate proteoglycan). This last GAG type can be biochemically modified into dermatan-sulphate, giving rise to a fourth family.

As already stated, a feature of all PGs is to have one or several GAG attachment sites, hence the proteins are located in the ECS or at the membrane of cells with carbohydrate moieties occupying the space around them. As this project focuses mostly on CSPGs, I will shortly describe the nature of the CS chain: it comprises a disaccharide alternating glucuronic acid (GlcA) and N-acetylgalactosamine (GalNAc). Several sulphation patterns produced by two distinct pathways appear in CS. The first one is the 4-O sulphation pathway and it leads to the A and E form. The A form is the most represented in the adult brain, it has a sulphate group on the GalNAc in position 4, and the addition of a sulphate group in position 6 leads to the E form. The other pathway, the 6-O sulphation pathway, is the most present in the developing brain and adds a 6-O sulphate group on the GalNAc first, generating the C form. Upon addition of a 2-O sulphation on the GlcA, it forms the CS-D (Miyata & Kitagawa, 2017).

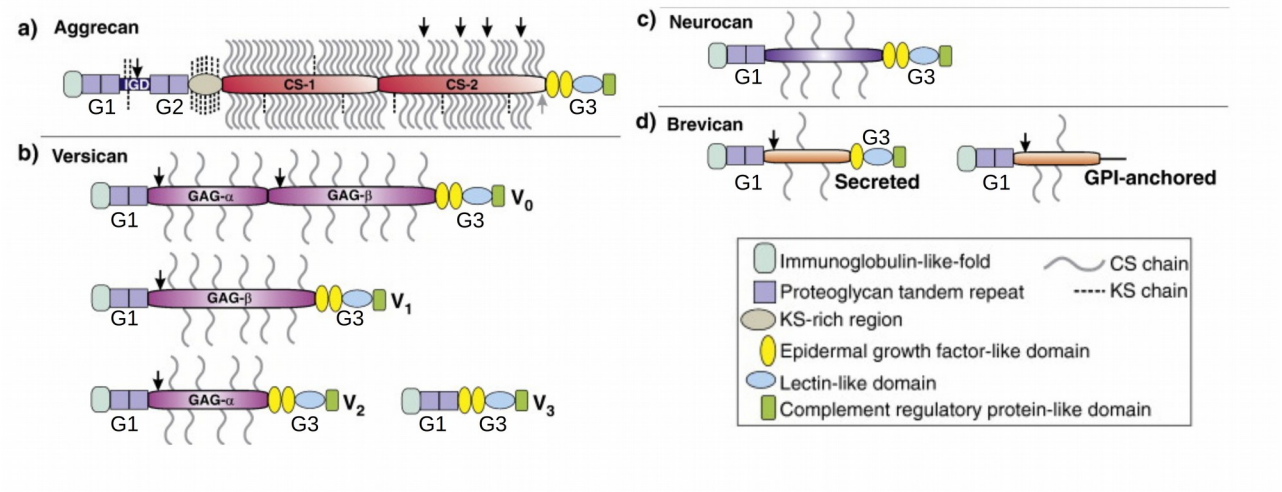

Figure 4: Representation of the four lecticans and their different splice variants: (a) Aggrecan, (b) Versican, (c) Neurocan, (d) Brevican. The main cleavage sites by matrix proteases are marked by an arrow. KS = keratan sulphate, CS = chondroitin sulphate. Modified from Stanton et al., 2011.

Among the CSPGs of the brain, there is one dominant subset of proteins: the lecticans (Yamaguchi, 2000, Figure 4). Their expression in the central nervous system is much stronger, with two members out of four being largely specific to the brain: Neurocan and Brevican. The other two members of this family are Aggrecan and Versican. Lecticans have a dumb-bell-like structure with a central part where the CS chains are attached and a globular domain on each end of the protein. The N-terminal part of the lectican (called G1) binds HA. It also possesses an IgG-like loop and a proteoglycan tandem repeat domain (PTR). Conversely to the other family members, Aggrecan has a second globular

domain on the N-terminal end (called G2), only comprising the PTR domain. Finally, the C-terminal part (called G3) comprises three domains: EGF repeats, a c-type lectin domain (from which comes the name lectican) and a complement regulatory protein-like domain. Among these four PGs, Brevican is the only one with a GPI-anchored variant (Seidenbecher et al., 1995), and thus can be found within the cell membrane.

Lecticans and Phosphacan (another CSPG of the brain) are linked together by other types of proteins. The Tenascins have the role of stabilising the ECM by linking the G3 domain of the CSPGs and forming polymers (Lundell et al., 2004). To our current knowledge, there are only two types of Tenascins expressed in the brain: Tenascin-C and Tenascin-R (TnC and TnR respectively). The first one is more often associated to a younger form of the ECM while the latter has increasing levels of expression as the organism reaches adulthood (Krishnaswamy et al., 2019). They oligomerise to form trimers for TnR and hexamers for TnC.

Another group of proteins of interest for the HA-based ECM are the so called Hyaluronan and Proteoglycan Link Proteins (HAPLN). There are four isoforms, named HAPLN1 to HAPLN4, out of which HAPLN3 is not expressed in the brain. HAPLNs ensure a stronger bond between the HA chain and the PGs attached to it (Binette et al., 1994). Studies to this date have shown that there were some preferential binding partners for each HAPLN. It appears that HAPLN2 (also referred to as Brain Link Protein 1 (Bral1)) is colocalised with Versican at the nodes of Ranvier (Oohashi et al., 2002, Figure 5b) while HAPLN1 mostly interacts with Aggrecan (Carulli et al., 2010). Finally, the HAPLN4 (also known as Bral2) is essential to address the Brevican to the PNNs, suggesting a stronger interaction between the two proteins (Bekku et al., 2012).

In the end, this complex of proteins and GAGs complex forms a network, a net-like structure more or less tight around the neurons and glia cells. The exact structure of the ECM however is dynamic and not uniform in the whole brain. Each brain region has specific needs and the ECM, as the regulator of the ECS and its properties, adapts to these needs. Hence, each region of the brain has a different ECM composition (Dauth et al., 2016).

I.3.b. - Structures and functions of the hyaluronan-based ECM

The meshwork described before is found throughout the whole brain with slight alterations to its composition that can have strong effects on the intricate balance of the neuronal networks and on the activity of glia cells. It is designated under the name of *diffuse ECM*, in contrast to a *condensed ECM*.

The strongest shift in the ECM composition happens during development and it participates actively in the processes of brain maturation (Bandtlow & Zimmermann, 2000). The ECM plays a preponderant role in axon guidance, cell development, dendrite

sprouting and synaptic plasticity (Avram et al., 2014). Over the time course that leads from a juvenile brain to an adult brain, the ECM undergoes several changes, with, for example, Neurocan (and the CSPG Phosphacan) having strong expressions in early-life but being almost absent from the adult brain (Carulli et al., 2010, Meyer-Puttlitz et al., 1995). Meanwhile, the core proteins of the ECM also see their CS moieties change: the sulphation patterns of the CS shifts around the same period away from 6-sulphation (Miyata et al., 2012).

Once the brain has reached its mature state, the ECM still plays a role in adult neuronal plasticity. Genetic manipulation to delete specific genes encoding ECM components may lead to changes in neuronal properties. As an example, a deletion of the Brevican gene leads to an impaired long-term potentiation (LTP) in hippocampal cells (Brakebusch et al., 2002); the same goes for a deficiency in TnR (Saghatelyan et al., 2001). Saghatelyan and colleagues (2004) even expanded on the role of TnR, showing the protein is involved in the migration of newly formed neuroblasts in the adult brain. Finally, TnC plays a role in the long-term depression in the CA1 region of the hippocampus (Evers et al., 2002).

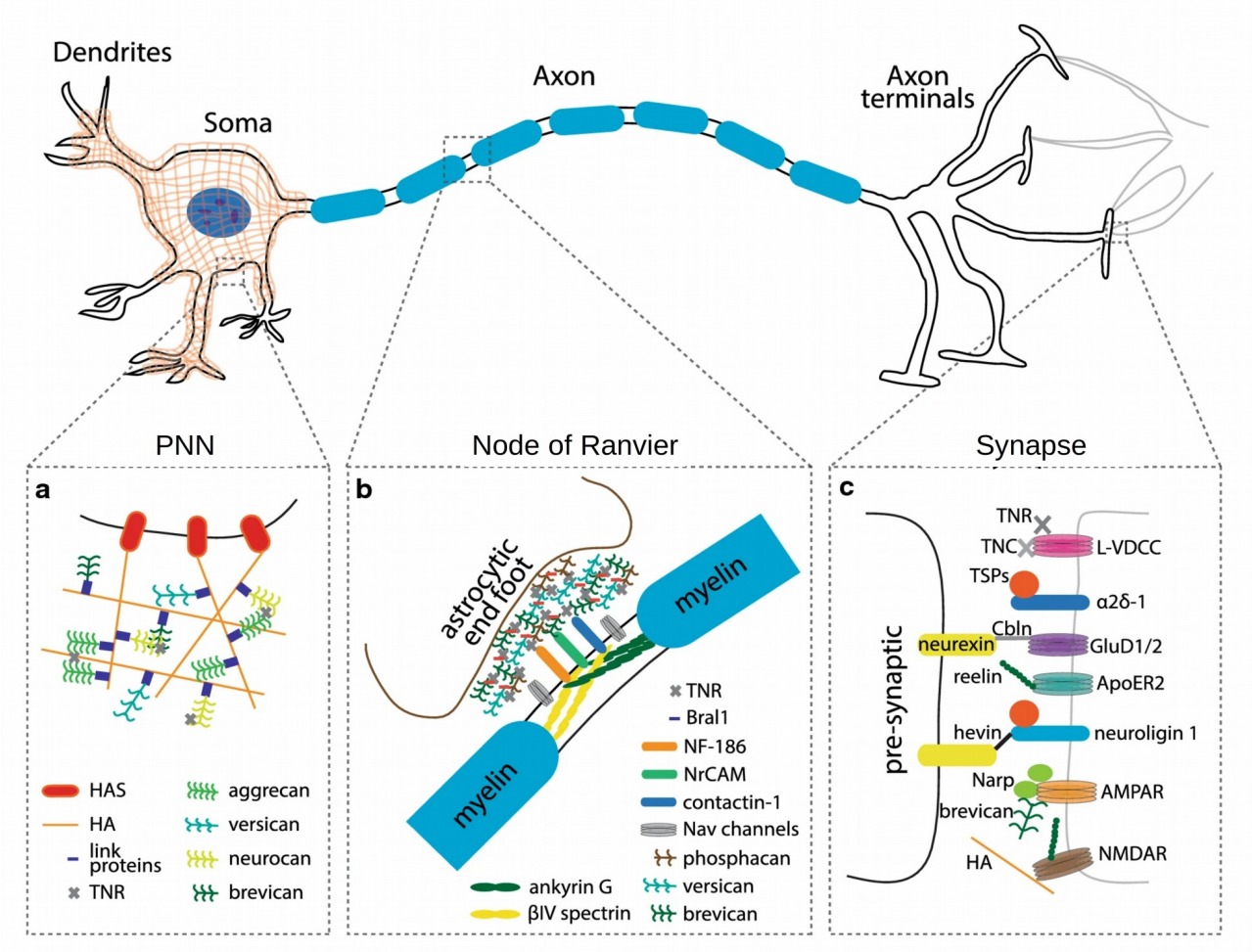

Figure 5: Representation of the different ECM structures around neurons in the brain. (a) Perineuronal net structure, a dense ECM composed of HA and lecticans that typically enwraps interneurons. (b) ECM structure at the node of Ranvier, highly enriched in Versican, HAPLN2 (also named Bral1) and Brevican. (c) The perisynaptic ECM has many interactions with actors of the synaptic transmission, synaptic plasticity and development. From Krishnawamy et al. (2019).

The core proteins are not the only part of the ECM with a role to play in plasticity mechanisms and experiments targeting the CS moieties have shown interesting results. The digestion of the CS chains by chondroitinase ABC (ChABC) leads to a reopening of a juvenile-like plasticity in the visual cortex (Pizzorusso et al., 2002) and is also able to improve axonal regeneration following injuries (Bradbury et al., 2002).

Generally, the return to juvenile plasticity is associated with the loss of ECM structures which are the hallmark of a mature brain: the PNNs (Figure 5a). The PNNs are a condensed form of ECM wrapped around specific cells, generally fast-spiking Parvalbumin interneurons (although they are not limited to this type only). Around the end of the critical period, the ECM changes and the PNNs appear around the interneurons, closing this period of heightened plasticity. A digestion of the PNNs with ChABC was shown to reopen plasticity in the visual cortex (Pizzorusso et al., 2002), to erase fear memories acquired in early-life (Gogolla et al., 2009), and to improve the retention of long-term memory (Romberg et al., 2013). Similarly, a genetically-induced disruption of PNN formation leads to maintained high plasticity into adulthood (Carulli et al., 2010, Romberg et al., 2013).

Interneurons are an important part of the brain networks and one of the supposed functions of PNNs is to protect these neurons from harm, for example against oxidative stress (Morawski et al., 2004). A more defined function of this structure is the capture of external factors such as Sema3A, necessary for a control of their innervation (de Winter et al., 2016). However, their range of action is not limited to a barrier function, PNNs also influence the electrical activity of the neurons they protect as their composition, notably Brevican, affects their electrophysiological properties (Favuzzi et al., 2017). It was shown that a lower level of Brevican within the PNN increases the excitability of interneurons. Hence a modification of the ECM around interneurons could lead to changes in the overall network activity.

Another specific structure of the ECM is set around the nodes of Ranvier, mainly composed of Versican, Brevican and HAPLN2, little is actually known about the function of these structures (Oohashi et al., 2002). Similarly, the dandelion-clock like structure is also an ECM structure which function is yet unknown. The dandelion-clock like structures appear around the same time as PNNs but are localised around cortical astrocytes and not interneurons (Hayashi et al., 2007).

Finally, another important structure of the ECM in the brain is the perisynaptic ECM. The HA-based ECM surrounds the synapse and, based on its ability to regulate the positioning and recruitment of AMPA receptors at the synapse (Frischknecht et al., 2009), the composition of NMDA receptors (Schweitzer et al., 2013) and the recruitment of L-type Ca^{2+} channels (Kochlamazashvili et al., 2010) it also has an important role to play in the

synaptic cleft. Moreover, it is an actor of modulatory signalling, with ECM cleavage being triggered by homeostatic plasticity mechanisms (Valenzuela et al., 2014) and dopaminergic signalling (Mitlöhner et al., 2020). This makes the ECM part of the complex regulatory mechanism of synaptic activity and plasticity.

I.3.c. - Proteolysis of the ECM and matricryptins, the ECM as a signal

Due to its repulsive or attractive action on neurons, as well as its ability to limit or reinforce plasticity, the brain ECM must be regulated in some way. To this end, neural cells produce enzymes that they secrete in the ECS to cleave specific ECM components. The HA and CSPGs are the target of several families of enzymes. The major ones are matrix metalloproteinases (MMPs, reviewed in Rempe et al., 2016), and specifically A disintegrin and metalloproteinase with thrombospondin motifs (ADAMTSs, reviewed in Kelwick et al., 2015). Together, these two families of proteases cleave the PGs composing the ECM into smaller fragments (for a review on the cleavage of lecticans, see Fontanil et al., 2021).

Following the cleavage by proteases, the fragments of PGs are in the ECS. Although there is no clear consensus, the fragments are believed to be cleared out by internalisation in the neighbouring cells, e.g. microglia (Nguyen et al., 2020). This is mediated via numerous receptors the ECM has at the cell surface. Indeed there are some receptors such as cell adhesion molecules or integrins. Some studies point to specific receptors for the ECM, notably the CD44 receptor, known to bind HA (reviewed in Wlodarczyk et al., 2011).

Cleaved fragments of the PGs may also constitute an entirely different molecular signal when compared to the full-length PGs. Such ECM fragments that are part of a signalling mechanism are called matricryptins. Whereas full-length ECM components act on a subset of ECM receptors, matricryptins may have their own receptors. Therefore cleavage of the ECM can be more than just a way to regulate the matrix integrity itself. It is a paradigm shift in the signalling coming from the ECS (Davis et al., 2000).

II Aims of the study

The basis of the epileptic phenotype is a disturbed E/I balance that leads to seizures with consequences at the behavioural level and also within neuronal networks. A dysregulation of the plasticity mechanisms is suspected to be one of the main reasons leading to the change in the E/I balance (Jarero-Basulto et al., 2018).

In addition to neurons and astrocytes, the ECM appears as a participant in some processes of plasticity as modifications to its composition affect neuronal functions, such as short-term plasticity (Frischknecht et al., 2009) or LTP (Brakebusch et al., 2002). Moreover, the degradation of ECM components is an integrative part of some forms of plasticity (Mitlöhner et al., 2020, Valenzuela et al., 2014) and the roles of the ECM in the developing brain are reminiscent of some changes observed in epilepsy (Avram et al., 2014). Nevertheless, the role of the ECM in epilepsy is not clear and investigations on the modifications of ECM in epileptic models have mostly focused on PNNs with few exceptions (*e.g.* Arranz et al., 2014, Kurazono et al., 2001).

In this thesis, I want to address the changes seen in the ECM composition between different types of models instead of a single chemically induced one. In addition, I want to further develop on the observation of Yuan and colleagues (2002) about a possible correlation between the state of the ECM and the extent of the epileptic phenotype, to see whether or not it is possible to link the state of the ECM to the strength of the epilepsy. The aims of my project are the following

1. Assess the severity of the epileptic phenotype of a diverse range of mouse models of epilepsy with generalised seizures: the Bassoon mutant mice.
2. Compare the effect of a cKO of the Bassoon protein in inhibitory neurons, and excitatory neurons on the epileptic phenotype.
3. Compare the severity and nature of the epileptic phenotype between the Bassoon mutants and the KA injected model.
4. Compare the changes in the main components of the HA-based ECM between the Bassoon mutants and the KA injected model.
5. Explore whether there is a link between regulation of ECM proteins and the severity of the epileptic phenotype.

III Material and Methods

All chemical products were purchased from Roth except when the provider is otherwise specifically stated.

III.1 - Animal housing and mutant genetic details

The mice were housed in standard conditions (21°C) on a 12-12hrs light-dark cycle. Food and water were provided *ad libitum*.

All the Bassoon mutant lines were bred in a C57BL/6N genetic background. We bred a total of 5 different Bassoon mutant lines included in our experiments. Among the mutant lines, 3 affect constitutively all synapses and 2 are cKOs to specific cell-lines (forebrain excitatory neurons and inhibitory neurons). Details of each line are summarised in Table 1 and Figure 3 along with publications describing their phenotype further. The animals used for the KA experiments were from a C57BL/6J background, bred in similar conditions. All animals used in the following experiments were between 3-7months.

The animal experiments were carried under the license TVA 2-DZNE-1316 and TWZ.

Line	Abbreviation	Genetic modification	Control used
$Bsn^{\Delta Ex4/5}$	Bsn1	The exons 4 & 5 of the *Bsn* gene are replaced by a LacZ-Neomycin cassette. A short version of Bassoon is still expressed (Altrock et al., 2003).	Wild-Type C57BL/6N
BGT	Bgt	A gene-trap in the intron between exons 1 & 2 of the *Bsn* gene lead to absence of *Bsn* expression (Hallermann et al., 2010).	Wild-Type C57BL/6N
Bsn2	Bsn2	LoxP sequences frame the exon 2 of the *Bsn* gene.	Not applicable
Bsn3	Bsn3	Bsn2 line crossed with a CMV-Cre line, leading to a full KO.	Bsn2
B2E	B2E	Bsn2 line crossed with an Emx-Cre line, leading to a KO specifically in forebrain excitatory neurons (Annamneedi et al., 2018).	Bsn2
B2I	B2I	Bsn2 line crossed with an Dlx5/6-Cre line, leading to a KO specifically in inhibitory interneurons.	Bsn2

Table 1: Description of the genetic modifications carried on each Bassoon line.

III.2 - Solutions and buffers

Buffer	Protocol	Composition
Tris Buffer Saline (TBS)	Western Blot	50mM Tris, 150mM NaCl, pH 7.6
TBS-T	Western Blot	0.1% Tween-20 in TBS
Milk solution	Western Blot	5% non-fat dried milk in TBS-T
SDS sample buffer (4x)	Western Blot	250mM Tris, 1% SDS, 40% Glycerol, 5% 2-mercaptoethanol, 0.02% Bromophenol blue, pH 6.8
Electrophoresis Buffer	Western Blot	25mM Tris, 192mM Glycin, 0.1% SDS, pH 8.3
Blotting Buffer	Western Blot	25mM Tris, 192mM Glycin, 0.2% SDS, 10% Methanol, pH 8.3
Phosphate Buffer Saline (PBS)	Immuhisto-chemistry	2.7mM KCl, 1.5mM KH2PO4, 137mM NaCl, 8 mM Na2HPO4, pH 7.4
Blocking solution	Immuhisto-chemistry	5% BSA, 0.3% Triton X-100 in PBS
Antibody solution	Immuhisto-chemistry	2% BSA, 0.1% Triton X-100 in PBS
Cryoprotection solution	Immuhisto-chemistry	10% PBS, 30% Ethylene Glycol, 30% Glycerin
Solution A	Fractionation	0.32M sucrose, 5mM HEPES, pH 7.4
Solution B	Fractionation	0.32M sucrose, 5mM Tris, pH 8.1
Sucrose gradient	Fractionation	0.85/1.0/1.2M sucrose, 5mM Tris, pH 8.1

Table 2: Composition of the buffers and solutions used in the different protocols.

III.3 - Antibodies

Antibody	Host species	Reference	Provider	WB	IHC
Brevican	Guinea Pig		LIN	1:1000	1:500
Brevican	Rabbit		LIN	1:1000	
Aggrecan	Rabbit	AB1031	Millipore	1:500	
Neurocan	Sheep	AF5800	R&D Systems	1:200	
Tenascin-R	Goat	sc-9875	Santa-Cruz	1:200	
Tenascin-C	Rabbit	#12221	Cell Signaling Tech	1:1000	
Hapln1	Goat	AF2608	R&D Systems	1:200	
Hapln4	Goat	AF4085	R&D Systems	1:200	
CS-56	Mouse	C8035	Millipore		1:500
GFAP	Rabbit	173002	Synaptic Systems		1:500
Iba1	Guinea Pig	234004	Synaptic Systems		1:500

Table 3: List of primary antibodies used and their respective dilutions for WB and IHC.

Fluorescently labelled secondary antibodies in use for WB are from Invitrogen (Alexa Fluor 680 & 790, dilution 1:15 000) while antibodies in use for IHC are from Dianova (Cy3 & Cy5, dilution 1:500). Secondary antibodies coupled to peroxidase (POD) are from Jackson Immuno Research (dilution 1:5 000).

III.4 - Surgery and electrode implantation

Surgeries and EEG recordings were performed in the DZNE Magdeburg by Shaobo Jia (Dept. Molecular Neuroplasticity).

For the surgery, the animal received a constant isoflurane flow at 1 – 1,5% O_2 to maintain the anaesthesia. The surgeon fixed the head to a stereotactic frame and coated the eyes with gel to prevent them from drying during the operation.

The top of the head was cleaned with 75% Ethanol and the operator removed the fur to reveal the skin. Once the skin was apparent, a RYMDAL spray ensured local anaesthesia and analgesia (Xylocaine pump spray, NaCl 0,9%) and the animal was left for 5min before any other manipulation. After 5min the surgeon cut open the skin to reveal the skull and cleaned the bone with 3% H_2O_2. The ground screw was put in place at the following coordinates: AP -3,50; ML -3,5 and the recording electrode at: AP -1,94; ML -1,5 (electrode E363/96/1.6/Spc, Bilaney consultants GmbH) in pre-drilled holes. Two more anchor screws were fixed in the skull to maintain the dental cement, which is used to stabilise the electrode and ground screw. Once the dental cement had a sticky texture, the operator fixed a 3D printed cap over it (polylactic acid, composed of two chambers, one for wireless transmitters and one for battery). The transmitters were then attached to the electrode and ground screw (A3028, Open Source Instruments). The animal recovered from surgery during 3 days while its weight was monitored and a RYMDAL spray was provided daily to avoid infections.

III.5 - Kainic acid injection

KA injections were performed in the DZNE Magdeburg by Shaobo Jia (Dept. Molecular Neuroplasticity).

For intra-hippocampal KA injection, a 22 gauge cannula (diameter: 0.711/0.483 mm; length: 8.65 mm) was positioned above the right hippocampal CA1 area (AP, -1.94; ML, +1.0; DV, 0.3 mm). KA monohydrate (K0250, Sigma Aldrich, Germany) was dissolved in distilled sterile water at 20mM as stock solution and kept at -20°C.

30min before injection, the stock solution was diluted in distilled sterile water to 10mM and loaded into a 10µL Hamilton syringe (35 gauge needle, NF35BV-2, World Precision Instruments, Sarasota, FL, USA). The Hamilton syringe was controlled by a MicroSyringe Pump Controller (Micro 4, World Precision Instruments, Sarasota, FL. USA). Animals with implantations were anaesthetised and fixed to the stereotactic frame. Through the

cannula, 120nL KA were administered to the hippocampal CA1 area (AP, -1.94; ML, +1.0; DV, 1.3 mm) at 3nL.s^{-1}. After injection, animals were monitored for behavioural and electrographic seizures. Animals with stage IV or V seizures according to Racine's scale were recruited into the following stages of the experiment. An injection of Lorazepam (6mg.kg^{-1} i.p.) terminated the *status epilepticus* 1.5h after the first seizure. The number of convulsions during the first hour after KA administration was recorded every 10min to control that animals assigned to control and treatment groups showed seizures of equal severity. The analysis was performed by an experimenter blinded to the group assignments.

Animals were then recorded with an EEG cap as previously described for up to 7d after injection (KA1wk group) or up to 30-35d after injection (KA4wk group).

III.6 - EEG recording, analysis and seizure counting

The EEG recordings were carried out at the DZNE Magdeburg, under the care of Shaobo Jia (Dept. Molecular Neuroplasticity).

After a period of recovery for the animals in individual cages (5-7 days), the transmitters and the electrodes transmitted their recordings wirelessly to the LWDAQ+ software (Open Source Instruments). The recordings ran for at least 4 full days (96h) up to 12 days (288h).

With the help of LWDAQ Neuroarchiver (Open Source Instruments), the recordings were cut into 4s frames with a glitch threshold at 200 counts to remove artefacts. In each of this 4s frames, the ECP19 processor extracted 6 properties from the EEG trace (whose detailed calculation can be found in Hashemi, 2020). The software stored the properties of a chosen set of traces in a library. The traces included therein were selected from the first 5h of each day of recording, outside of the Neuroarchiver usual reading frame.

Concerning the KA-injected animals, the first 3 days following the injection were not included in the analysis as they were too close to the injection to represent a chronic phase. They were nevertheless checked for seizures to verify that the KA injection had the desired effect. The 3h following injection were checked in the Sham animals for the absence of seizures.

For the Bassoon mutants, a library of 143 ictal intervals was compiled to be used as references by the software. The library for the KA animals is compiled similarly out of their own recordings, with 171 events for the KA1wk and 287 events for the KA4wk.

The library is then used to classify the remainder of the recording. The software computes a space based on the 6 properties (from the ECP19 processor) and places each 4s frame in this space before comparing their distance with the closest trace of the library. The 4s frame was considered ictal if the distance to a library point was below an 0.1 threshold

distance. It was then confirmed manually whether or not the frames identified as ictal during this process were or not part of an actual seizure. Ictal-like events with a duration below 8s were not considered as seizures.

Moreover the precision of the library was tested against two animals fully reviewed by eye, for each library. One without seizures to make sure that it was not a false negative and one with seizures to make sure that all possible seizures were properly detected by the library. The library was considered accurate once all seizures from the second animal could be selected and it was confirmed that the animal without any detected seizures indeed had none.

III.7 - Seizure onset classification

To classify the seizures, two scientists looked separately at the onset of each seizures and classified them into two categories: hypersynchronous (HYP) or low-voltage fast onset (LVF). They then compared their classifications and whenever a discrepancy was found, looked back at the seizure together to decide which category it belongs to. A third category (called “undefined”) was considered when no agreement could be found or the seizure trace did not fit in any of the two categories.

III.8 - Perfusion and extraction of the brain

Animals were sacrificed with CO_2 followed by cervical dislocation. Quickly after death, the animal is tied face-up and the rib cage is opened to reveal the heart. With the help of a peristaltic pump (Cyclo I, Roth) the heart is perfused with PBS until it replaces the blood in the body, then we switch to a 4% PFA in PBS solution for 15min. Once the body is fixated, the brain is collected into 4% PFA in PBS for post-fixation overnight (4°C). The brain is left in a 1M sucrose solution (in PBS) for cryoprotection. A couple of days later, we freeze it in 2-methyl-butane at -80°C. The brains are stored at -80°C until further use.

III.9 - Preparation of brain slices for immunohistochemistry

Slices from the Bsn3 and KA1wk animals were obtained with a cryomicrotome (Leica Biosystems, CM3050S). The slices were cut on the sagittal plane from the right hemisphere only (Bsn3) or a coronal plane (KA1wk). The slices were 40µm thick and cut at -16°C (object temperature)/-20°C (ambient temperature), stored as serial free floating sections in the cryoprotection buffer at -20°C until further use.

III.10 - Immunohistochemistry

A series of 3-5 slices by animal was carefully chosen for each staining. Before any incubation, the slices are rinsed in PBS (3x10min). This washing step is repeated between each incubation. Then, we incubate the slices in a blocking solution (PBS, 5% BSA, 0,3%

Triton X-100) for 1h before the incubation with the primary antibodies in the antibody solution (PBS, 2% BSA, 0,1% Triton X-100, 48-72hrs at 4°C). We incubate overnight with the secondary AB in the same solution. Finally, we rinse the slices one last time and mount them between slide and coverslip in Fluoromount-G™ with DAPI (Invitrogen, Thermo Fisher Scientific).

All staining are accompanied by a negative control where the first incubation is done without primary antibodies. Before any analysis, the negative control were checked for the absence of fluorescence signal under a fluorescence microscope (Zeiss, Axioplan 2). In case there was a signal, the corresponding channel was disregarded for qualitative and quantitative analysis.

III.11 - Microscopy and image analysis

The stained brain slices were observed under a confocal microscope (TCS SP5, Leica Microsystems) with the 10x objective. The image were taken at 1024 x 1024px resolution with 15% overlap to ensure a proper image stitching over a Z-stack of 17 images 0.59µm apart (9.399µm in total).

The images are stitched together and analysed with the help of FIJI (Schindelin et al., 2012, Preibisch et al., 2009). The hippocampus regions are delimited with the selection tool and each is measured for mean value, area and integrated density. Comparison between intensity levels was only carried out between slices treated in the same conditions, with the exact same image capture settings.

III.12 - Subcellular fractionation of the brain

CO_2 was used to sacrifice the animal, then, the skull was open to extract the brain and freeze it in liquid nitrogen. The brains are stored at -80°C until further use.

Before the fractionation, the brains were thawed in PBS. We then use a Potter S (Braun Biotech International) to homogenise the brain in Buffer A (10mL for 1g of original tissue; 12-14 strokes at 900rpm) with protease inhibitors (cOmplete, EDTA-free protease inhibitor cocktail, Roche). The obtained homogenate is centrifuged at 1000x g for 10min to separate the nuclear fraction and debris (pellet) from the other components (supernatant). The pellet is centrifuged a second time at 1000x g for 10min after resuspension in the same volume of buffer A (10mL for 1g of original tissue) and the pellet is discarded while the supernatants are pooled together.

Part of the supernatant is kept as “Homogenate” fraction and the remainder is further separated. A centrifugation at 12000x g for 20min separates the supernatant (termed “S2”) from the membrane fraction (termed “P2”). The P2 is resuspended in the original volume of buffer A and centrifuged a second time at 12000x g for 20min. The supernatants S2 are pooled together and some of the P2 pellet is kept. The remainder of P2 is suspended in

1,5mL for 1g of original tissue of buffer B before being laid on top of a sucrose gradient (1,2M, 1,0M and 0,85M). A high speed centrifugation at 85000x g for 2h separates different fractions in each of the phases between two concentrations. We collect the Myelin fraction between 0,32M and 0,85M, the Light Membrane fraction between 0,85M and 1,0M and finally the Synaptosome fraction between 1,0M and 1,2M. The pellet is discarded.

The S2 is further separated into soluble fraction and microsomes with a 100 000x g centrifugation for 1h. The microsome fraction (the pellet) is discarded while the supernatant is kept as the “Soluble” fraction (also referred to as “S3”).

In order to remove the CS chains on the proteins we are interested in, the samples are digested with ChABC (C3667, Sigma-Aldrich). The digestion is done with 1:400 of a 0.1U.µL^{-1} solution of ChABC in the sample, for 90min at 37°C.

We store the fractions at -80°C until further use.

III.13 - SDS PAGE gel preparation

Tris-Glycine gels were cast following the Laemmli buffer system. There are two types of gel depending on the molecular weight of the protein of interest that we want to develop, 5-20% and 2,5-10% (Table 4).

First, we prepare the gel casting chamber with aluminium plates, 0,75mm spacers and a glass plate. The chamber is plugged to a peristaltic pump. To create the gradient, the pump has two chambers under constant agitation. The first chamber corresponds to the lowest Acrylamide percentage and the second, which slowly dilutes into the other over the course of the casting, contains the highest percentage solution.

Once the whole separating gel solution is pumped in, we let the gradient polymerise for 2h with isopropanol on top to avoid the meniscus formation. After 2h the isopropanol is removed and we pour the stacking gel solution before adding the combs. The gels are left at room temperature for at least 1h, then the gels are stored at 4°C until further use.

III.14 - SDS-PAGE, Western Blot & Immunoblot detection

The protocol ran under permanent cooling at 8°C.

In order to quantify the amount of a specific protein in the samples, I use the sodium dodecyl sulphate polyacrylamide gel electrophoresis (SDS-PAGE) under fully denaturing conditions. The samples are diluted in 4x SDS loading buffer and boiled for 5min at 95°C. Before use, the samples are centrifuged shortly at maximum speed, the supernatant only is used. We load 15-20µg of sample into gradient Tris-Glycin gels: 2.5-10% for Aggrecan and 5-20% for all other proteins. All gels have alternatively a control and a KO or treated sample to account for possible gel heterogeneity. The gels are clamped in an

electrophoresis chamber filled with Electrophoresis Buffer (Mighty Small II MINI Vertical Electrophoresis Unit, Hoefer). The current provided is of 8mA per gel until the samples are out of the stacking gel, then it is changed to 12mA per gel. We wait until the molecular weight of interest for our proteins are within the stacking gel.

Gel type	Composition
Separation Buffer (20%)	8.25mL 1.5M Tris/HCl pH 8.8, 7.5mL 87 % glycerol, 16.5mL 40 % acrylamide, 330µL 10 % SDS, 330µL 0.2M EDTA, 22µL TEMED, 120µL 0.5 % bromophenol blue, 75µL 10% APS, 1.2% (v/v) 2,2,2-trichlorethanol (TCE)
Separation Buffer (5%)	8.25mL 1.5M Tris/HCl pH 8.8, 17.94mL dH_2O, 1.89mL 87% glycerol, 4.12mL 40% acrylamide, 330µL 0.2M EDTA, 330µL 10 % SDS, 22µL TEMED, 118µL 10% APS, 1.2% (v/v) TCE
Separation Buffer (10%)	8.25mL 1.5M Tris/HCl pH 8.8, 7.5 mL 87 % glycerol, 8.25mL 40 % acrylamide, 8.25mL dH_2O, 330 µl 10 % SDS, 330 µl 0.2M EDTA, 22µL TEMED, 120µL 0.5 % bromophenol blue, 75µL 10 % APS, 1.2% (v/v) TCE
Separation Buffer (2.5%)	8.25mL 1.5M Tris/HCl pH 8.8, 20mL dH_2O, 1.89mL 87% glycerol, 2.06mL 40 % acrylamide, 330µL 0.2M EDTA, 330 µl 10 % SDS, 22µL TEMED, 118µL 10% APS, 1.2% (v/v) TCE
Stacking Buffer (5%)	6mL 0.5M Tris/HCl pH 6.8, 7.84mL dH_2O, 5.52mL 87% glycerol, 3.90mL 30% acrylamide, 240µL 0.2M EDTA, 240µL 10% SDS, 17.2µL TEMED, 140µL phenolred, 137µL 10% APS

Table 4: Composition of the solutions used to cast the gels.

After the SDS-PAGE, the gels are illuminated with UV light for 5min for the TCE to bind the proteins. This image, similar to a Coomassie, is used as a control that the proteins ran properly in the gel before the next step.

We then transfer the proteins to a polyvinylidene fluoride membrane (PVDF, Immobilon®-FL, 0.45µm pore, Millipore) shortly activated in methanol. The transfer happens in a chamber filled with TG Blotting Buffer (Mighty Small Transfer Tank, Hoefer). For the 2,5-10% gels the blotting time is 2h15min, 1h45min for the 5-20% gels, at 200mA in both cases.

After the transfer, the membrane is exposed once more to UV light. The image of the TCE staining is then used as a loading control during quantification.

Following this, the membrane is blocked with a 5% non-fat milk solution in TBS-T for 30min at RT°. A quick wash in TBS-T is performed before the incubation of the membrane with the primary antibody diluted in the 5% milk solution overnight at 4°C. Washes with TBS-T (3x10min) are followed by the secondary antibody for 1h at RT. The POD-associated antibodies are diluted in milk solution whereas the fluorescent ones are in TBS-T. Once more the membranes are washed with TBS-T (3x10min) before imaging.

The POD labelled membranes are developed with an ECL Chemocam Imager (INTAS Science Imaging Instruments GmbH) while the fluorescently labelled blots were scanned with an Odyssey scanner (LI-COR® Biosciences).

The quantification is done with ImageJ and the values are normalised to the TCE images and then to the average value of the WT animals following the protocol of Mitlöhner et al. (2020).

III.15 - Sample preparation for proteomics

The membrane samples (referred as “P2” in III.12) of 4 animals of the Bsn2, Bsn3, B2E and B2I lines were sent to the Proteomic Core Facility of the EMBL Heidelberg (Germany). The Bsn2 animals were used as controls as stated in Table 1.

The following steps were realised by the EMBL Proteomic Core Facility (Heidelberg).

Shortly, the disulphide bridges of the samples were reduced in dithiothreitol 10mM (50mM HEPES, pH 8.5, 56°C, 30min) and freed cysteines were alkylated with 2-chloroacetamide 20mM (50mM HEPES, pH 8.5, RT°, 30min). Following the SP3 protocol (Hughes et al., 2014 & 2018), the peptides were prepared with trypsin (sequencing grade, Promega) at 1:50 protein ratio (37°C, overnight). The next day, the recovery of peptide combined supernatant collection on magnet and elution wash of beads, both in HEPES 50mM. The peptides were labelled with TMT10plex isobaric label reagent (ThermoFisher) following manufacturer’s instructions. For further sample clean-up, an OASIS® HLB µElution plate (Waters) was used. Offline high pH reverse phase fractionation was then carried out on an Agilent 1200 Infinity high-performance liquid chromatography system, with a Gemini C18 column (3µm, 110Å, 100 x 1.0 mm, Phenomenex).

III.16 - Mass spectrometry data acquisition

The following experiment was realised by the EMBL Proteomics Core Facility (Heidelberg).

The liquid chromatography MS-MS was carried out on an UltiMate 3000 RSLC nano LC system (Dionex) fitted with a trapping cartridge (µ-Precolumn C18 PepMap 100, 5µm, 300 µm i.d. x5mm, 100 Å) and an analytical column (nanoEase™ M/Z HSS T3 column 75µm x250mm C18, 1.8 µm, 100 Å, Waters). The trapping lasted 6min on a constant flow of 0.05% trifluoroacetic solution at 30µL/min in the trapping column. Subsequently, the peptides ran through the analytical column with a constant flow (0.3µL/min) of 0.1% formic acid solution in water, slowly replaced by 0.1% formic acid in acetonitrile. The outlet of the analytical column was coupled to an Orbitrap Fusion™ Lumos™ Tribrid™ Mass Spectrometer (ThermoFisher) using the Nanospray Flex™ ion source in positive ion mode.

The peptides were introduced into the Fusion Lumos via a Pico-Tip Emitter 360 µm OD x 20 µm ID; 10 µm tip (New Objective) and an applied spray voltage of 2.4 kV (capillary temperature: 275°C). Full mass scan was acquired with mass range 375-1500 m/z in profile mode in the orbitrap with resolution of 120000. The filling time was set at a maximum of 50ms with a limitation of 4.10^5 ions. Data dependent acquisition was performed with an Orbitrap resolution of 30000, with a fill time of 94ms and a limitation of 1.10^5 ions. A normalized collision energy of 38 was applied. MS^2 data was acquired in profile mode.

III.17 - Mass spectrometry data analysis

The following analysis was realised by the EMBL Proteomics Core Facility (Heidelberg).

IsobarQuant and Mascot (v2.2.07) were used to process the acquired data, which was searched against a Uniprot *Mus musculus* (UP000000589) proteome database containing common contaminants and reversed sequences. The following modifications were included into the search parameters: Carbamidomethyl (C) and TMT10 (K) (fixed modification), Acetyl (Protein N-term), Oxidation (M) and TMT10 (N-term) (variable modifications). For the full scan (MS1) a mass error tolerance of 10 ppm and for MS/MS (MS2) spectra of 0.02Da was set. Further parameters were set: Trypsin as protease with an allowance of maximum two missed cleavages; a minimum peptide length of 7 amino acids; at least two unique peptides were required for a protein identification. The false discovery rate on peptide and protein level was set to 0.01.

III.18 - Survival analysis

The survival analysis was conducted with the data of the five Bassoon lines (not including Bsn2 animals, see Table 1) from the LIN records. It comprised the records of all the animals genotyped between 1st January 2017 to 1st August 2020.

The Kaplan-Meier plot and the Cox proportional hazard models are fitted with “spontaneous deaths” only considered as the event. Any other type of death or use in an experiment lead to a censored data point at the appropriate time.

The animals are genotyped when they are weaned, at 3 weeks of age. Hence, the survival analysis did not take into account any event prior to this time point. In order to estimate the amount of animals lost before the genotype was known, the number of animals of each genotype was calculated and compared to the expected amounts with a Mendelian model for the same total amount of animals. The expected proportions were as follows: 25% KO, 50% heterozygous, 25% Ctrl. Concerning the cKOs (B2E and B2I), there are no heterozygous, hence only KO and Ctrl were compared with 1:1 proportions being expected.

III.19 - Statistical analysis

All statistical analysis was conducted with the R statistical software (https://www.r-project.org/) with the help of the following packages: broom, car, corrplot, dplyr, edfReader, emmeans, ggfortify, glmnet, ggplot2, reshape2, plyr, psych, scales, survminer, tidyr.

In order to help in our decisions concerning quantified results, we used several statistical tests, reported along with the corresponding p-value. Post-hoc tests were carried away only on results of significant ANOVAs, with personalised contrasts on least-square means. Following the post-hoc tests, the p-values were corrected with the false discovery rate method (fdr).

The correlation analysis was carried out with Spearman's correlation as the distribution of seizure properties was heavily skewed toward 0 due to the non-epileptic animals being included in the matrix. The tests of the correlation were corrected with the fdr method.

As a general rule, a p-value of under $5{,}00.10^{-2}$ was considered significant, however some results with a convincing effect, yet higher p-value, are also discussed as possible changes (but did not lead to post-hoc tests). For exploratory purposes some uncorrected p-value are also briefly discussed.

IV Results

IV.1 - Spontaneous deaths in Bassoon mutants suggest an early-onset epilepsy

Knowing that the Bsn1 mutants develop epilepsy early in life (Altrock et al., 2003), we wanted to investigate in a non-invasive yet reliable way the possible apparition of an epileptic phenotype in the other Bassoon mutant lines, as well as confirm the observed results in Bsn1.

To do so, we measured the number of animals in each line that died from spontaneous death (Figure 6). These death are unexplained and unexpected deaths that cannot be linked to any particular reason such as a disease or an infection. We suspect that they may be related to the development of an epileptic phenotype.

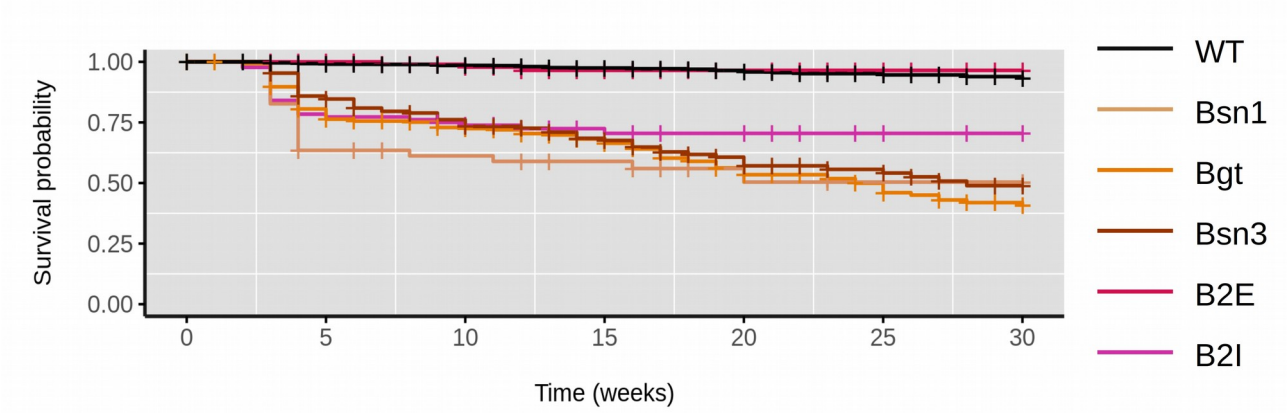

Figure 6: Kaplan-Meier survival plot of the different Bassoon lines from 3 weeks up to 30 weeks of age. The event counted in this plot are spontaneous deaths, any death with a clearly defined cause (disease, infection…) led to a censored data point at the appropriate time.

The mutants' death rates were compared to the spontaneous death rate of WT animals in a Kaplan-Meier curve (Figure 6). The Kaplan-Meier curve highlights the higher death rate of the Bassoon mutants compared to the WT. As soon as the 3rd and 4th week of life, the mutants from the Bsn1, Bgt, Bsn3 and B2I lines have an increased rate of spontaneous deaths. The Bsn1 line has a strong decrease in survival during these first weeks (~40% of individuals die of spontaneous death by the 5th week), but in the end, Bgt and Bsn3 lines have a similar survival rate as the Bsn1 by the 20th week up to the 30th, with about 50% of surviving animals. On the other hand, the B2I animals have a slightly less severe phenotype with ~25% of spontaneous death at 16 weeks (with no further events until the 30th week). Finally, the B2E animals are undistinguishable from the WT animals, with a survival rate close from 100%.

A quantification of the increased risk of spontaneous death in these lines was carried out with a Cox proportional hazard model, with the WT animals as the reference. The Cox proportional hazard model is a good fit (likelihood ratio test = 467,5 (6df), $p < 2{,}00.10^{-16}$). There are no differences between sexes over all the different lines considered (coefficient = -0,04, p = 0,76, female as the reference), nor for the B2E line when compared to the WT littermates (coefficient = -0,05, p = 0,92). All other Bassoon strains have a significantly higher risk of spontaneous death when compared to WT (Bsn1, coefficient = 3,02, $p < 2{,}00.10^{-16}$; Bgt, coefficient = 2,86, $p < 2{,}00.10^{-16}$; Bsn3, coefficient = 2,68, $p < 2{,}00.10^{-16}$; B2I, coefficient = 2,43, $p < 2{,}00.10^{-16}$). This corresponds to an 11-fold risk increase for the B2I (lowest coefficient), 14,5 for the Bsn3, 17,4 for the Bgt and finally 20-fold for the Bsn1 line. Of note, the number of Bsn1 (n = 52) and B2I (n = 88) animals are much lower than the numbers included in the other lines (B2E n = 210, Bgt n = 287, Bsn3 n = 172), which leads to a lower precision of the estimated risk coefficient.

One caveat of the above-mentioned analysis is that it only takes into account animals that have survived past their 3rd week of life, when they are genotyped. In order to improve the precision of our survival estimation, especially in the period prior to the 3 weeks of age, we calculated the proportions of animals of each genotype in each line and compared it to expected Mendelian ratios. The results for each line are reported in Table 5.

Animal line	**Homozygous (%)**		**Heterozygous (%)**		**Ctrl (%)**		**χ^2 (p-value)**
	Observed	Expected	Observed	Expected	Observed	Expected	
Bsn1	52 (6%)	216 (25%)	446 (52%)	432 (50%)	365 (42%)	216 (25%)	164.7 ($<2{,}0.10^{-16}$)
Bgt	287 (13%)	568 (25%)	1204 (53%)	1137 (50%)	782 (34%)	568 (25%)	184.9 ($<2{,}0.10^{-16}$)
Bsn3	172 (12%)	364 (25%)	699 (48%)	728 (50%)	584 (40%)	364 (25%)	134.1 ($<2{,}0.10^{-16}$)
B2I	88 (54%)	81 (50%)			73 (46%)	81 (50%)	1.22 (0,27)
B2E	210 (38%)	280 (50%)			350 (62%)	280 (50%)	34.5 ($4{,}3.10^{-9}$)

Table 5: Comparison of the observed animal numbers with the expected Mendelian numbers in the Bassoon lines. The p-values were calculated for the comparison of Observed Homozygous against the Expected number.

With the exception of the B2I line (54% of homozygous for 46% of Ctrl, p = 0,27), there is an obvious lack of homozygous animals in all the Bassoon lines when compared to the expected number. First, the constitutive mutant lines have a high mortality at a young age, seemingly, the Bsn1 line is the one with the highest infantile death rate (only 6% of homozygous against 42% of Ctrl, $p < 2{,}00.10^{-16}$). Whether it happens *in utero*, at the spermatozoid or oocyte level, or after birth remains unknown.

On the other hand, the B2E line shows a lower than expected number of homozygous animals (38% only for 62% Ctrl, $p = 4{,}30.10^{-9}$) but the animals that survive past the 3wk line have a survival rate in line with the one from the WT (Figure 6). Conversely, the B2I do not show any unexpected homozygous death before 3 weeks but then have ~25% spontaneous deaths over the following 27wk (Figure 6).

Concerning the heterozygous animals, they also have a lower than expected number, as they are supposed to have a 2:1 ratio with Ctrl animals, which is not the case here. The effects of a Bassoon haploinsufficiency is evident, especially in the Bsn1 line (446 heterozygous for 365 Ctrl, ratio = 1,22) and Bsn3 line (699 heterozygous for 584 Ctrl, ratio = 1,20). The Bgt heterozygous are also affected, albeit at a seemingly lower rate (1204 heterozygous for 782 Ctrl, ratio = 1,54). This argues in favour of an effect of Bassoon in the early development phases or on the survivability of gametes, even when it is only down-regulated. Following the first weeks, the heterozygous animals do not develop any harmful phenotype based on previous reports about the Bsn1 line (Altrock et al., 2003).

IV.2 - All investigated models display epileptic seizures

To test for the presence of seizures in the Bassoon mutants, an EEG recording of all the Bassoon lines was carried out. A surface electrode was set above the brain to record the brain activity and find potential seizures. The constitutive Bassoon mutants – Bsn1, Bgt and Bsn3 – were expected to display epileptic seizures as it had already been reported in the Bsn1 line (Altrock et al., 2003). Concerning the conditional Bassoon mutants – B2E and B2I – it was unclear whether or not they would develop epilepsy.

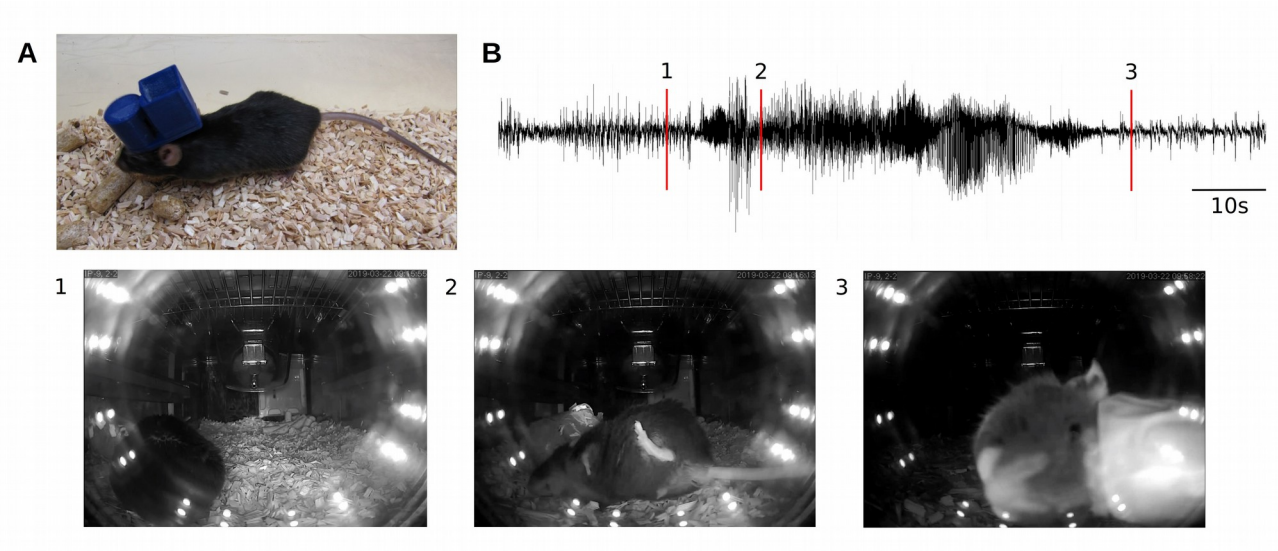

Figure 7: Long-term EEG recording in the Bassoon mice. (A) Mouse with a wireless emitter for the EEG signal transmission. (B) Seizure trace from a B2I animal. The red lines mark events observed on the camera before (1), during (2) and after (3) a seizure. 1. The animal is asleep. 2. Shortly after the start of the seizure, the animal falls to the side with uncontrolled jerks. 3. After the end of the seizure, the animal remains immobile with repeated paw to mouth movements.

The EEG activity of all recorded animals showed clear differences between Ctrl animals and either Bassoon mutants as well as KA-injected animals one and four weeks post-injection (KA1wk and KA4wk respectively). Noteworthy, two animals from the Bsn1 line died following the implantation of the electrode (before recording) and one Bgt animal died during the recording. Unfortunately the emitter was off at the time of death thus no EEG trace corresponding to this event is available.

With the exception of the B2E animals where not all animals showed seizures (40%, n = 5), all the other Bassoon lines had seizures among 100% of their individuals (n = 4 – 5). Conversely, the KA injection did not lead to such a high rate of epileptic animals with 41,7% (n = 12) after 1wk and 55,6% (n = 9) after 4wk.

Noteworthy, one of the Ctrl animals from the B2E batch (Bsn2 line) displayed a few seizures over the course of the recording. Overall, this represents a low proportion of epilepsy onset within the Ctrl mice of all the Bassoon line experiments (3,8%, n = 26), and the stressful nature of the electrode implantation might be at the origin of the seizures. Among the saline-injected Ctrl for the KA experiment, no seizure occurred (n = 18) (summarised in Table 6).

Animal group	% animals with seizures	Total number
Bsn2	3,8	26
Bsn1	100,0	4
Bgt	100,0	5
Bsn3	100,0	5
B2E	40,0	5
B2I	100,0	5
Sham	0,0	18
KA1wk	41,7	12
KA4wk	55,6	9

Table 6: Proportion of animals of each recorded group displaying seizures.

In order to show that the seizure traces observed during the recording sessions were indeed accompanied by behavioural consequences, the EEG recording of the B2I line was conducted with video-recording and the video was studied during the seizures detected via the EEG recording. The animals had convulsions and typical tonic-clonic seizure behaviour during the heightened EEG activity recognised as seizures (Figure 7).

Taken together, these results show that the KA-injected animals have a lower epilepsy onset rate than Bassoon mutants. The only exception is the B2E line, where Bassoon is deleted in the excitatory neurons only (Annamneedi et al., 2018) and the mutation does not lead systematically to an epileptic phenotype. This finding is quite striking in

comparison to the B2I line where the deletion of Bassoon in interneurons does lead to an epileptic phenotype in all cases.

IV.3 - The Bsn3 line has the most severe epileptic phenotype

In order to assess the severity of the epileptic phenotype in the different Bassoon mutant lines, the frequency of seizures, their average length and, in an effort to combine both number of seizures and duration, the proportion of time spent in seizures over all the recording period (expressed in %) was measured. As a comparison point, the established KA model was also analysed for the same variables. Each group of recorded animals was composed of one type of Bassoon mutants or KA-injected animals with their corresponding Ctrl. A total of seven groups were analysed: Bsn1, Bgt, Bsn3, B2E, B2I, KA1wk and KA4wk.

Concerning the frequency, there is a clear difference between the mutants or injected animals and their respective Ctrl (Two-way ANOVA, Treatment/Genotype nested within Group, $F(7, 77) = 25{,}66$, $p < 2{,}2.10^{-16}$). A direct comparison between the mutants or KA-injected animals (excluding the Ctrl animals) with their counterparts from the other lines showed a strong effect of the Group variable on the frequency of seizures ($F(6,38) = 15{,}53$, $p = 6{,}58.10^{-9}$) (Figure 8B). Out of all the lines, two stand out as the ones with most frequent seizures.

First, the Bsn3 line has the highest seizure frequency by far (4,19±0,59 seizure.day^{-1}), almost twice as many seizures as the second highest frequency in the Bgt line (2,12±0,45 seizure.day^{-1}, $p = 2{,}3.10^{-3}$). Both Bsn3 and Bgt have significantly higher seizure rates than the B2E line (0,11±0,11 seizure.day^{-1}, Bgt $p = 6{,}0.10^{-3}$, Bsn3 $p < 1{,}0.10^{-4}$) which is expected when considering that not all B2E animals display recurrent seizures (Table 6). Bgt, however, is considered to have a similar rate to B2I (1,18±0,39 seizure.day^{-1}, $p = 0{,}17$) and Bsn1 (1,09±0,52 seizure.day^{-1}, $p = 0{,}22$), while Bsn3 has a higher frequency (both, $p < 1{,}0.10^{-4}$). Hence, Bsn3 is the Bassoon line with the most frequent seizures.

As a comparison point, the KA1wk group (0,54±0,24 seizure.day^{-1}) and KA4wk group (0,33±0,14 seizure.day^{-1}) have a lower frequency only when compared to Bgt (respectively, $p = 6{,}0.10^{-3}$ and $p = 2{,}5.10^{-3}$) and Bsn3 (both, $p < 1{,}0.10^{-4}$).

The severity of the epileptic phenotype, however, is not limited to the frequency of the seizures but it is also defined by their strength. In our case we measured the duration of seizures in each model and compared their average seizure duration, taking into account animals without seizures as null values (Figure 8C).

The seizure duration is different between Ctrl and mutant or injected animals (Two-way ANOVA, Treatment/Genotype nested within Group, $F(7, 77) = 15{,}87$, $p = 1{,}0.10^{-12}$). The direct comparison of the mutants and KA-injected animals led to a significant effect of the

Group variable (excluding Ctrl) on the duration of the seizures ($F(6, 38) = 4,38$, $p = 1,9.10^{-3}$). Unlike the seizure frequency, it is difficult to distinguish a specific group from the others.

The animal group with the highest seizure duration is the Bsn3 group (51,9±6,00s), which has significantly higher values than the B2E only (18,9±11,9, $p = 3,7.10^{-2}$). Following as the second line with the longest seizure duration is the Bsn1 group (43,1±7,36s), then the B2I and Bgt line (35,0±4,95s and 31,9±3,39s respectively). There are no significant differences between any of the Bassoon lines when it comes to seizure duration (with the exception of Bsn3 and B2E), suggesting it is not a value that can easily separate the different Bassoon lines from one another.

The comparison with the KA1wk (9,26±3,37s) and the KA4wk (21,8±8,50s) shows that the Bsn3 has a higher seizure duration (respectively, $p = 2,0.10^{-3}$ and $p = 3,4.10^{-2}$) than the KA models. This is also true for Bsn1 in comparison with KA1wk ($p = 3,0.10^{-2}$) but not KA4wk ($p = 0,15$).

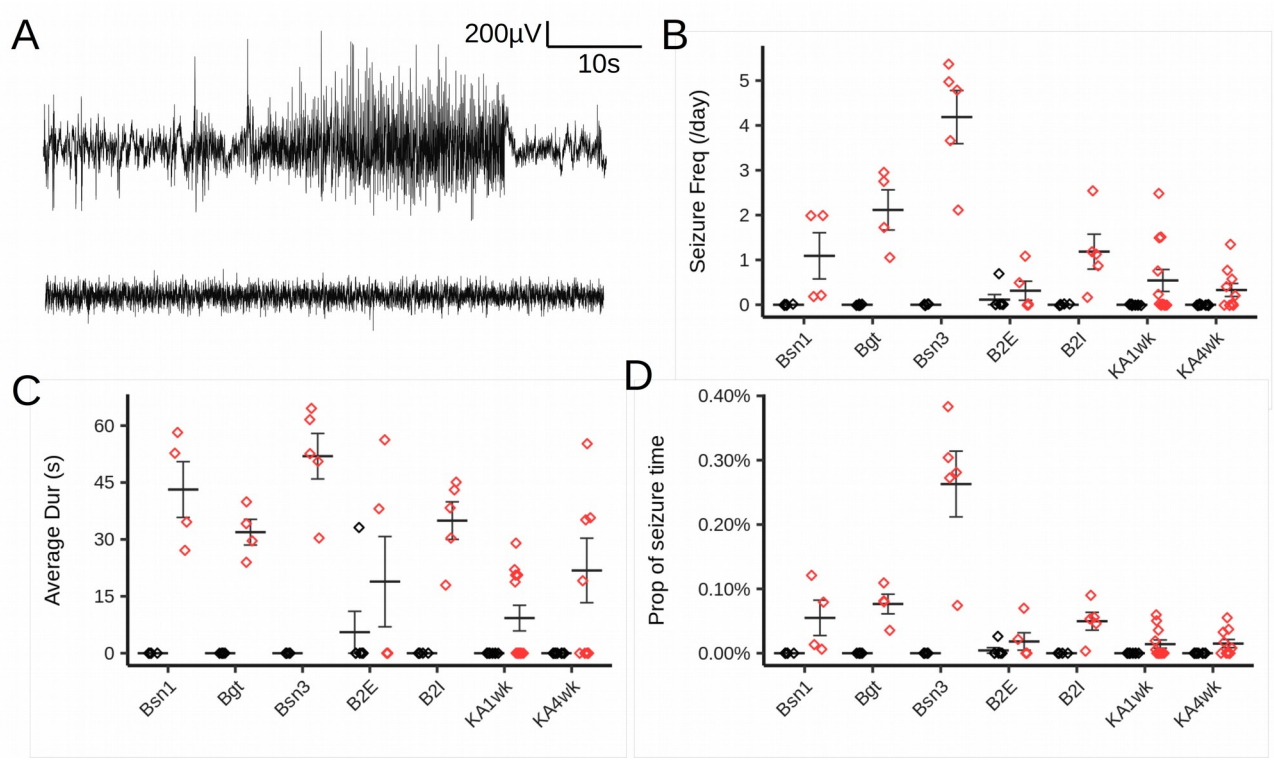

Figure 8: Seizure properties of the different epilepsy models, Bassoon lines and KA-injected animals. (A) Example of the EEG recording from a Bsn3 animal during a seizure (top) and a Ctrl littermate (bottom). (B) Average number of seizure per day in the different epilepsy models. There is a difference between the treated animals and mutants and their respective Ctrl ($F(7, 77) = 25,66$, $p < 2,00.10^{-16}$). (C) Average duration (in s) of seizures in the different epilepsy models. Comparison of Ctrl and treated or mutant animals ($F(7, 77) = 15,87$, $p = 1,00.10^{-12}$). (D) Proportion of the recording time spent in a seizure state (in %). Comparison of Ctrl and treated or mutant animals ($F(7, 77) = 27,41$, $p < 2,00.10^{-16}$). Black points: Ctrl animals; Red points : Bassoon mutants or KA-injected animals.

To take into account both the duration of seizures and their frequency, we calculated the amount of time spent in seizures during the recording period. As not all recordings were exactly the same length, it is normalised as the proportion of recording time spent in seizures (shortened as “time proportion”) (Figure 8D). As for the duration measurements, the animals without seizures were considered to have a null value.

As expected, the Ctrl animals are different from the mutants and injected animals (Two-way ANOVA, Injection/Genotype nested within Group, $F(7,77) = 27,41$, $p = p < 2,00.10^{-16}$) and the Group variable (excluding Ctrl) has an effect on the time proportion ($F(6,38) = 20,53$, $p = 1,51.10^{-10}$).

It appears that only the Bsn3 line is different from the others with a much higher time proportion (0,26%±0,05). This result is expected as the Bsn3 line has both the highest frequency and duration of seizures, leading to a much higher time proportion than the Bgt (0,08%±0,02, $p < 1,0.10^{-4}$), the Bsn1 (0,06%±0,03, $p < 1,0.10^{-4}$), the B2I (0,05%±0,01, $p < 1,0.10^{-4}$) and the B2E (0,02%±0,01, $p < 1,0.10^{-4}$). Interestingly, all the other lines, despite slight differences, do not show any significant differences.

When bringing the KA groups into the picture, both the KA1wk group (0,01%±0,01, $p < 1,0.10^{-4}$) and the KA4wk group (0,02%±0,01, $p = 1,0.10^{-4}$) have a lower time proportion than the Bsn3. The only other group that could have a slightly higher time proportion is the Bgt group, notably when compared to both KA1wk ($p = 7,3.10^{-2}$) and KA4wk ($p = 7,8.10^{-2}$), although this remains a trend.

These findings argue for a much stronger epileptic phenotype of the Bsn3 line. The fact that it experiences longer seizures at a higher rate than most, if not all, of the other groups also shows that a generalised deletion of Bassoon does have a stronger phenotype than only a partial deletion as observed in B2E or B2I. Finally, this analysis brings a new information concerning the strength of the Bassoon mutants’ epilepsy: it is at least as severe as the one observed in the KA model.

IV.4 - Diverse seizure onsets for diverse epilepsy models

The pattern of the EEG recording at the onset of a seizure may be informative on the neuronal networks involved in the seizure generation. Thus, we classified the onset of each seizure in one of the two most described onset types: LVF, an onset based on the synchronicity of inhibitory activity (Elahian et al., 2018), and HYP, an onset based on a failure of the inhibitory network (Köhling et al., 2016) (example of traces in Figure 9A). Our purpose was to decipher whether different network types were involved in the observed seizures. Only animals with more than 3 seizures during the recording period were included in this analysis.

There are no significant differences in the proportion of LVF onsets between the different Bassoon lines. The Bsn3 line has a strong proportion of LVF onsets (83,6±0,06%, n = 5),

similar to the one observed in B2I (68,9±20,0%, n = 4) and Bgt (57,7±15,3%, n = 4). The other Bassoon lines (B2E and Bsn1) do not have enough animals to properly estimate the proportion of either onset in the population (n = 2). An interesting finding is the complete absence of LVF onsets in the KA4wk animals (0,0±0,0%, n = 5), whereas the KA1wk have at least some (34,2±17,8%, n = 4).

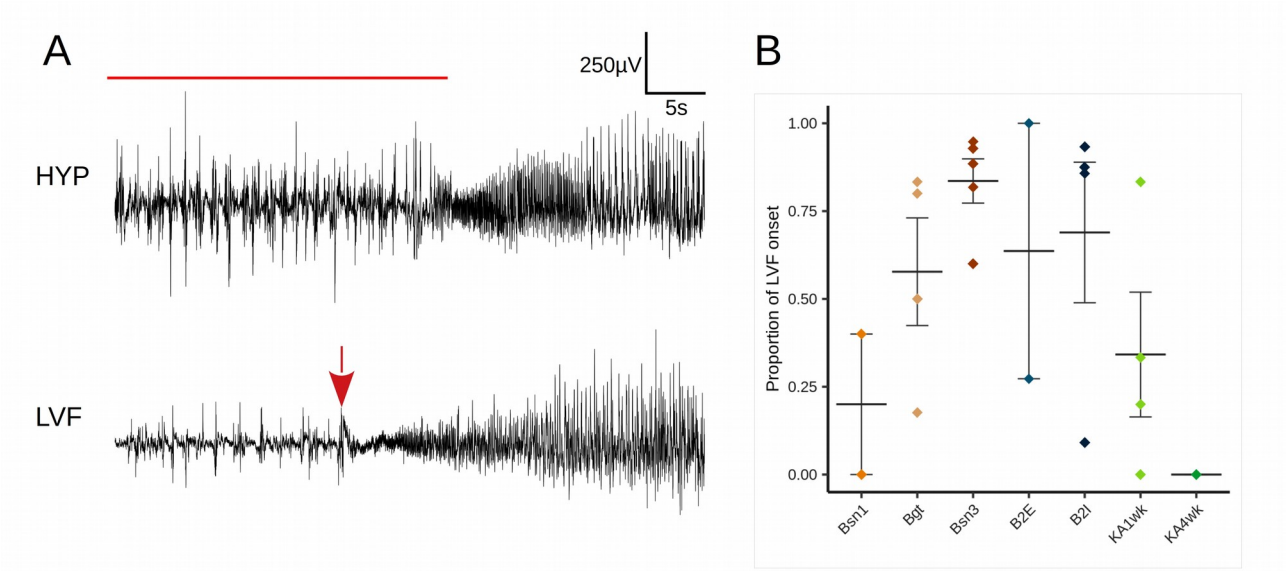

Figure 9: The seizure onsets are different between the epilepsy models. (A) Top – Example of a hypersynchronous (HYP) onset with strong regular spikes leading to the seizure activity, marked by the red line above the EEG signal. Bottom – Example of a low voltage fast (LVF) onset with a low amplitude activity that gradually increases after a sentinel spike at the start of the seizure marked with a red arrow. (B) Plot of the proportion of the LVF type of onset in the animals with at least 3 seizures during the recording period.

In the end, this analysis would require a higher number of animals, although it can already be deduced from this that Bsn3 tends to have a vast majority of LVF onsets, a tendency that is not as marked in the KA1wk (p = 0,11) and significantly lower in the KA4wk group (p = 0,03). A similar tendency is seen between the B2I animals and the KA4wk group (p = 0,08), suggesting a majority of LVF onsets in this line as well. Moreover, the complete lack of LVF onsets in the KA4wk but not in the KA1wk could mark a difference due to the evolution of the epileptic phenotype over the weeks (although not significant).

IV.5 - Differential regulation of the ECM between epilepsy models

To study the involvement of the ECM in the different epilepsy models, we collected the brains of the animals following the EEG recordings and isolated their subcellular fractions. The following three subcellular fractions were analysed for the expression level of different essential proteins of the HA-based ECM: the homogenate fraction (Hom), the soluble fraction (Sol) and the synaptosome fraction (Syn).

The quantified proteins include the main lecticans and their cleaved fragments. So Aggrecan and its 250kDa fragment, Brevican and its 90kDa fragment and finally Neurocan and its 130 and 90kDa fragments were included in the analysis. As no full-length Neurocan could be seen in the synaptosome fraction and the low expression in the homogenate could not be quantified in any reliable way, these were not taken into account. I also included four of the main binding partners of the lecticans, namely HAPLN1, HAPLN4, TnC and TnR. The latter could only be measured in the homogenate fraction, but not subcellular fractions.

Considering the amount of data, a Principal Component Analysis (PCA) was carried out to find the underlying structure of the multiple ECM variables and detect whether or not some of the epileptic models cluster together. It appears that there are no obvious clusters forming away from the Ctrl animal values (Figure 10A).

Although no clear clusters are forming (Figure 10A), some KA-injected animals distinguish themselves from the Bassoon mutants by a high value on the 1^{st} PC (13,9% variance explained). The 2^{nd} PC (10,1% variance explained) easily separates the Bsn3 animals from the others, with the Bsn3 having lower values than any other animal, with the exception of two KA4wk mice. Of note, the KA4wk and constitutive Bassoon mutants (Bsn1, Bgt, Bsn3) tend to have a null or negative value on the 2^{nd} PC, whereas the KA1wk tend to have positive ones. The other PCs do not bring more information concerning possible similarities or differences between the epileptic models in use (data not shown).

The only molecules found to be changed between the mutant/injected animals and the Ctrl ones were lecticans (Figure 10B). The HAPLN1 sees its lowest p-value in the soluble fraction (Two-way ANOVA, Injection/Genotype nested within Group, $F(7, 55) = 1,28$, $p = 0,28$). HAPLN4 follows a similar pattern with the value in the homogenate having the lowest p-value ($F(7, 55) = 1,36$, $p = 0,24$). Concerning the tenascins, TnR is unlikely to see any regulation ($F(7, 55) = 0,31$, $p = 0,95$) and TnC also does not reach significance, with the value in synaptosomes being the one with the lowest p-value ($F(7, 55) = 1,49$, $p = 0,19$).

Coming back to the lecticans and starting with Aggrecan, there is a difference between the Ctrl animals and their injected/mutant counterparts in the soluble fraction (Two-way ANOVA, Injection/Genotype nested within Group, $F(7, 55) = 2,52$, $p = 2,56.10^{-2}$). The regulation of the full-length protein, however, does not seem to affect the amount of the 250kDa fragment of Aggrecan in the same fraction ($F(7, 55) = 1,32$, $p = 0,95$).

The Neurocan has an opposite pattern when compared to Aggrecan. Indeed, the full-length protein is not affected in the soluble fraction (Two-way ANOVA, Injection/Genotype nested within Group, $F(7, 55) = 1,47$, $p = 0,20$), but the 90kDa cleaved-fragment has a marked tendency for a change in the soluble fraction ($F(7, 55) = 1,95$, $p = 7,95.10^{-2}$). This same 90kDa fragment is affected in the homogenate ($F(7, 55) = 4,56$, $p = 4,51.10^{-4}$).

Finally, Brevican is highly regulated as it shows a significant difference between Ctrl and mutants/injected animals in the homogenate (Two-way ANOVA, Injection/Genotype nested within Group, $F(7, 55) = 3,64$, $p = 2,70.10^{-3}$), the soluble fraction ($F(7, 55) = 2,69$, $p = 1,82.10^{-2}$) and the synaptosome ($F(7, 55) = 2,30$, $p = 3,97.10^{-2}$). As for Aggrecan, the regulation seen in the full-length PG does not seem to affect the level of the 90kDa cleaved-fragment in either of the subcellular fractions.

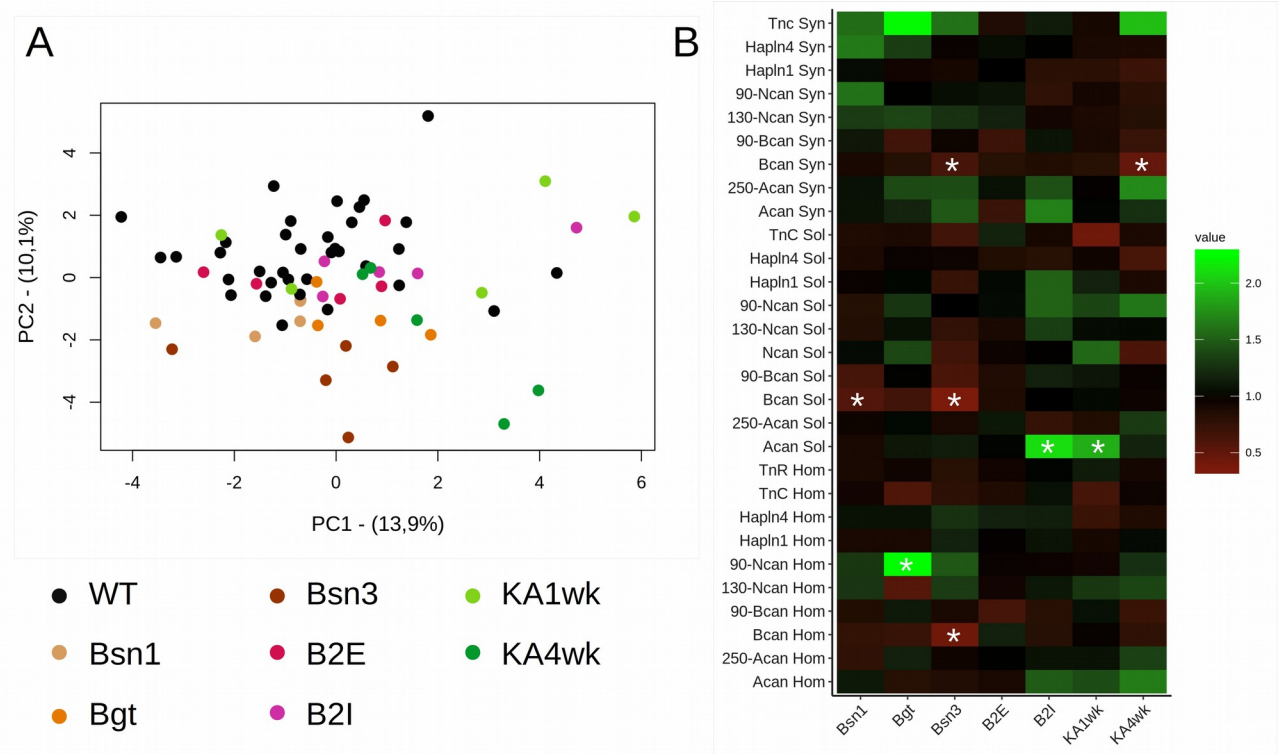

Figure 10: Overview of the regulation of ECM components in the different epilepsy models used. (A) Plot of the first two Principal Components (PCs). No clear cluster appears, nonetheless, the Bsn3 mice consistently show a low value on the second PC along with some KA4wk, but not KA1wk mice. The first PC does not separate any of the groups, although none of the Bassoon mice seem to have values above 2 on this PC, whereas Ctrl as well as KA1wk and KA4wk mice do (and one B2I). (B) Heatmap of the regulation of all the observed ECM components in the different models, normalised to their respective Ctrl. Results with a significant difference when compared to their respective Ctrl are marked with a star (Two-way ANOVA, Injection/Genotype nested within Group).

IV.5.a. - Brevican amounts are consistently lower in the Bsn3 line

Changes in the amount of Brevican were expected as the protein is a target of neuronal plasticity mechanisms (Mitlöhner et al., 2020, Valenzuela et al., 2014). It is important to note, however, that these mechanisms rely on the enzymatic cleavage of Brevican. In our case, no increase in the cleavage product could be detected along with the lower levels of full-length protein, indicating a different type of regulation.

In the homogenate, it appears evident that Bsn3 mice have a much lower expression of Brevican (0,43±0,08) when compared with their Ctrl (1,00±0,14, $p = 3,0.10^{-4}$) (Figure 11A).

This decreased amount of Brevican compared to Ctrl is also observed, albeit as a tendency, in the Bgt line (0,73±0,09, p = 0,09) and the Bsn1 line (0,76±0,08, p = 0,11). Interestingly, the KA4wk animals also have a trend for a decrease in the amount of Brevican (0,77±0,05, p = 0,12) while the KA1wk do not show such a regulation (0,98±0,06, p = 0,89), however the difference between the two KA groups is not significant (p = 0,12). Still, this finding highlights a possible evolution of the ECM state following the course of epilepsy after the injection of KA in the brain.

In the end, the Bsn3 animals distinguish themselves by a lower amount of Brevican in the homogenate when compared to all the other groups (KA1wk ($p = 6{,}0.10^{-4}$), KA4wk ($p = 1{,}8.10^{-2}$), B2E ($p < 1{,}0.10^{-4}$), B2I ($p = 9{,}6.10^{-3}$), Bgt ($p = 4{,}1.10^{-2}$) and Bsn1 ($p = 2{,}8.10^{-2}$)). Of note, with the exception of the KA1wk (p = 0,22), all the groups have a lower amount of Brevican in homogenate than the B2E line, which can be explained by its slightly higher amount (1,15±0,12) when compared to the KA4wk ($p = 1{,}1.10^{-2}$), B2I ($p = 2{,}6.10^{-2}$), Bgt ($p = 9{,}6.10^{-3}$), Bsn1 ($p = 1{,}1.10^{-2}$) and of course Bsn3 groups. Despite this increase, the B2E mice are not considered having a different level of Brevican when compared to their Ctrl littermates (p = 0,31).

In the soluble fraction, Brevican follows a similar pattern to the one observed in the homogenate (Figure 11C). Of note, under normal circumstances, the soluble fraction hosts most of the Brevican produced in the brain. The Bsn3 mice have a much lower amount of Brevican (0,36±0,07) when compared to their Ctrl (1,00±0,26, $p = 1{,}5.10^{-3}$), as well as the other groups (B2I (1,00±0,09, $p = 1{,}5.10^{-3}$), KA1wk (1,03±0,08, $p = 1{,}5.10^{-3}$) and KA4wk (1,03±0,09, $p = 2{,}0.10^{-3}$)). Only one other group has a significantly lower amount of Brevican when compared to their Ctrl: the Bsn1 line (0,58±0,08, p = 0,04), which also has differences with B2I ($p = 3{,}7.10^{-2}$), KA1wk ($p = 2{,}6.10^{-2}$) and KA4wk ($p = 5{,}4.10^{-2}$, tendency). To a lesser extent, the Bgt line has a similar phenotype (0,68±0,03), although it is not marked enough to be statistically distinguishable from the Ctrl (p = 0,12).

Finally, in the synaptosomes, only a subfraction of the total Brevican is found. We observe a similar pattern as for the homogenate and soluble fraction (Figure 11B). The Bsn3 mice (0,64±0,07) have a significantly lower amount of Brevican when compared with their Ctrl mice (1,00±0,08, p = 0,05), albeit not as marked. Surprisingly, the KA4wk group (0,49±0,13) also displays a lower level of Brevican in the synaptosome when compared to their Ctrl (1,00±0,18, $p = 5{,}5.10^{-3}$). Despite this changes in two groups, their magnitude was not sufficient to detect a difference between the different groups (excluding Ctrl animals) (ANOVA, F(6, 26) = 1,31, p = 0,28). This finding suggests that higher numbers would be required to distinguish the differences in the regulation of Brevican amounts at the synapse between the epilepsy models.

In conclusion, the constitutive mutants for Bassoon seem to have reduced Brevican levels. More specifically, the Bsn3 mice have a much lower amount of Brevican in both soluble fraction and synaptosomes, as well as overall in the homogenate. This comes as

an interesting parallel to its epileptic phenotype, also the strongest among the different models in use in this thesis. It is interesting to point out that KA4wk has a lower Brevican level in the synaptosomes which is not a difference that appears in the KA1wk group, at an earlier time point (Figure 11B).

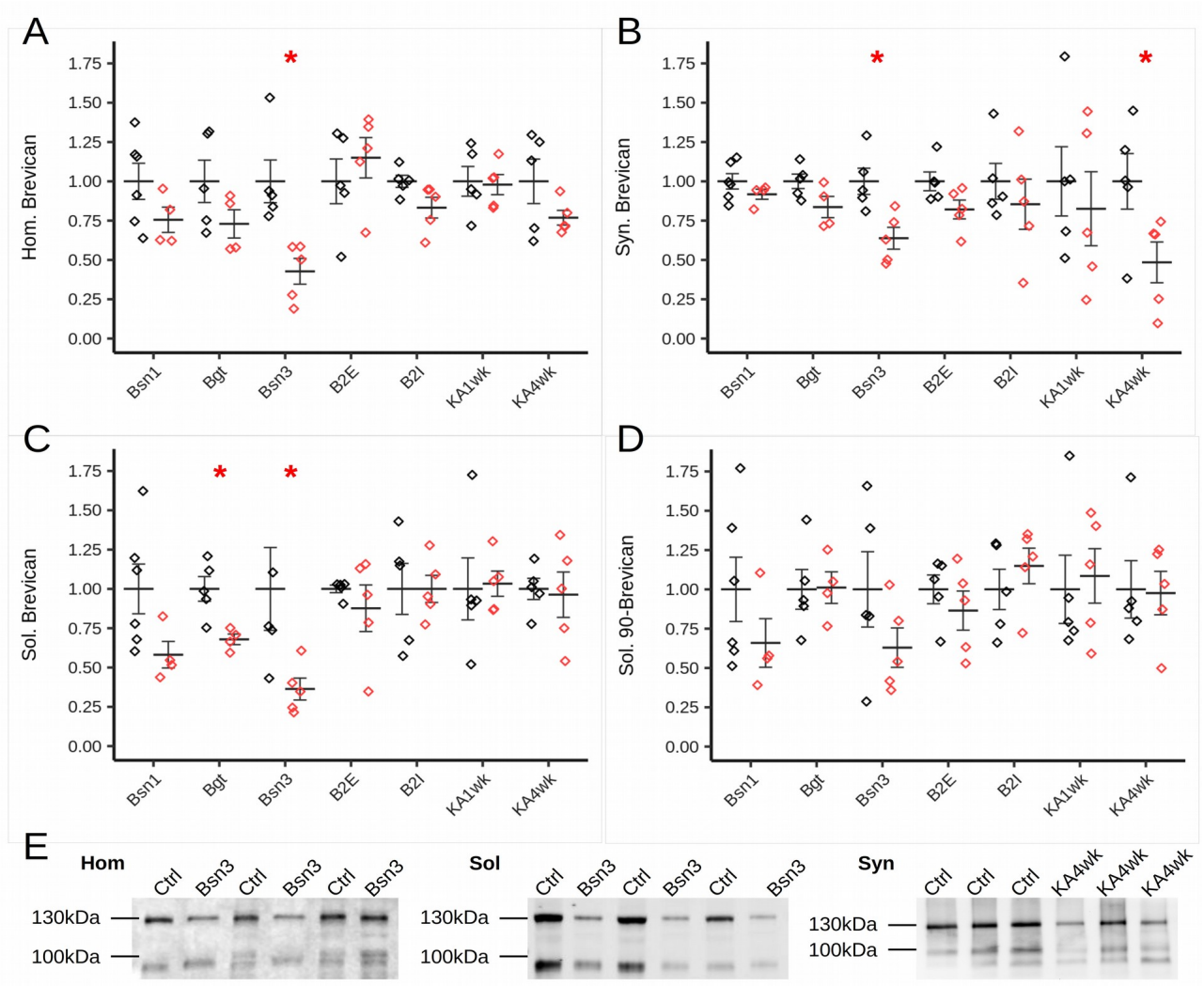

Figure 11: Levels of Brevican in the different subcellular fractions of the Bassoon lines and KA-injected animals with their respective Ctrl. A significant difference between Ctrl (black) and mutant/ injected animal (red) is marked by a red star. (A) Brevican amount in the homogenate fraction (Hom), with a marked decrease for Bsn3 mice ($p = 3{,}0.10^{-4}$) and a tendency for Bsn1, Bgt, KA4wk mice. (B) Brevican amount in the synaptosome fraction (Syn). Bsn3 mice have a lower expression ($p = 0{,}05$), this time also observed in the KA4wk animals ($p = 5{,}5.10^{-3}$). (C) Brevican amount in the soluble fraction (Sol) with Bsn3 ($p = 1{,}5.10^{-3}$) and Bsn1 mice ($p = 3{,}7.10^{-2}$) having a lower amount, and a tendency for less Brevican in Bgt animals. In this fraction, KA4wk mice does not show any decrease. (D) Amount of 90kDa cleaved-fragment of Brevican in the soluble fraction. There is a tendency for lesser amounts in Bsn1 and Bsn3 mice but none are significant. (E) Examples of Brevican blots (from left to right) in the homogenate and soluble fraction of Bsn3 mice and in the synaptosomes of KA4wk mice. Black points: Ctrl animals; Red points : Bassoon mutants or KA-injected animals.

IV.5.b. - Increase in soluble Aggrecan in the B2I and KA1wk animals

Among the regulated lecticans, it appears that there is a difference between the Ctrl and mutant/injected animals in the amount of Aggrecan in the soluble fraction ($F(7, 55) = 2,52$, $p = 2,56.10^{-2}$). The differences detected with the Ctrl animals, however, are not strong enough to be able to statistically distinguish the epilepsy models from one another ($F(6, 26) = 1,16$, $p = 0,36$).

Aggrecan is first and foremost known for its role as a component of the PNNs around interneurons, which are severely affected in epilepsy (Rankin-Gee et al., 2015). The components of the PNNs are tethered to the membrane and would not appear in the soluble fraction. The regulation of Aggrecan in the soluble fraction is a novel observation that links Aggrecan to epilepsy, not as a part of the PNN, but as a soluble PG (Figure 12A).

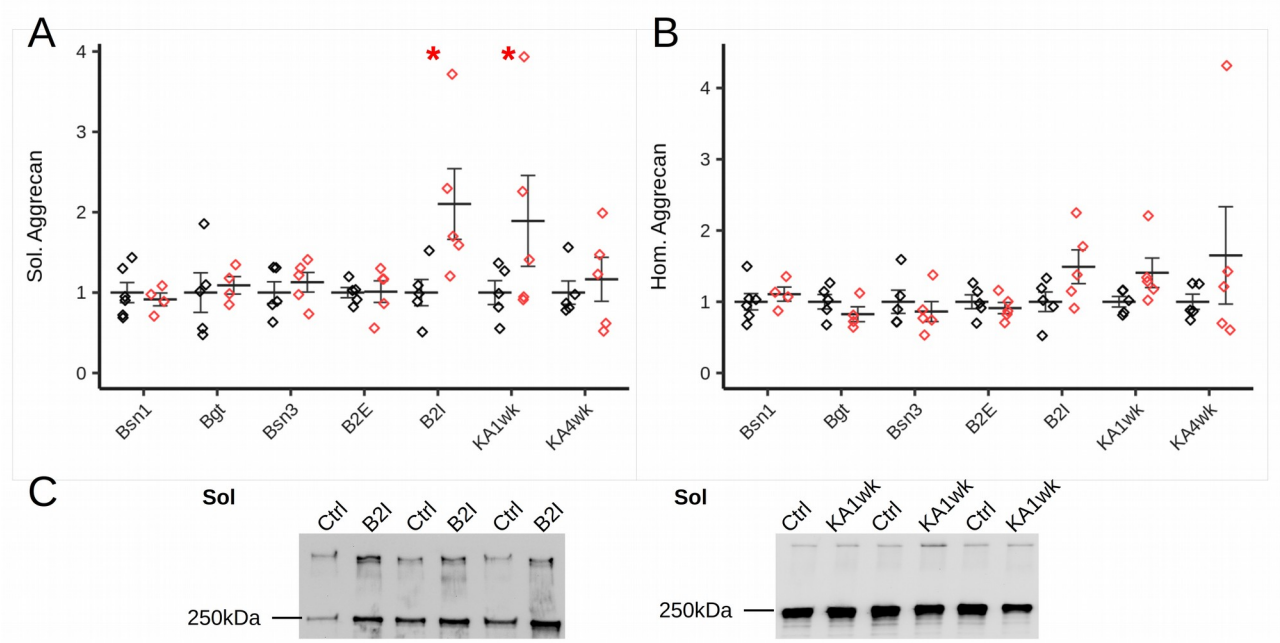

Figure 12: Amounts of Aggrecan in (A) soluble fraction and (B) homogeante. (A) Amount of Aggrecan in the soluble fraction (Sol). The B2I and KA1wk mice have a significantly higher amount compared to their Ctrl ($p = 2,2.10^{-3}$, and $p = 1,2.10^{-2}$ respectively, marked by a red star) while no other group has a significant difference. (B) Amount of Aggrecan in the homogenate. There are no detected changes in any group (Two-way ANOVA, Injection/Genotype nested within Groups, $F(7, 55) = 1,24$, $p = 0,30$). (C) Examples of blots for Aggrecan levels (from left to right) in the soluble fraction of B2I mice and of KA1wk mice. Black points: Ctrl animals; Red points : Bassoon mutants or KA-injected animals.

Only two lines have higher amounts of soluble Aggrecan compared with their respective Ctrl (Figure 12A). The KA1wk animals have higher levels of Aggrecan ($1,89 \pm 0,57$, $p = 1,2.10^{-2}$) comparable to the one observed in the B2I animals ($2,10 \pm 0,44$, $p = 2,2.10^{-3}$).

None of the other models depart from the values of their respective Ctrl, including the KA4wk group, which suggest an evolution of the ECM from the KA1wk to the KA4wk.

In the end, the B2I line has a strong up-regulation of Aggrecan in the soluble fraction. No other model has a comparable phenotype, except for the KA1wk animals but not KA4wk. This raises a question concerning the possible importance of soluble Aggrecan, away from PNNs. Moreover, the overall level of Aggrecan, in the homogenate (Figure 12B), does not seem to be affected in any group (Two-way ANOVA, Injection/Genotype nested within Groups, $F(7, 55) = 1,24$, $p = 0,30$), a finding that suggests a shift of Aggrecan into the soluble fraction rather than the production of more Aggrecan overall.

IV.5.c. - The Bgt line has higher levels of the 90kDa Neurocan fragment

Neurocan is a PG associated to a juvenile ECM supporting the brain development (Krishnaswamy et al., 2019). The amount of Neurocan in the adult ECM is limited and the cleaved fragments are much more preponderant. In the different epilepsy models of this study, it appears that there is a regulation of the 90kDa Neurocan fragment in homogenate (Two-way ANOVA, Injection/Genotype nested within Group, $F(7, 77) = 4,56$, $p = 4,51.10^{-4}$, Figure 13A), but not of the 130kDa ($F(7,77) = 1,59$, $p = 0,16$, Figure 13B). Furthermore, the amount of 90kDa Neurocan is different between groups ($F(6, 26) = 5,68$, $p = 7,04.10^{-4}$).

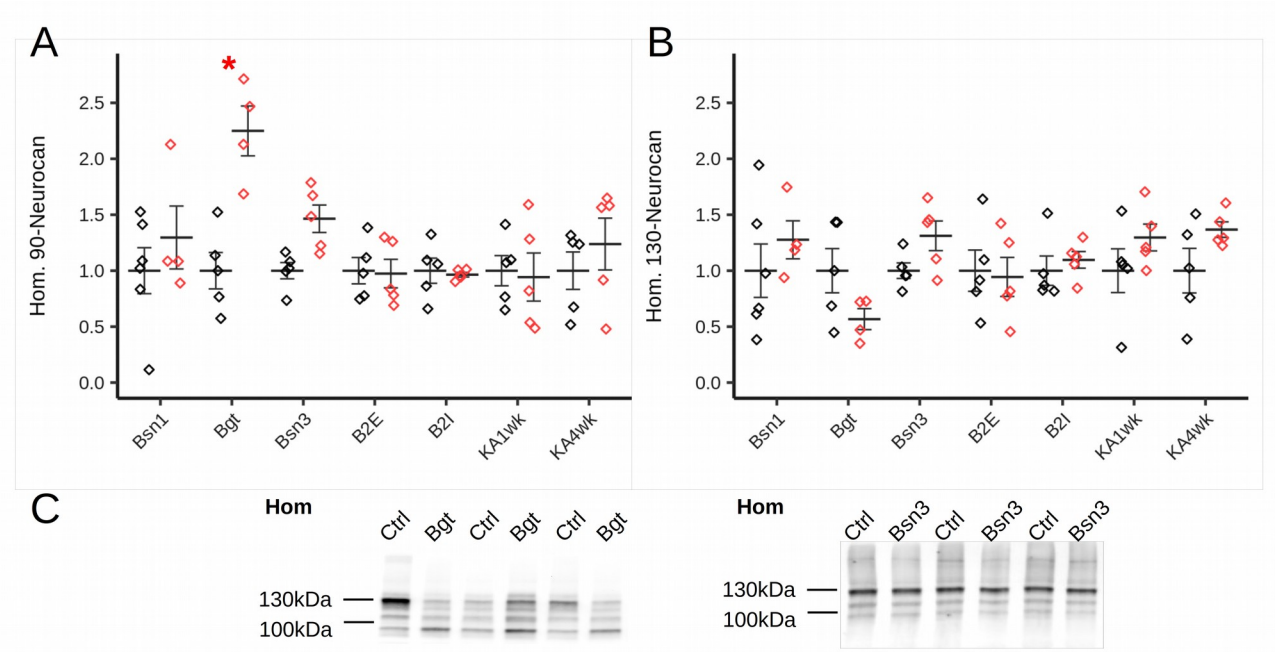

Figure 13: Amounts in the homogenate fraction of (A) the 90kDa cleaved-fragment of Neurocan and (B) of the 130kDa cleaved-fragment of Neurocan. (A) The Bgt line has a much higher level of 90kDa Neurocan than its Ctrl ($p = 1{,}0.10^{-4}$), a finding that extends to the Bsn3 line as a tendency ($p = 5{,}2.10^{-2}$). (B) The 130kDa Neurocan does not display any significant difference between the epileptic animals and their respective Ctrl ($F(7,55) = 1{,}59$, $p = 0{,}16$), unlike the 90kDa fragment. (C) Examples of Neurocan blots (from left to right) of homogenate fraction in Bgt animals and Bsn3 animals. Black points: Ctrl animals; Red points : Bassoon mutants or KA-injected animals.

The only group that displays a changed amount of 90kDa Neurocan in homogenate is the Bgt line (2,25±0,22) when compared to its Ctrl (1,00±0,16, $p = 1{,}0.10^{-4}$). It also has a higher 90kDa Neurocan level when compared to all the other models: B2E (0,97±0,13, $p = 5{,}0.10^{-4}$), B2I (0,96±0,02, $p = 5{,}0.10^{-4}$), Bsn1 (1,30±0,28, $p = 1{,}0.10^{-2}$), Bsn3 (1,46±0,12, $p = 2{,}5.10^{-2}$) and also the KA1wk (0,94±0,22, $p = 5{,}0.10^{-4}$) and KA4wk models (1,24±0,23, $p = 4{,}6.10^{-3}$).

Although the Bsn3 has a slight increase in 90kDa Neurocan in homogenate (1,46±0,12), it did not reach a significant level when compared to its Ctrl ($p = 5{,}24.10^{-2}$). Furthermore, its marked lower levels when compared with the Bgt line suggests that the effect in the Bsn3 line is milder, if it exists at all.

This increase in the 90kDa cleaved fragment of Neurocan in the Bgt mice is not seen in either of the soluble fraction (1,28±0,11, not shown) nor the synaptosomes (1,00±0,16, not shown). This means that the change happens away from the synapse and the soluble ECM, probably on a structure attached to the membrane, such as PNNs or the ECM at the nodes of Ranvier.

It is important to note that, although the total amount of the 130kDa fragment in homogenate is not significantly lower in the Bgt line (Figure 13B), it shows a strong

tendency for a down-regulation of this specific cleavage product (0.57±0.09), which is not the case in the other two constitutive Bassoon mutants (Bsn1 (1.28±0.17), Bsn3 (1.31±0.13)). These results were not further investigated due to the lack of significance of the ANOVA. Nevertheless, they are a hint towards a differential regulation of the two Neurocan cleaved fragments.

IV.6 - Brevican levels negatively correlates with seizure properties in the Bassoon lines

To further our understanding of the dynamics of the ECM in epilepsy, we ran a correlation analysis (Spearman's correlation) between the individual EEG data extracted from the recordings and the data of the immunoreactivity levels of ECM molecules in the brain fractions of the same animals. Based on these results we could link distinct the amount of distinct ECM molecules to the frequency of seizures, their average length and the proportion of time during the recording spent in seizures. Each subcellular fraction has been evaluated separately from the others as they contain information about different parts of the ECM and the Western Blot experimental design did not allow for proper comparison of the fractions between themselves.

The correlation matrices are also separated between the Bassoon mutants and the KA-injected animals. Our purpose here is to decipher the possible differences between the two types of models in the regulation of their HA-based ECM. Of note, the KA correlation matrix includes less animals (n = 20) than the Bassoon mutant correlation matrix (n = 49) and the range of values of the seizure properties is smaller in the KA matrix, especially due to the low amount of animals with seizures present in the correlation analysis for the KA-injected animals (n = 4) in comparison to the Bassoon mutants (n = 21).

First of all, the strongest correlations are in between the seizure properties (Figure 14). The duration and frequency have a 0,95 correlation coefficient while duration and time proportion have 0,96, and time proportion and frequency 0,99 (all $p < 2{,}0.10^{-16}$). Such a link shows that the animals with the highest number of seizures also tend to have the longest ones. It reinforces the idea that a neuronal network prone to seizures affects both the frequency at which seizures are triggered in the brain and the likelihood to maintain the brain in an ictal state for a longer period of time. As for the correlations between ECM components and the seizure properties, only two candidates were found in the homogenate (Figure 14A & B).

In the Bassoon animals, the full-length Brevican levels correlate negatively with the seizure length ($r = -0{,}44$, $p = 1{,}65.10^{-2}$), as well as seizure frequency ($r = -0{,}51$, $p = 2{,}97.10^{-3}$) and time proportion ($r = -0{,}51$, $p = 2{,}97.10^{-3}$) (Figure 15A). This is not the case in the KA-injected models of epilepsy (Figure 14B).

The other candidate is the 90kDa fragment of Neurocan (Figure 15B). As for Brevican, it correlates with seizure length ($r = 0,40$, $p = 3,78.10^{-2}$), seizure frequency ($r = 0,44$, $p = 1,65.10^{-2}$) and time proportion ($r = 0,43$, $p = 1,65.10^{-2}$). This PG fragment has a positive correlation with the seizures, suggesting a stronger epileptic phenotype results in a higher rate of cleavage of the Neurocan core protein into the 90kDa fragment, or it increases the stability of the cleaved fragment. Since the 130kDa fragment gets cleaved into the 90kDa fragment (Rauch et al., 2001), one would expect a down-regulation of the 130kDa fragment going along with this cleavage up-regulation, however, there are no significant correlation between the two cleaved fragments in either of the Bassoon line matrix or the KA model matrix.

Interestingly, the correlation between Brevican and the seizure properties is conserved also in the soluble fraction for the Bassoon matrix (Figure 14C, Figure 15C): seizure length ($r = -0,50$, $p = 2,33.10^{-3}$), seizure frequency ($r = -0,55$, $p = 5,08.10^{-4}$) and time proportion ($r = -0,56$, $p = 5,08.10^{-4}$). The values of the correlation factor are even higher in this fraction than in the homogenate, suggesting the pool of soluble Brevican has a stronger link with seizures than the overall level.

Finally, in the synaptosomes (Figure 14E, Figure 15D), the amount of Brevican is also correlated with seizure length ($r = -0,55$, $p = 6,71.10^{-4}$), seizure frequency ($r = -0,52$, $p = 1,43.10^{-3}$) and time proportion ($r = -0,52$, $p = 1,43.10^{-3}$). As for the soluble fraction, it appears as though the correlation in synaptosome is stronger than in homogenate.

In addition to Brevican, Aggrecan in its full-length form in synaptosomes correlates with seizure length ($r = 0,35$, $p = 4,12.10^{-2}$), seizure frequency ($r = 0,39$, $p = 2,65.10^{-2}$) and time proportion ($r = 0,38$, $p = 2,74.10^{-2}$) (Figure 15E & F). The 250kDa cleaved fragment of Aggrecan also correlates with seizure length ($r = 0,39$, $p = 2,65.10^{-2}$), seizure frequency ($r = 0,46$, $p = 6,64.10^{-3}$) and time proportion ($r = 0,46$, $p = 7,46.10^{-3}$), with slightly higher correlation coefficients than the full-length PG. This finding is exciting as the function of Aggrecan at the synapse is not often considered although it seems some plasticity mechanisms do lead to its cleavage around the synapse (*e.g.* Mitlöhner et al., 2020). The positive correlation suggest that higher amounts of Aggrecan are concomitant with a higher epileptic phenotype.

Of note, in the case of the synaptosomes in the Bassoon animals, the 130kDa fragment of Neurocan could be related to seizure properties. Indeed, there is a trend between the 130kDa fragment and the time proportion ($r = 0,31$, $p = 0,09$). On the other hand, the smaller 90kDa Neurocan does not have any correlation with seizure properties.

To conclude about the correlations between seizure properties and ECM components, each fraction has its specifics. A major point to be made is that the lecticans are the only ones with strong correlations to the seizure properties. The 90kDa fragment of Neurocan is of some importance in the homogenate (Figure 14A, Figure 15B) while Aggrecan and its

main 250kDa fragment correlate with seizure properties in synaptosomes only (Figure 14E, Figure 15E & F). Brevican, nevertheless, remains the main finding as it shows a strong and reliable negative correlation with all of the seizure properties in all the different fractions of the Bassoon animals (Figure 14A, C & E, Figure 15A, C & D). It is important to note that only the full-length PG is involved in this correlation and not the 90kDa cleaved fragment of Brevican.

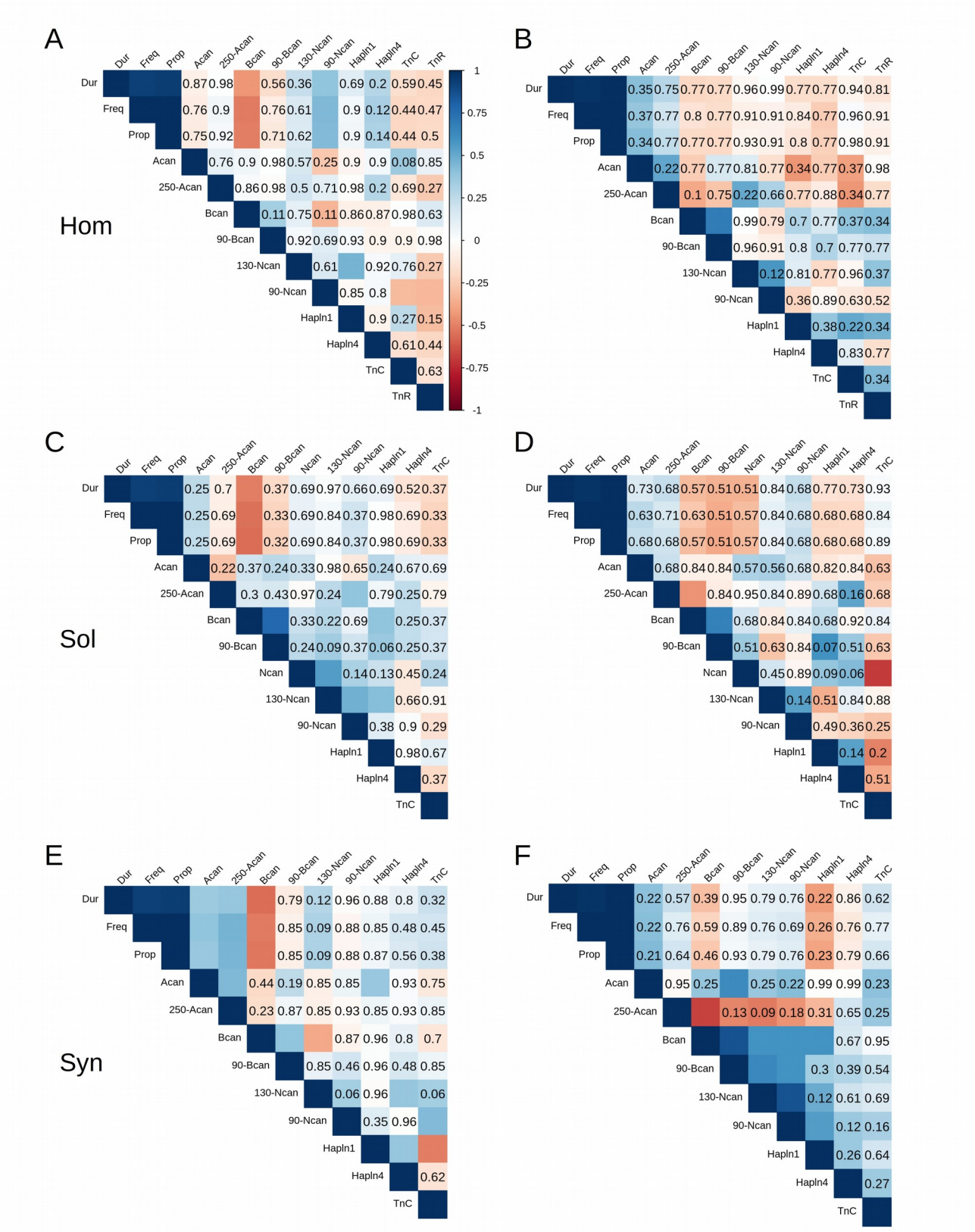

Figure 14: Spearman's correlation matrices of the ECM component levels and seizure properties in each of the 3 subcellular fraction (homogenate, A, B; soluble fraction, C, D; synaptosomes, E, F) for the batch of Bassoon animals (A, C, E) and KA-injected animals (B, D, F) (including Ctrl). P-values of non-significant correlations (p > 0,05) are written in the adequate square while significant ones are left without.

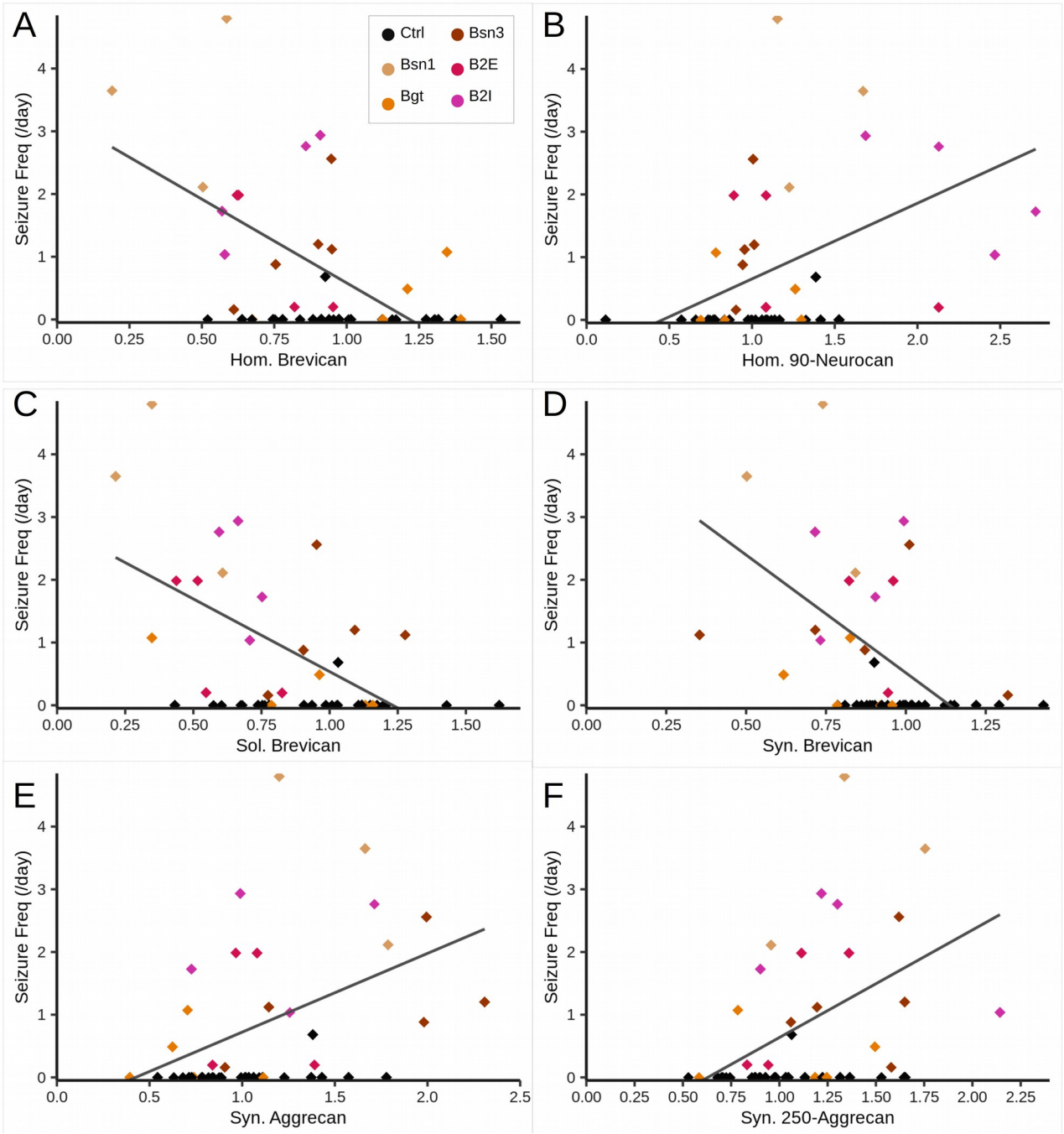

Figure 15: Scatterplots of significant correlations between seizure frequency (y-axis) and ECM components in the Bassoon animals. Correlation of seizure frequency with (A) Brevican in homogenate (r = -0,51, p = 2,9.10^{-3}); (B) 90kDa cleaved fragment of Neurocan in homogenate (r = 0,44, p = 0,02); (C) Brevican in soluble fraction (r = -0,55, p = 5,1.10^{-4}); (D) Brevican in synaptosomes (r = -0,52, p = 1,4.10^{-3}); (E) Aggrecan in synaptosomes (r = 0,39, p = 0,03); (F) 250kDa cleaved fragment of Aggrecan in synaptosomes (r = 0,46, p = 6,6.10^{-3}).

IV.7 - ECM component amounts are co-regulated differently in KA and Bassoon epilepsy models

Apart from the information brought by correlations between ECM components and seizure properties, the correlation matrices also highlight patterns of co-regulations of ECM components. These correlations are to be interpreted carefully as they come from two groups of epileptic animals based on two distinct model types. This analysis deciphers the similarities and differences in the matrix regulations between the two model types.

IV.7.a. - Correlation of the full-length Brevican with its cleaved fragment

First of all, there are only two significant correlations in common between the two matrices (Figure 16A, B), it is the positive correlation of full-length Brevican with its 90kDa cleaved fragment in the soluble fraction (Bassoon, r = 0,77, p = $1,65.10^{-9}$; KA, r = 0,67, p = 0,02) and in synaptosomes (Bassoon, r = 0,40, p = 0,03; KA, r = 0,87, p = $9,56.10^{-6}$). In both models the presence of more Brevican leads to an increase in the amount of its 90kDa cleaved fragment, and this tendency could be extended to the homogenate (Bassoon, r = 0,34, p = 0,11; KA, r = 0,69, p < $2,0.10^{-16}$), although in this last case the correlation in the Bassoon matrix does not reach a significant level.

IV.7.b. - The correlation between full-length Brevican and 130kDa Neurocan is negative in the Bassoon group and positive in the KA-injected group

The most striking difference between the KA and Bassoon matrices comes from the synaptosomal fraction (Figure 16C, D). While in the Bassoon matrix, the correlation between Brevican and the 130kDa cleaved fragment of Neurocan is negative (r = -0,37, p = 0,03), it is a positive one for the KA matrix (r = 0,59, p = 0,03). This could be due to the mutation of Bassoon, as most mutants appear to have a lower amount of Brevican compared to their Ctrl and a slightly higher amount of 130kDa fragment of Neurocan (Figure 10). However, it could also mean that the injection of a substance in the brain, independently of the injected substance (whether KA or saline in our case), brings about a different regulation of the ECM.

IV.7.c. - Tenascins and HAPLNs correlate with different ECM components in the Bassoon and KA-injected groups

There are a few more differences in between the Bassoon and KA matrices concerning significant correlations. Without going into all the possible correlations, there are a few others that reinforce the idea of differential regulations between the two types of epilepsy model.

To begin with, in the Bassoon matrix for the homogenate fraction, the 90kDa Neurocan fragment is correlated with TnR (r = -0,32, p = $2,65.10^{-2}$) and TnC as well (r = -0,32, p = $2,34.10^{-2}$) (Figure 14A). It could mean that the cleavage of Neurocan into its smaller

90kDa fragment impacts negatively the amount of tenascins in the Bassoon mutants, or that a lower amount of tenascins leads to higher cleavage of Neurocan. In parallel, such correlations are not as strong in the KA matrix (Figure 14B) and do not lead to any significant result.

Instead, the KA matrix for the soluble fraction shows a strong negative correlation between full-length Neurocan and TnC ($r = -0,69$, $p = 2,65.10^{-2}$) (Figure 14D). Lower amounts of Neurocan would imply higher amounts of TnC according to the KA matrix, a surprising finding as TnC and Neurocan are both elements of the juvenile ECM and are expected to be co-regulated in the same way (Krishnaswamy et al., 2019). In the Bassoon matrix for soluble fraction, this correlation does not reach significance (Figure 14C).

Finally, in the synaptosomal fraction of the Bassoon groups, the full-length Aggrecan correlates with HAPLN1 ($r = 0,38$, $p = 2,74.10^{-2}$) (Figure 14E, Figure 16E). This interaction is expected as HAPLN1 and Aggrecan interact in the PNNs (Giamanco et al., 2010). However, in synaptosomes, this interaction was not reported and it is interesting to point out that in the KA matrix for synaptosomal fraction, Brevican, instead of Aggrecan, correlates with HAPLN1 ($r = 0,60$, $p = 3,28.10^{-2}$) (Figure 14F, Figure 16F).

It could be that the different epilepsy models, Bassoon deficient mutants and KA-injected animals, lead to the preferential formation of different ECM complexes. The correlations differ between the two model types and this in synaptosome, soluble fraction and homogenate fraction. These differences highlight a possible shift in the ECM structure, with different affinities between ECM components. The mechanisms behind may be as simple as a regulation of the amount of the different components to prioritise one interaction over another (Figure 10), or more complex, including post-translational modifications or a relocalisation of pre-existent ECM components to a new fraction.

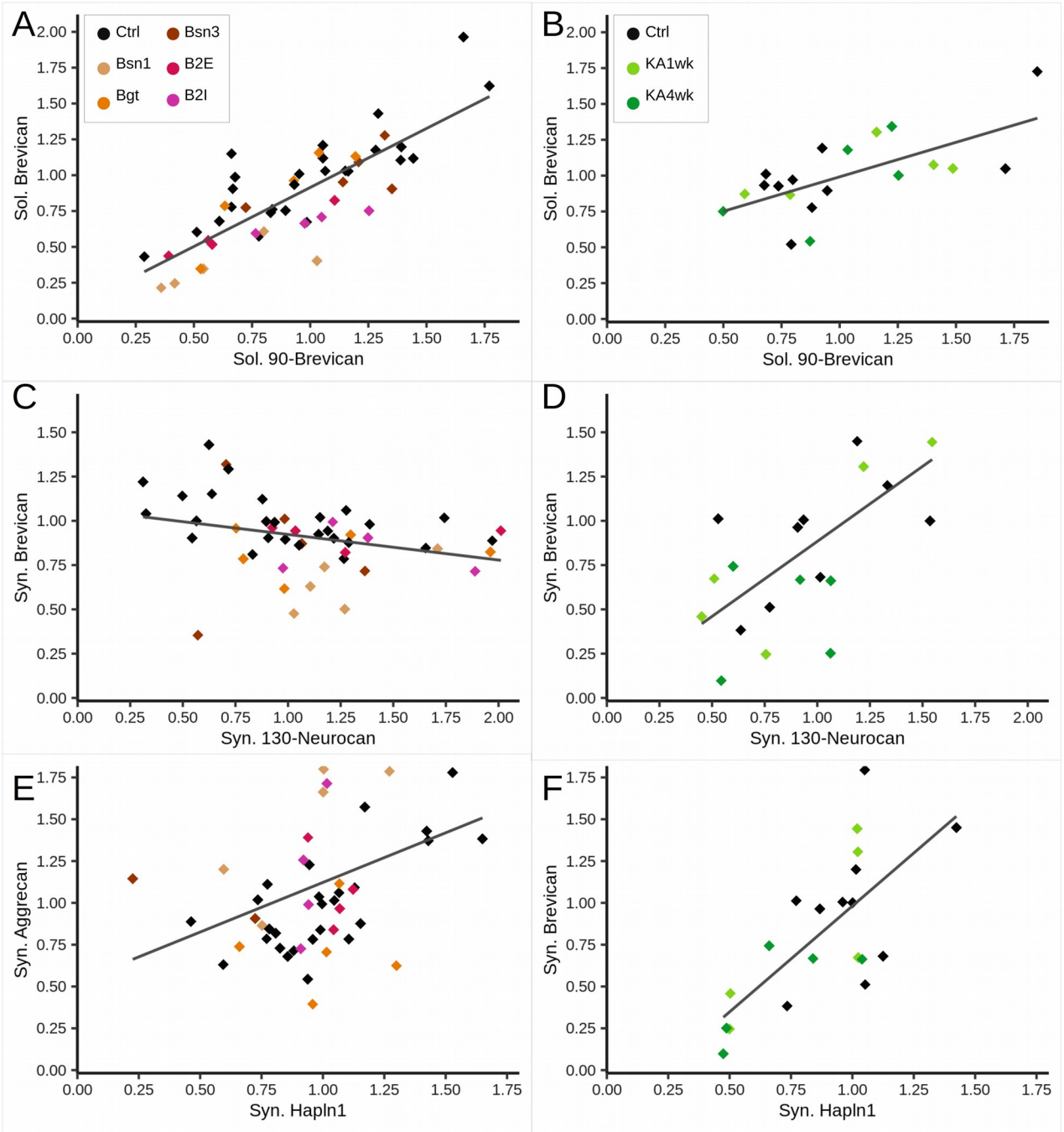

Figure 16: Scatterplots of significant correlations in between ECM components in Bassoon groups (A, C, E) and KA groups (B, D, F). (A) Correlation of Brevican and 90kDa fragment of Brevican in the soluble fraction of Bassoon groups (r = 0,77, p = 1,6.10^{-9}); (B) Correlation of Brevican and 90kDa fragment of Brevican in the soluble fraction of KA groups (r = 0,67, p = 0,02); (C) Correlation of Brevican and 130kDa fragment of Neurocan in synaptosomes of Bassoon groups (r = -0,37, p = 0,03); (D) Correlation of Brevican and 130kDa fragment of Neurocan in synaptosomes of KA groups (r = 0,59, p = 0,03); (E) Correlation of Aggrecan and HAPLN1 in synaptosomes of Bassoon groups (r = 0,38, p = 0,03); (F) Correlation of Brevican and HAPLN1 in synaptosome of KA groups (r = 0,60, p = 0,03).

IV.8 - The membrane fractions of Bsn3 and B2I mouse hippocampi contains increased CD44 levels

In order to identify protein changes in the hippocampus of Bassoon animals (Bsn3, B2E & B2I with Bsn2 as the Ctrl), a proteomics analysis of the membrane fraction samples (referred as P2, see III.12) was carried out. Out of 4273 proteins detected in this fraction, there were a few differentially regulated proteins in the Bassoon mutants (n = 105, see appendix 1).

A

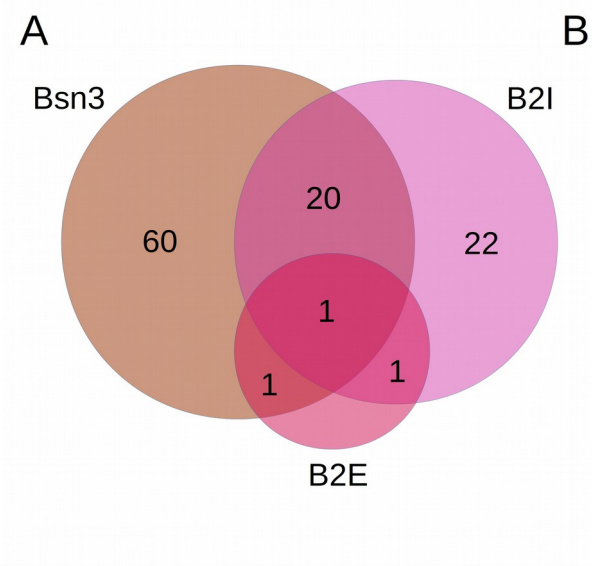

B

Gene Name	Regulated in			Reference
	Bsn3	B2I	B2E	
IGHV1	**Down**	**Down**	**Down**	-
Bassoon	**Down**	-	**Down**	Ghiglieri et al., 2009
CD44	**Up**	**Up**	-	Borges et al., 2004
BDNF	**Up**	**Up**	-	Lin et al., 2020
GFAP	**Up**	**Up**	-	Robel et al., 2016
CD34	**Down**	**Down**	-	Huse et al., 2017
PLGRKT	-	**Up**	-	-
Kir 2.3	**Down**	-	-	Xu et al., 2013
Kca 4.2	**Up**	-	-	Ambrosino et al., 2018
GAD65	**Up**	-	-	Kakizaki et al., 2021

Figure 17: The B2I and Bsn3 animals have some regulations compared to Bsn2 animals in common in the membrane fraction of the hippocampus. (A) Venn diagram of the hit proteins in the 3 Bassoon lines in comparison to Bsn2 animals. The B2E animals have only 3 strongly regulated proteins, among which 1 in common with B2I and Bsn3. Bsn3 and B2I share 21 proteins in common. (B) Table of some proteins of interest and their associated regulations in the Bassoon lines, with a publication linking the protein to an epileptic phenotype. Only significant regulations are noted.

The protein in common between all models is the IGHV1 immunoglobulin heavy variable (Figure 17A & B). It does not seem to have any link to an epileptic phenotype, but it is consistently down-regulated in all the Bassoon mutants.

As expected, Bassoon is down-regulated, a result that does not reach significance in the B2I as only the interneurons are affected, which represent a minor part (10-15%) of the total amount of neurons, and thus contribute only a minor fraction to total Bassoon (Figure 17B).

One protein of high interest among the hits is the CD44 protein, a receptor of HA at the cell membrane that modulates synaptic plasticity (Roszkowska et al., 2016, Skupien et al., 2014). This protein is up-regulated in B2I animals (2,50 fold, $p = 1{,}20.10^{-3}$) and in Bsn3 (2,03 fold, $p = 2{,}31.10^{-3}$) but not in B2E animals (1,00 fold, p = 0,99) (Figure 17B).

Interestingly, the two lines with stronger epileptic phenotypes have a higher level of CD44 in the hippocampus compared to their Ctrl, whereas B2E animals, which are not all epileptic, have a normal level of this protein.

Of note, the novel plasminogen receptor Plg-RKT (PLGRKT), a known MMP2 and MMP9 activator (Lighvani et al., 2011, Miles et al., 2020), was found to be up-regulated in the B2I line (1,53 fold, $p = 9{,}98.10^{-3}$) and it has a similar trend in Bsn3 animals (1,31 fold, $p = 3{,}61.10^{-2}$), but once more not in the B2E animals (0,91 fold, p = 0,89) (Figure 17B). This suggests ECM regulations might be higher in the Bsn3 and B2I lines when compared to their Ctrl or B2E.

Along with the ECM receptors, other types of proteins linked to epileptic phenotypes are regulated in the Bassoon lines. BDNF is up-regulated in both Bsn3 animals (3,12 fold, $p = 6{,}97.10^{-5}$) and B2I animals (2,02 fold, $p = 2{,}70.10^{-3}$), showing that these two lines have a phenotype similar to the one already observed in Bsn1 animals (Dieni et al., 2012, Heyden et al., 2011) (Figure 17B). BDNF is an important target for the regulation of neuronal activity and proliferation, functions which are affected in epilepsy (Lin et al., 2020).

In a parallel to other epilepsy models, the level of GFAP was found to be increased in the Bsn3 line (1,99 fold, $p = 2{,}02.10^{-3}$) and the B2I line (1,36 fold, $p = 9{,}71.10^{-2}$) (Figure 17B).This increase is a mark of astrocytic activation (Robel et al., 2016), which in turn could affect the level of ECM components produced by the astrocytes (Zhang et al., 2014). Moreover, the astrocytic activation is a hallmark of the epileptic phenotype (Robel et al., 2016).

Finally, a major finding at the level of the synapse is the regulation of GAD65, the enzyme producing the neurotransmitter GABA. It displays an increase in Bsn3 mice (1,73 fold, $p = 3{,}26.10^{-2}$) but no such regulation in B2E (0,76-fold, p = 0,75) nor B2I mice (1,08-fold, p = 0,82) (Figure 17B). This increase in the amount of the GABA producing enzyme could explain the amount of LVF onsets (Figure 9), considering there could be a higher inhibitory drive with more GABA produced.

IV.9 - Higher expression of ECM markers in the dentate gyrus of the Bsn3 mutants

The hippocampus is a central hub for seizures and we wanted to have a more precise overview of its ECM and which changes epilepsy brings to it. A comparison of the animals from the Bassoon line with the strongest epileptic phenotype (*i.e.* the Bsn3 line) to their Ctrl littermates showed a clear difference in the expression of some markers of the ECM.

The markers considered in this experiment were markers of the CS side chains. The WFA marker binds to a free GalNAc on the CS, whereas the CS-56 antibody recognises a specific pattern comprising CS-A (4-O sulphation on GalNAc), followed by CS-D (6-O

sulphation on GalNAc, 2-O sulphation on GlcA) (see I.3.a, Miyata & Kitagawa, 2017). In addition, the two most prominent lecticans were stained: Brevican and Aggrecan. The antibodies against Aggrecan and Brevican recognised the full-length core protein, as well as its cleaved fragments. The mean intensity of the signal of these four markers was measured in the different sub-regions of the hippocampus: CA1, CA2, CA3 and DG.

First, the Aggrecan staining highlights the CA2 region, as expected (Two-way ANOVA, $F(3,36) = 5,56$, $p = 3,05.10^{-3}$) (Figure 18A & C). The analysis shows that there is no significant interaction effect between the genotype and sub-regions ($F(3,36) = 1,52$, $p = 0,23$). Moreover, the genotype does not have any effect on the mean level of Aggrecan intensity ($F(1,36) = 0,05$, $p = 0,82$). This means that total Aggrecan staining in the hippocampus is not affected in any way in the Bassoon mutants.

Concerning Brevican, we have a similar picture to the one observed in Aggrecan, where the sub-region does have an effect (Two-way ANOVA, $F(3,120) = 8,35$, $p = 4,34.10^{-5}$) (Figure 18B & E). The interaction between genotype and sub-region, once more, is not relevant to the total Brevican staining intensity ($F(3,120) = 0,31$, $p = 0,82$) and nor is the genotype of the animals ($F(1,120) = 0,11$, $p = 0,74$).

When coming to the CS chains, there are interesting changes to be reported. For the CS-56 chains (Figure 18B & F), there are no detected changes as the interaction between genotype and sub-region is non-significant (Two-way ANOVA, $F(3,122) = 0,20$, $p = 0,90$), like the genotype ($F(1,122) = 0,94$, $p = 0,33$), although the Bsn3 animals have a slightly lower intensity of CS-56 signal (90,7±3,7 intensity (int)) when compared to Ctrl (95,4±5,6 int) regardless of the region. As for Brevican and Aggrecan, the sub-region has a significant effect on the amount of detected CS-56 ($F(3,122) = 6,81$, $p = 2,76.10^{-4}$). This difference is due to the DG having a much lower intensity (69,7±4,2 int) when compared to the CA1 subfield, used as the reference (102±6,4 int, $p = 3,33.10^{-3}$).

Finally, the WFA-detected CS chains show a striking change in their immunoreactivity levels between the Bsn3 and Ctrl animals (Figure 18B & D). The sub-region has an effect on the mean intensity of the signal ($F(3,120) = 18,8$, $p = 4,67.10^{-10}$), as expected as WFA marks the CA2 sub-region with a strong signal, just like Aggrecan. Despite the genotype alone not having an overall effect ($F(1,120) = 0,21$, $p = 0,65$), there is a significant interaction between genotype and sub-region ($F(3,120) = 3,24$, $p = 0,02$), meaning the Bsn3 animals do not have the same level of WFA intensity in at least one region. From the pictures (Figure 18B) it is easy to see that the DG of the Bsn3 animals has a much more intense WFA signal (133±17,3 int) when compared to the Ctrl (78,3±4,4 int, $p = 0,02$).

The amount of total immunoreactivity of both Brevican and Aggrecan is not affected in the Bsn3 animals (Figure 18C, E). The absence of change in these two lecticans is surprising when taking into account the increase in CS signal intensity detected by WFA (Figure 18D). This could mean that either the CSPGs present in the DG have a higher amount of

CS chain per core protein, or that another type of CSPG is produced to accommodate for a higher CS chain amount.

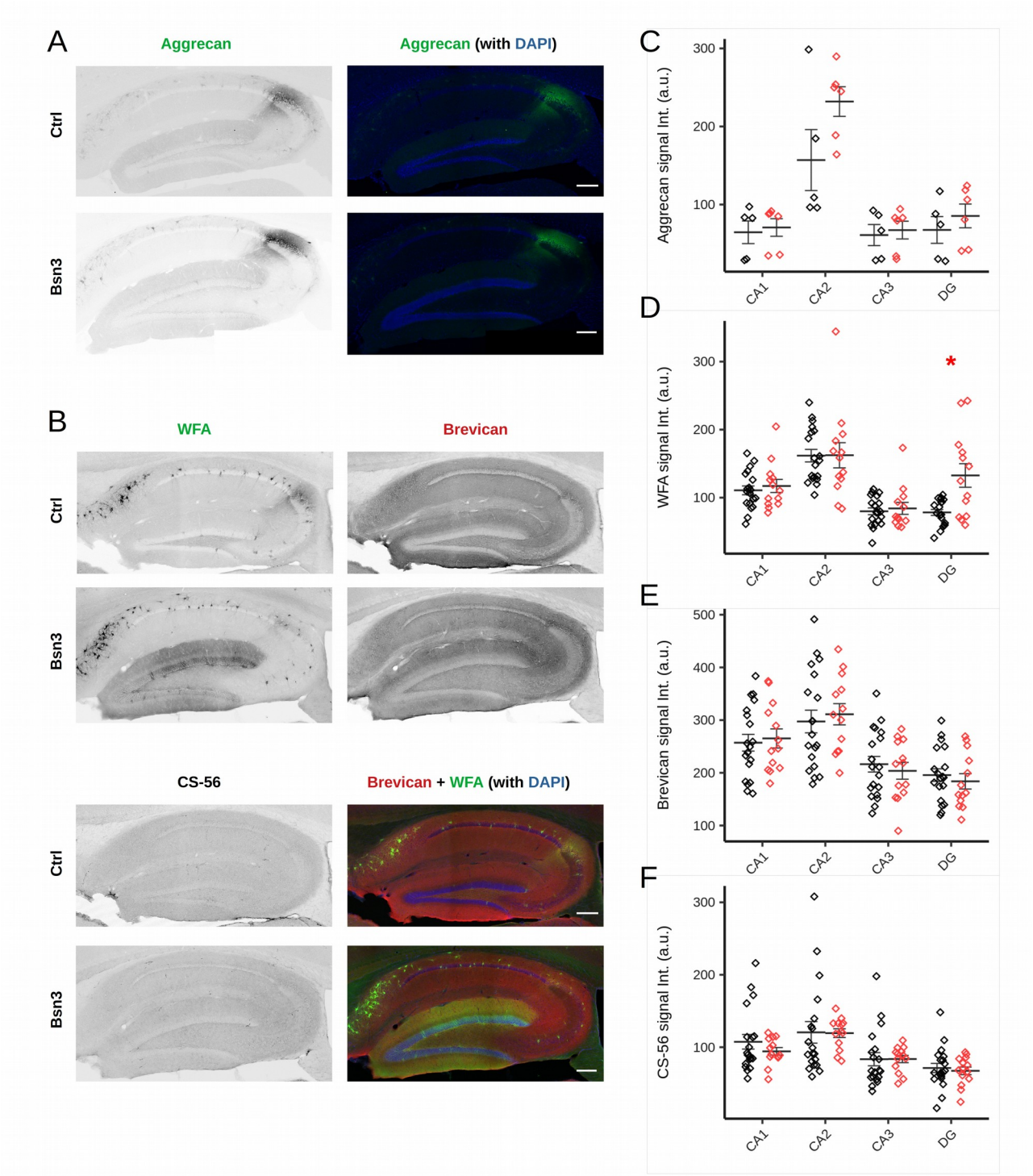

Figure 18: Bsn3 animals have a strong expression of WFA positive CS chains in the DG but not in any other sub-region of the hippocampus. (A) Example of Aggrecan staining. No notable changes can be observed between Ctrl and Bsn3 ($F(1,36) = 0,05$, $p = 0,82$). (B) Example of WFA, Brevican and CS-56 staining. For WFA ($F(1,120) = 0,21$, $p = 0,65$), Brevican ($F(1,120) = 0,11$, $p = 0,74$) and CS-56 ($F(1,122) = 0,94$, $p = 0,90$) the genotype does not have an overall effect. (C, D, E, F) Quantification of the mean intensity of the signal of (C) Aggrecan, (D) WFA, (E) Brevican and (F) CS-56. (D) There is an interaction between genotype and sub-region ($F(3, 120) = 3,24$, $p = 0,02$) with the DG having a much higher intensity in the Bsn3 than in the Ctrl ($p = 0,02$). Scale bar = 200µm.

IV.10 - The hippocampus of KA1wk mice shows WFA aggregates

In order to have a comparable analysis of the ECM in the KA-injected animals with the Bsn3 animals, we looked into the WFA marker in the hippocampus. The CS-56 marker could not be evaluated as its secondary antibody cross-reacted with some stellate structures located mostly in the hippocampus in the negative control of the KA-injected mice (data not shown).

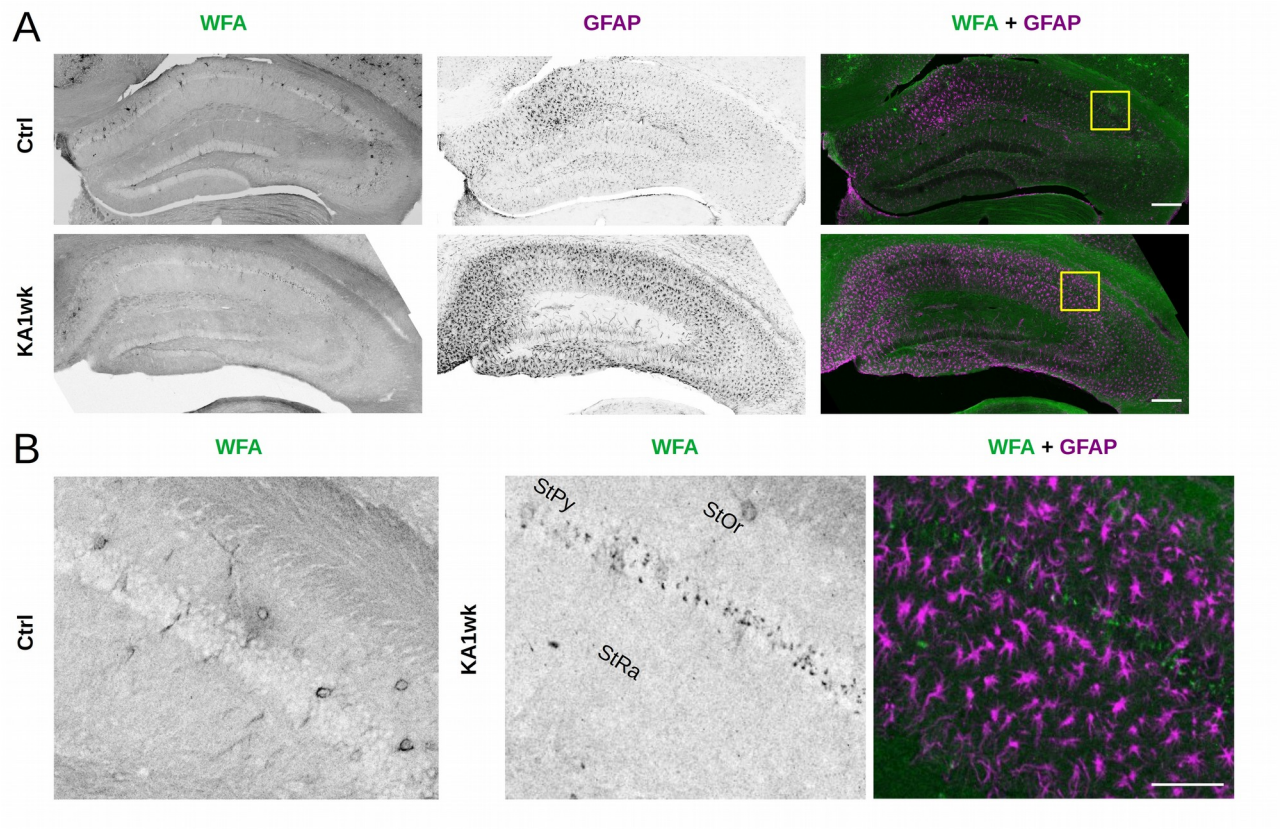

Figure 19: The CA1 region of KA-injected animals has WFA aggregates within the pyramidal cell layer that do not colocalise with GFAP. (A) Example of a WFA and GFAP staining on the hippocampus of a Sham injected and a KA1wk animal. (B) Zoom-in on the CA1 region delineated in (A) with the presence of WFA aggregates in KA1wk. StOr = stratum oriens, StPy = stratum pyramidale, StRa = stratum radiatum. (A) Scale bar = 200µm. (B) Scale bar = 50µm.

Interestingly, the observations were different from the ones made in the Bsn3 mice. Instead of a strong pericellular WFA staining in the DG (Figure 18B), the CS chains are forming small aggregates in the CA1 pyramidal layer (Figure 19B, Figure 20C). The exact nature of these aggregates is unknown, they may be localised within the cell bodies or form extracellular aggregates.

The treatment of the animal had an effect on the overall WFA staining intensity, with a stronger level in the KA-injected (149±9,40 int) than in the Sham animals (115±5,63 int) (Two-way ANOVA, $F(1, 60) = 7,12$, $p = 9,79.10^{-3}$) (Figure 20D). The increase in the WFA level is not localised in any specific region in the KA-injected animals as the interaction

between treatment and sub-region is not significant (F(3, 60) = 0,59, p = 0,63). Of note, however is the lack of significance of the sub-region factor in both treatments (F(3, 60) = 0,35, p = 0,79). This means that the injection alone of a solution in the hippocampus, unrelated to the nature of the solution, leads to changes in the ECM and notably a decrease of the WFA signal within the CA2, or a diffusion to other sub-regions that abolishes or down-regulates its usually prominent expression of WFA-detected CS chains (Figure 19, Figure 20).

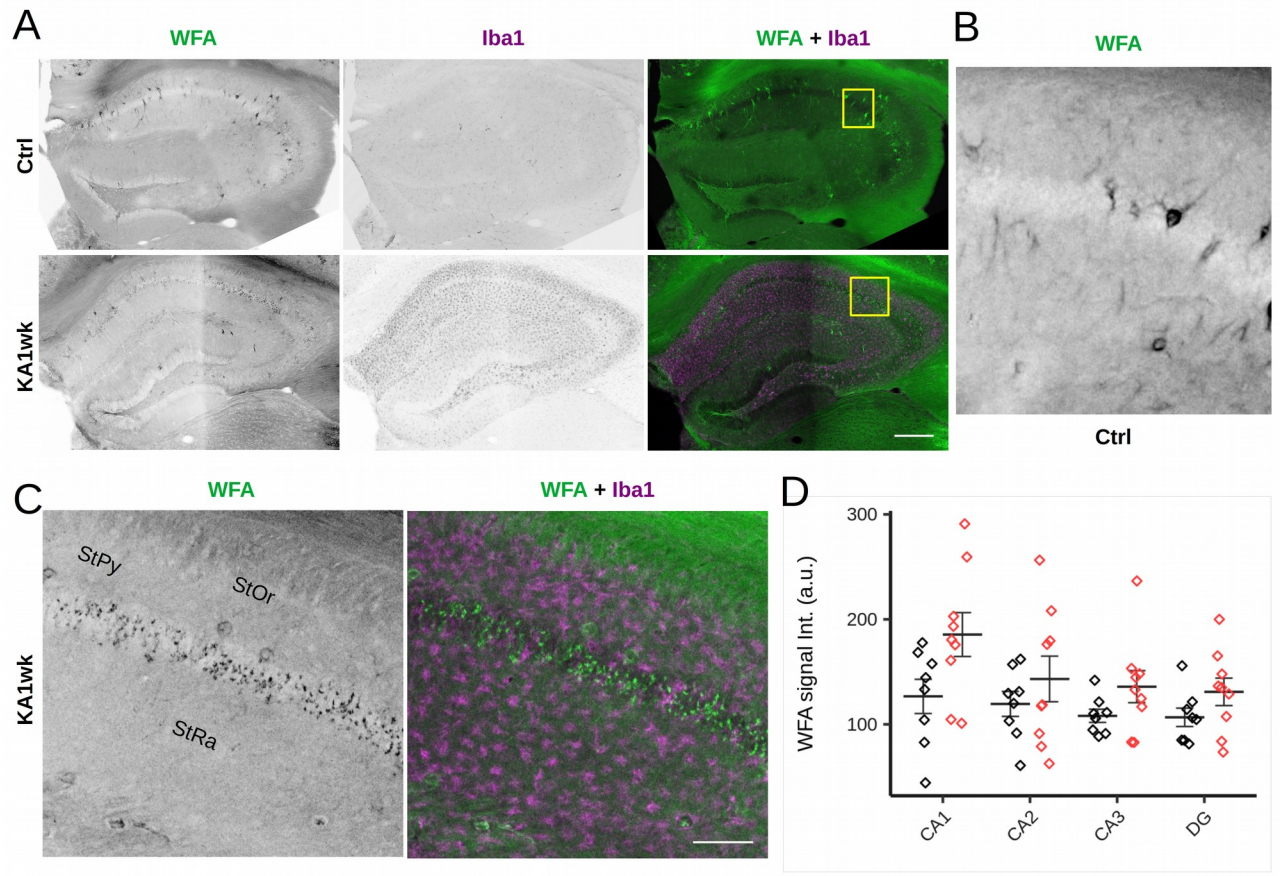

Figure 20: WFA aggregates in the CA1 sub-region of KA1wk animals do not colocalise with the Iba1 marker for microglia. (A) Example of a WFA and IbA1 staining on the hippocampus of Sham injected and KA1wk animals. (B) Zoom on the CA1 region of the Sham animal delineated in (A). (C) Zoom on the CA1 region of the KA1wk delineated in (A), it appears clearly that the WFA aggregates (green) do not colocalise with the Iba1 marker (purple). (D) Quantification of the mean intensity of the WFA staining in the Sham (black) and KA1wk animals (red). There is a significant effect of the genotype overall (F(1, 60) = 7,12, p = 9,79.10^{-3}), with the KA1wk having a higher WFA staining than the Sham animals. (A) Scale bar = 300µm. (C) Scale bar = 50µm.

To further investigate the WFA aggregates, co-stainings for GFAP and Iba1 were carried out to see whether or not the aggregates would colocalise with these glial markers (Figure 19A, Figure 20A). The GFAP staining shows a stronger staining in the KA-injected animals than in the Sham animals, a sign of the activation of astrocytes. Alongside this increase, the Iba1 staining shows an activation of the microglia that is not present in the

Sham animals. Despite the strong presence of both astrocytes and microglia, it appears that neither cell type colocalises with the WFA aggregates (Figure 19B, Figure 20C).

V Discussion

The main aim of this thesis was to elucidate the interplay between different types of epilepsy and the regulation of the ECM. Although it has been already shown that seizures alter the state of the ECM (Naffah-Mazzacorrati et al., 1999), the effects of epilepsy on the brain ECM in long lasting epilepsy are not fully known. With a focus on the HA-based ECM, I wanted to answer questions concerning the overall state of the ECM and how epilepsy (rather than the seizures alone) affects it.

The discussion will provide answer elements to the aims of this thesis (highlighted in chapter II). Throughout this discussion, I will shed some light onto the possible mechanisms behind some of the findings, as well as develop possible links to other known epileptic phenotypes.

V.1 - Epilepsy in the Bassoon mutant lines in comparison to a classical model

My project looked in depth into the epileptic phenotype of Bassoon mutants and compared it with the well established KA model. The latter is a model of MTLE and we were interested in unravelling which were the common points and differences between the Bassoon animals and the KA model.

Bassoon mutants do not suffer from MTLE, and the present experiments made it clear once more. The animals from the Bassoon lines develop epilepsy during the first weeks of life as the survival analysis concerning spontaneous deaths suggests (Figure 5), indicating a form of childhood epilepsy and confirming previous observations (Ghiglieri et al., 2009). One other strong difference is the absence of hippocampal sclerosis in the Bassoon mutants, if anything, the lack of Bassoon is responsible for the presence of more neurons rather than less (Annamneedi et al., 2018, Heyden et al., 2011). Conversely, the loss of neurons is a central feature of MTLE, both in animal models and patients although not always present (Thom, 2014). The model of supra-hippocampal KA injection we used does not have an immediate sclerosis following the seizure induction (Jia et al., unpublished).

V.1.a. - Severity of the epileptic phenotype in Bassoon mutants

First of all, the Bassoon mutants can all develop epilepsy. This finding extends the known neuronal functions of Bassoon to a role as a potential E/I balance regulator. This role could find its roots as early as the first synaptogenesis events. Bassoon plays a role in both inhibitory and excitatory synaptogenesis (Zhai et al., 2000). The inhibitory network is the first to form synapses during development (Anastasiades et al., 2017), and its importance for the proper development of neuronal circuits is central and, to some extent, this is proven by the differences in seizure severity observed between the B2E and B2I

lines. The B2I mice develop a stronger epileptic phenotype than the B2E ones (Table 6), possibly because the development of their neuronal network is more strongly affected. This first difference between the B2E and B2I emphasises the importance of inhibitory system dysregulation in the aetiology of epilepsy (see Khazipov, 2016) as an impairment of the excitatory circuit through the conditional deletion of Bassoon (*i.e.* the B2E line) did not lead to epilepsy as frequently as the same deletion in the inhibitory circuit.

The view of a neuronal development more strongly affected in B2I than in B2E animals, however, is somewhat challenged by the survival rates observed in the two conditional KO lines. A stronger dysregulation of neuronal network development likely would raise the risk of death in early-life or even at the embryo level, however, the B2E animals are the ones with a lower than expected number of homozygous mutants, while B2I have a normal number (Table 5). This trend is reversed at a later time point; once the animals reach 3 weeks of age, the B2I animals have a higher spontaneous death rate than the B2E (Figure 6), most likely due to their stronger epileptic phenotype.

Of note, the spontaneous death rate of the constitutive mutants – namely Bsn1, Bgt and Bsn3 – is higher than the one of B2I and B2E (Figure 6). About 50% of constitutive mutants die of unexplained spontaneous death by the age of 6 months, a confirmation of previous results from the Bsn1 mice (Altrock et al., 2003). It would be interesting to further distinguish whether the spontaneous deaths in the Bassoon animals happen following a seizure or are comparable to sudden unexplained deaths in epilepsy (Devinsky et al., 2016). In the second case, Bassoon mutants could be considered as interesting models to decipher the causes and mechanisms of such sudden deaths.

The Bassoon mutants display recurrent seizures and develop epilepsy, but with inter-individual and group differences, since they do not all develop this phenotype at a comparable level (Figure 8). Among the constitutive mutants, the Bsn3 line distinguishes itself by its high seizure frequency and longer seizure duration when compared to the other lines. One explanation concerning the milder epilepsy of the Bsn1 is that they express a truncated form of Bassoon (Altrock et al., 2003) and it could still keep part of its function at the synapse. On the other hand, the Bgt animals are known to have some residual expression of Bassoon as well, notably in the retina and auditory system (Hallermann et al., 2010). How this affects the epileptic phenotype remains to be evaluated.

In the end, the Bsn1 and Bgt lines are similar to the B2I in terms of seizure frequency and duration (Figure 8), however, Bsn3 is the line with the highest seizure rate in adult animals. If anything, the Bsn1 animals seem to have a much stronger phenotype during development. They have a tremendously low number of homozygous mutants compared to the expected number (Table 5) and it seems that their survival during the first weeks could be lower, although a study with higher animal numbers would be required to confirm such finding. The Bsn1 animals could be an interesting model of early-onset epilepsy,

whereas the Bsn3 line seems more appropriate for studying long-lasting consequences of such an epilepsy.

V.1.b. - The epileptic phenotype of Bassoon mutants is more severe than the one from KA-induced epilepsy

Interestingly, not all the KA animals displayed seizures during the recording period, both in early epilepsy (KA1wk) and during the chronic phase (KA4wk). In a sense, the KA models are comparable to the B2E mutants concerning their seizure frequency and duration. It could be interesting to further investigate the phenotype of the B2E animals in order to see if they have a similar phenotype to the KA-injected models with focal seizures (Bouilleret et al., 1999). Nevertheless, it remains likely that B2E develop a similar epileptic phenotype as the other Bassoon mutants, with generalised seizures (Altrock et al., 2003, Ghiglieri et al., 2009). In the end, the B2E animals could be used as an enhanced seizure susceptibility model like the SV2a heterozygous mutants (Kaminski et al., 2009).

On the other hand, with the exception of the B2E line, all Bassoon lines develop seizures (Table 6). Their phenotype shows a similar or higher time spent in seizures when compared to both the KA1wk group and the KA4wk group. Among all the lines, the Bsn3 line is the one that stands out the most.

V.1.c. - Speculation on the origin of the epilepsy in Bassoon mutants

The origin of the epileptic phenotype in the Bassoon mutants has yet to be identified, nevertheless, several hypotheses can be made about the mechanisms at play. Most likely, several of the presented mechanisms come together to tip the scale toward the high synchronous activity necessary to trigger a seizure.

First and foremost, Bassoon is a pre-synaptic protein with a role in synaptic transmission (Gundelfinger et al., 2016). That alone already makes it a candidate for triggering synaptic dysregulation upon mutations or deletion and, in turn, lead to a seizure-prone neuronal activity. The reports on the effects of the deletion of Bassoon, however, do not point toward a higher neuronal activity. In the Bsn1 mutants, several excitatory synapses have been found to be inactive in the hippocampus (Altrock et al., 2003) and the sustained synaptic activity is impaired as well (Mendoza-Schulz et al., 2014). This lower sustained activity is also present in the Bgt animals (Hallermann et al., 2010) along with a lack of $Ca_V2.1$ at the synapse, part of the vesicle fusion mechanism (Davydova et al., 2014). Consistent with the findings of a reduced synaptic activity, impairments in the LTP of Bsn1 mutants have been shown, with a lower increase in neuronal excitability than expected in striatal and CA1 neurons (Ghiglieri et al., 2009, Sgobio et al., 2010). Concerning the CA1 neurons, they may be affected by the inability of mossy fibre synapses to properly mature (Lanore et al., 2010).

Nevertheless, a reduced neuronal activity does not exclude the apparition of seizures, as seizures may arise from a synchronisation of inhibitory inputs (Khazipov et al., 2016). The presence of LVF onsets among the seizures observed in the Bassoon lines (Figure 9) reinforces the idea of an inhibitory synchronisation (Elahian et al., 2018). The proteomics analysis also adds further evidence to support this hypothesis, since the level of GAD65 – a GABA producing enzyme – is increased in Bsn3 and as a trend in B2I (Figure 17). This could point toward an increased inhibitory drive in the hippocampus, that could potentially extend to other brain structures. Indeed, Ghiglieri and colleagues (2009) report a larger interneuron dendritic tree in the striatum of Bassoon mutants, along with an abnormally strong LTP in these same interneurons. Conversely, the dendritic trees of excitatory cells in the striatum (Ghiglieri et al., 2009) and of the granule cells in the hippocampus (Sgobio et al., 2010), are smaller and more simple. The simplicity of the dendritic tree of excitatory neurons could be due to the extended one in inhibitory cells as the inhibitory input has some control over the development of dendrites in excitatory cells (Gupta et al., 2019). It is interesting to point out that in the B2E line, which is not as affected by seizures, the hippocampal granule cells have a more complex dendritic tree (Annamneedi et al., 2018). Most of these changes might be traced back to the developmental phase of the neuronal networks (Zhai et al., 2000), especially in the Bassoon mutants affecting inhibitory cells (Anastasiades et al., 2017).

Another explanation for the apparition of seizures comes from more recent research, with evidence that Bassoon is involved in the degradation of proteins at the pre-synapse through the control of the autophagy machinery (Okerlund et al., 2017). More recently, Hoffman-Conoway and colleagues (2020) showed that synaptic proteins were more heavily ubiquitinated, leading to higher degradation rates. One of the most highly ubiquitinated protein is the Sv2a protein, which leads to a higher seizure susceptibility when partially deleted (Kaminski et al., 2009) and is a target for the anti-seizure drug levetiracetam. Past this explanation, there is a more direct link between autophagy and epilepsy (Gan et al., 2015) and a dysregulation of autophagy leads to an epileptic phenotype, which is in line with the Bassoon mutants having a higher pool of ubiquitinated proteins and an epileptic phenotype. However, it could still be that the autophagy dysregulation seen in the Bassoon lines is a consequence of the epilepsy and not the cause (Gan et al., 2015).

V.2 - Changes to the extracellular matrix in epilepsy

The brain ECM, and more precisely the HA-based ECM, appears as a regulator of neuronal plasticity, axon guidance and cell motility. Its components are changed over the course of epilepsy with, for example, a higher expression of CS chains in the hippocampus of the pilocarpine epilepsy model in rats (Naffah-Mazzacorrati et al., 1999), a change that parallels the observations made in the Bsn3 mice, albeit limited to the DG

(Figure 18). This increase in CS goes along with a decrease in Aggrecan and HAPLN1, essential components of the PNNs around the Parvalbumin interneurons (McRae et al., 2012). Interestingly, the phenotype of Bsn3 animals does not display such a decrease in Aggrecan (Figure 18) and there is no overall difference in HAPLN1 (Figure 10B).

Different types of epilepsy models might have some overlaps in their regulations of ECM components, but they also might have differences that set them apart and could explain the different types of seizures, the spread of electrical activity to different regions and more.

V.2.a. - A link between Brevican and epileptic phenotypes

A first link between Brevican and an epileptic phenotype was observed by Yuan and colleagues (2002), with the increased cleavage of Brevican in the hippocampus along with a loss of synapses within the DG of KA-injected animals. There is, here, an interesting parallel to be made with the decreased amount of spines on the dendrites of hippocampal neurons in Bsn1 mice (Sgobio et al., 2010), especially with the knowledge that constitutive Bassoon mutants tend to have lower Brevican amounts (Figure 11), although only the Bsn3 line reaches significantly lower levels. To further reinforce the link between a lower Brevican and the observed phenotype in the Bassoon mutants, the impaired maintenance of LTP seen in the hippocampus of Bsn1 animals is quite similar to the one observed in Brevican KO animals (Brakebusch et al., 2002). A decreased amount of Brevican may not have exactly the same effects but could participate in the LTP phenotype observed in the Bassoon mutants.

One could argue that the amount of the cleaved fragment of Brevican is not increased in Bassoon animals as it is the case in the experiments of Yuan and colleagues (2002), but the adult Bassoon animals are far into the chronic phase of epilepsy. At that phase of epilepsy, cleavage of Brevican comes back to normal levels (Mayer et al., 2005).

Moreover, our model of early KA-induced epilepsy (KA1wk group) remains at the level of their Ctrl counterparts when it comes to the amount of either Brevican or its cleaved fragment (Figure 11). Even at a later time point (KA4wk group), the amount of Brevican is not changed in the homogenate, only in the synaptosomes. A lower amount of Brevican at the synapse might mean a more permanently plastic synapse (Valenzuela et al., 2014, Mitlöhner et al., 2020); but it might also make the synapse less functional, notably by altering its LTP (Brakebusch et al., 2002) or modifying the dynamics of AMPA receptors at the membrane (Frischknecht et al., 2009). That last hypothesis may underlie the lack of functionality of some synapses in the Bassoon mutants (Altrock et al., 2003).

The down-regulation of the amount of Brevican in the Bassoon mutants could be a consequence of astrocytic activation, as astrocytes produce some components of the ECM and particularly Brevican (Geissler et al., 2013, Zhang et al., 2014). The proteomics

analysis shows a much higher level of GFAP in the hippocampus of Bsn3 and B2I animals (Figure 17B), an increase similar to the one observed in the KA model (Bitsika et al., 2016). The activation of astrocytes is sufficient to cause seizures (Robel et al., 2015) and glia affects many mechanisms that could increase the overall network excitability (see Robel et al., 2016).

So far, it is not known whether there is a direct link between the pre-synaptic Bassoon protein and astrocytes. The astrocytic activation in Bassoon mutants may thus be a consequence of the epileptic phenotype.

Furthermore, there are evidences that Brevican regulates the excitability of PNN-sheathed interneurons. Notably, in Brevican KO animals, interneurons have a higher excitability (Favuzzi et al., 2017). The decreased Brevican could raise the excitability of interneurons and lead to synchronous firing as well as LVF seizures (Elahian et al., 2018). The correlation observed between the seizure properties and Brevican levels in homogenate, soluble fraction and synaptosomes could rely on such mechanism, with a lower amount of Brevican leading to a higher interneuron excitability, and in turn to more frequent or stronger seizures (Figure 14, Figure 15).

Further evidence of the importance of the ECM, and Brevican to some extent, is shown in experiments with quadruple KO for Brevican, Neurocan, TnC and TnR. In these quadruple KO hippocampal cells, the amount of excitatory synapses is increased while the inhibitory ones are decreased (Gottschling et al., 2019). This phenotype could be present in Bassoon animals and an interesting parallel is drawn as the GAD65 protein is also up-regulated in the hippocampus of the quadruple KO, similar to the observed results in Bsn3 and B2I (Figure 17). However, the electrophysiological alterations in the quadruple KOs are quite different from the one documented in Bassoon mutants (Jansen et al., 2017), notably the early component of LTP is affected, whereas the late component is in Bassoon animals.

Whether or not this decrease in Brevican amounts is a cause or a consequence of epilepsy, it remains that it resembles a phenotype observed in epileptic patients suffering from TLE (Favuzzi et al., 2017). Nevertheless, the absence of neuronal loss and the early-onset of the epileptic phenotype suggest that Bassoon mutants are not TLE models.

V.2.b. - A role for other lecticans in the epileptic phenotype

Generally, Aggrecan is considered the most prominent component of the PNNs, thus a part of the dense meshwork surrounding the Parvalbumin interneurons (Yamaguchi, 2000). In the B2I line and the KA1wk animals however, the soluble Aggrecan is up-regulated (Figure 12), while the overall Aggrecan level is not. Most likely, the soluble Aggrecan in both models leaves is originally from another subcellular compartment.

One hypothesis to explain such a change is the “shedding” of Aggrecan from the PNNs into the soluble fraction. Following this train of thoughts, the interneurons without Aggrecan could still have PNNs, albeit with a strongly altered composition (Giamanco et al., 2010), notably a lack of WFA-specific CS chains. The lack of Aggrecan around the interneurons reinstates plasticity (Rowlands et al., 2018) and this newly-found plasticity could lead to the formation of epileptic circuits.

In the Bassoon animals, the seizures properties do not correlate with the soluble Aggrecan, but do so positively with the Aggrecan and its cleaved-fragment from the synaptosomes (Figure 14). This shows that the regulation of Aggrecan in the soluble fraction is more specific to the B2I line, a quite logical finding considering the Aggrecan is mostly found in the PNNs around inhibitory interneurons (Yamaguchi, 2000), which lack Bassoon in the B2I line. On the other hand, the role of Aggrecan at the synapse in epilepsy is highlighted by its strong correlation with seizure properties (Figure 14). Little is known about the role of Aggrecan outside of the PNNs and further investigation would be needed, although it has already been shown to be present around the synapse and digested following plasticity-inducing signalling (Mitlöhner et al., 2020).

Finally, Neurocan is also linked to the epileptic phenotype in the Bassoon mutants. Its 90kDa cleaved-fragment correlates positively with seizure properties in homogenate, but not in any sub-cellular fraction (Figure 14). This is an interesting finding as Neurocan is up-regulated in a model of spontaneous epilepsy in rats, and this even before the onset of seizures (Kurazano et al., 2001). Generally, Neurocan is linked to a juvenile ECM that is more plastic (Rauch et al., 2001). In the adult Bassoon mutants, however, the protein might be cleaved quickly by the proteases and thus only its fragment is easily detected. In this case, it is difficult to decipher whether the increase in the cleaved fragment would have similar capacities as the full-length protein. If the properties are similar, then a higher level of Neurocan might be responsible for the enlargement of inhibitory dendritic trees observed in the Bassoon animals (Sullivan et al., 2018).

V.2.c. - ECM correlations as hints to co-regulations and ECM structure

Apart from the correlations between ECM and seizure properties, the correlations from ECM protein to ECM protein also are of interest.

As a matter of fact, the correlations between expression of some ECM proteins may be indicative of their interactions or whether they form ECM structures together. Moreover, the distinction between Bassoon mutants and KA-injected animals reveals different correlations between the two groups (Figure 14). The injection within the brain of a substance, either KA or saline solution, must have distinct effects on the ECM, different from the one observed within the Bassoon mutants.

Some of the significant correlations show links between lecticans and HAPLNs or tenascins (Figure 14). Interestingly, these correlations are not seen in the homogenate at all, a finding that points towards more specific regulations for each subcellular compartment rather than overall changes of the ECM. In the soluble fraction of Bassoon animals, the HAPLN1, normally known for its preferred interaction with Aggrecan for the formation of PNNs (Carulli et al., 2010), correlates with Brevican levels. It could be that the structure of the PNNs is affected in the Bassoon mutants, although at the level of the hippocampus, it does not seem that PNNs change as they are still strongly marked by Aggrecan and WFA (Figure 18).

All these correlations show some of the underlying regulations of the ECM and how it responds to heightened or altered activity. It is of interest to know more about the links between the ECM proteins to increase awareness of how it is affected globally and not only at the single protein level.

V.2.d. - Changes to the ECM cell receptor in the epileptic animals

To add to the changes in the ECM, the results from the proteomics study show an increase in CD44 in both B2I and Bsn3 lines, but not the B2E line that has a milder epileptic phenotype. CD44 is an ECM receptor, more precisely a receptor for HA, at the cell membrane (Roszkowska et al., 2016). This increase in CD44 is also observed in the KA model (Bitsika et al., 2016), although at a much higher level following the injection, and an increase is also noted following status epilepticus (Borges et al., 2004).

In both cases, this increase points towards a role of the ECM in the epileptic phenotype. In fact, CD44 plays a role in synaptic plasticity (Skupien et al., 2014, Roszkowska et al., 2016) and its down-regulation leads to a lower excitatory drive at the synapse (Roszkowska et al., 2016). No study to our knowledge has looked into the effects of CD44 over-expression at the synapse, nonetheless it is logical to think it would have the opposite effect to its down-regulation, *i.e.* a reinforcement of the excitatory drive. This would add to the E/I imbalance necessary for the epileptic phenotype.

V.3 - Changes to the hippocampal ECM in Basson and KA-injected epilepsy models

As the hippocampus is known to be undergo an extensive range of plastic changes in epilepsy (Jarero-Basulto et al., 2018, Thom, 2014), it seems logical to think that there are plasticity inducing changes in the ECM in the hippocampus of epilepsy models.

In the Bsn3 mutants, along with the strong seizures, there is a much higher level of CS chains in the DG (Figure 18). Similar observations have been made in the brain of TLE patients (Perosa et al., 2002), with an increased content of CS, as well as HA. Either the production of CS is increased in the DG, or its degradation is impaired in some way. Although it does not exclude an increase in the production rate of CS, no proteins related

to their production was increased in the results of the proteomics experiment. Moreover, degradation of CS relies on the lysosomal pathway (Yamada, 2015) and although there are evidences for changes in the proteasome degradation pathway in Bassoon mutants (Hoffmann-Conoway et al., 2020, Okerlund et al., 2017), little investigation has been carried out on a potential increase of lysosomal activity in Bassoon (Waites et al., 2013).

Of note, the CS chains in the DG of Bsn3 animals are detected by WFA, and not CS-56. Currently, the WFA detected chains are believed to preferentially link to Aggrecan (Giamanco et al., 2010), but it could also be that another CSPG (different from either Aggrecan or Brevican) is up-regulated in the DG to accommodate for the increased amount of CS.

In addition, the increased CS content of the DG may explain the increased neurogenesis observed in the Bassoon mutants (Annamneedi et al., 2018, Heyden et al., 2011). Indeed, a higher CS content in the DG is linked to higher neurogenesis (Yamada et al., 2018). Importantly, the new-born neurons project mossy fibres to the CA3 region (Cope & Gould, 2019) and the abnormal generation of neurons would be responsible for MFS in epilepsy (Thom, 2014). Interestingly, the increased neurogenesis in Bassoon animals could underlie their epileptic phenotype, although MFS has not been described in the Bassoon mutants and not been found in the B2E line (Annamneedi et al., 2018), it remains that mossy fibres in the Bassoon animals have an impaired transmission during their development (Lanore et al., 2010). Experiments to limit the neurogenesis would be interesting in the Bassoon mutants, as they have already proven their efficacy to prevent seizures in chemically-induced epilepsy models (Cho et al., 2015). It even appears that the amount of newborn neurons is linked to the frequency of the seizures (Zhou et al., 2019). It could then be that the Bsn3 animals have more seizures because of a stronger phenotype than the one already observed in B2E or Bsn1 (Annamneedi et al., 2018, Heyden et al., 2011).

Conversely, in the KA-injected animals, the DG is not the most affected region of the hippocampus but rather the CA1 (Figure 19, Figure 20). In this region, the WFA-detected CSs are not up- or down-regulated, instead there are some clusters forming in the pyramidal cell layer, likely aggregates of CS. The origin and precise localisation of these CS aggregates is unknown. One hypothesis, especially when considering the already documented degradation of PNNs in chemically-induced epilepsy (McRae et al., 2012, Rankin-Gee et al., 2015), is that these clusters are CS chains from the PNNs that are internalised and digested. However, it appears that neither the astrocytes nor the microglia are responsible for the digestion of these CS chains (Figure 19, Figure 20).

Looking for the cells that could be at the origin of the aggregation of WFA-detected CS, we looked into astrocytes and microglia in the hippocampus. It appeared both astrocytes and microglia are activated in KA-injected animals. This is of importance as the astrocytes are among the cells producing components of the ECM (Geissler et al., 2013, Zhang et

al., 2014) and microglia could affect the ECM. In the KA-injected animals, the activation of microglia is already documented (Eyo et al., 2017) and changes to the ECM are able to affect its activation, such as an increase in TnC for example (Haage et al., 2019). Although TnC is not up-regulated in our KA models (Figure 10), there are some changes in Neurocan and Aggrecan that could affect the microglia and its state. Changes to the ECM could thus be targeted to regulate the activation of microglia, leading to anti-epileptogenic effects as demonstrated by Fu and colleagues (2020).

VI Conclusion and outlooks

Despite a major focus on the role of glutamate and GABAergic neurotransmission in epilepsy, little is known about the causes of the E/I imbalance. Staley (2015) discusses that the brain network cannot be in a permanent state of imbalance, otherwise the circuits would trigger seizures without any interruption. Hence, epilepsy is all about an increased susceptibility to seizures that represents a recurrent – but not permanent – E/I imbalance.

Considering this, the Bassoon animals are an interesting new model of generalised epilepsy. The functionality of the synapses is affected in adults (Ghiglieri et al., 2009, Sgobio et al., 2010) as well as during development (Lanore et al., 2011) and this could underlie the early-onset and the continuation of the epileptic phenotype into adulthood. Its generalised seizures suggest an overall neuronal network dysregulation. Most likely, this network dysregulation is more reliant on inhibitory interneurons, as the B2I animals systematically display seizures whereas the B2E do not. The use of the B2I animals might prove more convenient as a generalised epilepsy model than the Bsn3, as it is evident in this model that epilepsy derives from impairments of the inhibitory circuits. In the Bsn3 animals, an interplay of not only excitatory and inhibitory, but also modulatory impairments may be at the root of the epileptic phenotype. This would, in a way, explain their more frequent seizures and stronger epileptic phenotype.

Importantly, ECM changes are also observed in the Bassoon mutant model: lower amounts of Brevican are detected in animals with more seizures. The exact mechanisms by which a down-regulation of Brevican affects the synapses and the neuronal network remain to be unveiled, as well as the effect of seizures on the overall Brevican. However, the ECM components are not equally affected in the KA model, suggesting that there are some regulations that are specific to each model, with TLE having a distinct ECM when compared to the early-onset generalised seizures of Bassoon mutants. This is highlighted once more in the hippocampus, with a CS-rich DG in Bassoon mutants while KA animals have clusters of CS in the CA1 that suggest it is being digested.

The changes in the ECM may directly influence the neuronal transmission (Favuzzi et al., 2017), and in addition, they may induce the higher neurogenesis typically observed in the Bassoon mutants (Heyden et al., 2011) which would in turn aid in the formation of recurrent circuits and genesis of seizures (Zhou et al., 2019).

In the end, it may be that the epileptic phenotype in TLE models (*e.g.* KA-injected animals) and the Bassoon mutants are underlined by the same mechanism: an aberrant neurogenesis. Although the details of how neurogenesis leads to epilepsy might differ in the two types of epilepsy, it would be interesting to see whether the attenuation of neurogenesis could also reduce the frequency of seizures in the Bassoon mutants (Zhou et al., 2019). Furthermore, the ECM modifications observed in Bassoon animals may be at

the origin of the increased neurogenesis in the first place. Several new treatments targeting the ECM and its digestion have been recently proposed and tested in TLE models (Broekaart et al., 2020, Korotkov et al., 2018). Extending the tests for such treatments to generalised seizures might finally improve the diversity of proposed anti-epileptic drugs in a useful and significant way.

VII References

Abramovici, S., & Bagić, A. (2016). Chapter 10 - Epidemiology of epilepsy. In M. J. Aminoff, F. Boller, & D. F. Swaab (Eds.), *Handbook of Clinical Neurology* (Vol. 138, pp. 159–171). Elsevier. https://doi.org/10.1016/B978-0-12-802973-2.00010-0

Altrock, W. D., tom Dieck, S., Sokolov, M., Meyer, A. C., Sigler, A., Brakebusch, C., Fässler, R., Richter, K., Boeckers, T. M., Potschka, H., Brandt, C., Löscher, W., Grimberg, D., Dresbach, T., Hempelmann, A., Hassan, H., Balschun, D., Frey, J. U., Brandstätter, J. H., … Gundelfinger, E. D. (2003). Functional Inactivation of a Fraction of Excitatory Synapses in Mice Deficient for the Active Zone Protein Bassoon. *Neuron*, *37*(5), 787–800. https://doi.org/10.1016/S0896-6273(03)00088-6

Ambrosino, P., Soldovieri, M. V., Bast, T., Turnpenny, P. D., Uhrig, S., Biskup, S., Döcker, M., Fleck, T., Mosca, I., Manocchio, L., Iraci, N., Taglialatela, M., & Lemke, J. R. (2018). De novo gain-of-function variants in KCNT2 as a novel cause of developmental and epileptic encephalopathy. *Annals of Neurology*, *83*(6), 1198–1204. https://doi.org/10.1002/ana.25248

Anastasiades, P. G., Marques-Smith, A., Lyngholm, D., Lickiss, T., Raffiq, S., Kätzel, D., Miesenböck, G., & Butt, S. J. B. (2016). GABAergic interneurons form transient layer-specific circuits in early postnatal neocortex. *Nature Communications*, *7*, 10584. https://doi.org/10.1038/ncomms10584

Angenstein, F., Hilfert, L., Zuschratter, W., Altrock, W. D., Niessen, H. G., & Gundelfinger, E. D. (2008). Morphological and metabolic changes in the cortex of mice lacking the functional presynaptic active zone protein bassoon: a combined 1H-NMR spectroscopy and histochemical study. *Cerebral Cortex (New York, N.Y.: 1991)*, *18*(4), 890–897. https://doi.org/10.1093/cercor/bhm122

Annamneedi, A., Caliskan, G., Müller, S., Montag, D., Budinger, E., Angenstein, F., Fejtova, A., Tischmeyer, W., Gundelfinger, E. D., & Stork, O. (2018). Ablation of the presynaptic organizer Bassoon in excitatory neurons retards dentate gyrus maturation and enhances learning performance. *Brain Structure & Function*, *223*(7), 3423–3445. https://doi.org/10.1007/s00429-018-1692-3

Arranz, A. M., Perkins, K. L., Irie, F., Lewis, D. P., Hrabe, J., Xiao, F., Itano, N., Kimata, K., Hrabetova, S., & Yamaguchi, Y. (2014). Hyaluronan deficiency due to Has3 knock-out causes altered neuronal activity and seizures via reduction in brain extracellular space. *The Journal of Neuroscience: The Official Journal of the Society for Neuroscience*, *34*(18), 6164–6176. https://doi.org/10.1523/JNEUROSCI.3458-13.2014

Avoli, M., de Curtis, M., Gnatkovsky, V., Gotman, J., Köhling, R., Lévesque, M., Manseau, F., Shiri, Z., & Williams, S. (2016). Specific imbalance of excitatory/inhibitory signaling establishes seizure onset pattern in temporal lobe epilepsy. *Journal of Neurophysiology*, *115*(6), 3229–3237. https://doi.org/10.1152/jn.01128.2015

Avram, S., Shaposhnikov, S., Buiu, C., & Mernea, M. (2014). Chondroitin sulfate proteoglycans: structure-function relationship with implication in neural development and brain disorders. *BioMed Research International*, *2014*, 642798. https://doi.org/10.1155/2014/642798

Bandtlow, C. E., & Zimmermann, D. R. (2000). Proteoglycans in the developing brain: new conceptual insights for old proteins. *Physiological Reviews*, *80*(4), 1267–1290. https://doi.org/10.1152/physrev.2000.80.4.1267

Barker-Haliski, M., & White, H. S. (2015). Glutamatergic Mechanisms Associated with Seizures and Epilepsy. *Cold Spring Harbor Perspectives in Medicine*, *5*(8), a022863. https://doi.org/10.1101/cshperspect.a022863

Bekku, Y., Saito, M., Moser, M., Fuchigami, M., Maehara, A., Nakayama, M., Kusachi, S., Ninomiya, Y., & Oohashi, T. (2012). Bral2 is indispensable for the proper localization of brevican

and the structural integrity of the perineuronal net in the brainstem and cerebellum. *The Journal of Comparative Neurology*, *520*(8), 1721–1736. https://doi.org/10.1002/cne.23009

Binette, F., Cravens, J., Kahoussi, B., Haudenschild, D. R., & Goetinck, P. F. (1994). Link protein is ubiquitously expressed in non-cartilaginous tissues where it enhances and stabilizes the interaction of proteoglycans with hyaluronic acid. *The Journal of Biological Chemistry*, *269*(29), 19116–19122.

Bitsika, V., Duveau, V., Simon-Areces, J., Mullen, W., Roucard, C., Makridakis, M., Mermelekas, G., Savvopoulos, P., Depaulis, A., & Vlahou, A. (2016). High-Throughput LC-MS/MS Proteomic Analysis of a Mouse Model of Mesiotemporal Lobe Epilepsy Predicts Microglial Activation Underlying Disease Development. *Journal of Proteome Research*, *15*(5), 1546–1562. https://doi.org/10.1021/acs.jproteome.6b00003

Borges, K., McDermott, D. L., & Dingledine, R. (2004). Reciprocal changes of CD44 and GAP-43 expression in the dentate gyrus inner molecular layer after status epilepticus in mice. *Experimental Neurology*, *188*(1), 1–10. https://doi.org/10.1016/j.expneurol.2004.03.019

Bouilleret, V., Ridoux, V., Depaulis, A., Marescaux, C., Nehlig, A., & Le Gal La Salle, G. (1999). Recurrent seizures and hippocampal sclerosis following intrahippocampal kainate injection in adult mice: electroencephalography, histopathology and synaptic reorganization similar to mesial temporal lobe epilepsy. *Neuroscience*, *89*(3), 717–729. https://doi.org/10.1016/S0306-4522(98)00401-1

Bradbury, E. J., Moon, L. D. F., Popat, R. J., King, V. R., Bennett, G. S., Patel, P. N., Fawcett, J. W., & McMahon, S. B. (2002). Chondroitinase ABC promotes functional recovery after spinal cord injury. *Nature*, *416*(6881), 636–640. https://doi.org/10.1038/416636a

Brakebusch, C., Seidenbecher, C. I., Asztely, F., Rauch, U., Matthies, H., Meyer, H., Krug, M., Böckers, T. M., Zhou, X., Kreutz, M. R., Montag, D., Gundelfinger, E. D., & Fässler, R. (2002). Brevican-deficient mice display impaired hippocampal CA1 long-term potentiation but show no obvious deficits in learning and memory. *Molecular and Cellular Biology*, *22*(21), 7417–7427. https://doi.org/10.1128/mcb.22.21.7417-7427.2002

Broekaart, D. W., Bertran, A., Jia, S., Korotkov, A., Senkov, O., Bongaarts, A., Mills, J. D., Anink, J. J., Seco-Moral, J., Baaijen, J., Idema, S., Chabrol, E., Becker, A., Wadman, W., Tarrago, T., Gorter, J. A., Aronica, E., Prades, R., Dityatev, A., & van Vliet, E. A. (2020). The matrix metalloproteinase inhibitor IPR-179 has antiseizure and antiepileptogenic effects. *The Journal of Clinical Investigation*. https://doi.org/10.1172/JCI138332

Brückner, G., Grosche, J., Hartlage-Rübsamen, M., Schmidt, S., & Schachner, M. (2003). Region and lamina-specific distribution of extracellular matrix proteoglycans, hyaluronan and tenascin-R in the mouse hippocampal formation. *Journal of Chemical Neuroanatomy*, *26*(1), 37–50. https://doi.org/10.1016/s0891-0618(03)00036-x

Buckmaster, P. S. (2004). Laboratory animal models of temporal lobe epilepsy. *Comparative Medicine*, *54*(5), 473–485.

Carstens, K. E., Phillips, M. L., Pozzo-Miller, L., Weinberg, R. J., & Dudek, S. M. (2016). Perineuronal Nets Suppress Plasticity of Excitatory Synapses on CA2 Pyramidal Neurons. *The Journal of Neuroscience: The Official Journal of the Society for Neuroscience*, *36*(23), 6312–6320. https://doi.org/10.1523/JNEUROSCI.0245-16.2016

Carulli, D., Pizzorusso, T., Kwok, J. C. F., Putignano, E., Poli, A., Forostyak, S., Andrews, M. R., Deepa, S. S., Glant, T. T., & Fawcett, J. W. (2010). Animals lacking link protein have attenuated perineuronal nets and persistent plasticity. *Brain: A Journal of Neurology*, *133*(Pt 8), 2331–2347. https://doi.org/10.1093/brain/awq145

Chabrol, E., Navarro, V., Provenzano, G., Cohen, I., Dinocourt, C., Rivaud-Péchoux, S., Fricker, D., Baulac, M., Miles, R., Leguern, E., & Baulac, S. (2010). Electroclinical characterization of

epileptic seizures in leucine-rich, glioma-inactivated 1-deficient mice. *Brain: A Journal of Neurology*, *133*(9), 2749–2762. https://doi.org/10.1093/brain/awq171

Chen, Z., Brodie, M. J., Liew, D., & Kwan, P. (2018). Treatment Outcomes in Patients With Newly Diagnosed Epilepsy Treated With Established and New Antiepileptic Drugs: A 30-Year Longitudinal Cohort Study. *JAMA Neurology*, *75*(3), 279. https://doi.org/10.1001/jamaneurol.2017.3949

Chistyakov, D. V., Astakhova, A. A., Azbukina, N. V., Goriainov, S. V., Chistyakov, V. V., & Sergeeva, M. G. (2019). High and Low Molecular Weight Hyaluronic Acid Differentially Influences Oxylipins Synthesis in Course of Neuroinflammation. *International Journal of Molecular Sciences*, *20*(16). https://doi.org/10.3390/ijms20163894

Cho, K.-O., Lybrand, Z. R., Ito, N., Brulet, R., Tafacory, F., Zhang, L., Good, L., Ure, K., Kernie, S. G., Birnbaum, S. G., Scharfman, H. E., Eisch, A. J., & Hsieh, J. (2015). Aberrant hippocampal neurogenesis contributes to epilepsy and associated cognitive decline. *Nature Communications*, *6*, 6606. https://doi.org/10.1038/ncomms7606

Cope, E. C., & Gould, E. (2019). Adult Neurogenesis, Glia, and the Extracellular Matrix. *Cell Stem Cell*, *24*(5), 690–705. https://doi.org/10.1016/j.stem.2019.03.023

Danzer, S. C. (2019). Adult Neurogenesis in the Development of Epilepsy. *Epilepsy Currents*, *19*(5), 316–320. https://doi.org/10.1177/1535759719868186

Dauth, S., Grevesse, T., Pantazopoulos, H., Campbell, P. H., Maoz, B. M., Berretta, S., & Parker, K. K. (2016). Extracellular matrix protein expression is brain region dependent. *The Journal of Comparative Neurology*, *524*(7), 1309–1336. https://doi.org/10.1002/cne.23965

Davis, G. E., Bayless, K. J., Davis, M. J., & Meininger, G. A. (2000). Regulation of tissue injury responses by the exposure of matricryptic sites within extracellular matrix molecules. *The American Journal of Pathology*, *156*(5), 1489–1498. https://doi.org/10.1016/S0002-9440(10)65020-1

Davydova, D., Marini, C., King, C., Klueva, J., Bischof, F., Romorini, S., Montenegro-Venegas, C., Heine, M., Schneider, R., Schröder, M. S., Altrock, W. D., Henneberger, C., Rusakov, D. A., Gundelfinger, E. D., & Fejtova, A. (2014). Bassoon specifically controls presynaptic P/Q-type Ca(2+) channels via RIM-binding protein. *Neuron*, *82*(1), 181–194. https://doi.org/10.1016/j.neuron.2014.02.012

de Winter, F., Kwok, J. C. F., Fawcett, J. W., Vo, T. T., Carulli, D., & Verhaagen, J. (2016). The Chemorepulsive Protein Semaphorin 3A and Perineuronal Net-Mediated Plasticity. *Neural Plasticity*, *2016*, 3679545. https://doi.org/10.1155/2016/3679545

Devinsky, O., Vezzani, A., Najjar, S., De Lanerolle, N. C., & Rogawski, M. A. (2013). Glia and epilepsy: excitability and inflammation. *Trends in Neurosciences*, *36*(3), 174–184. https://doi.org/10.1016/j.tins.2012.11.008

Devinsky, O., Hesdorffer, D. C., Thurman, D. J., Lhatoo, S., & Richerson, G. (2016). Sudden unexpected death in epilepsy: epidemiology, mechanisms, and prevention. *The Lancet Neurology*, *15*(10), 1075–1088. https://doi.org/10.1016/S1474-4422(16)30158-2

Dieni, S., Matsumoto, T., Dekkers, M., Rauskolb, S., Ionescu, M. S., Deogracias, R., Gundelfinger, E. D., Kojima, M., Nestel, S., Frotscher, M., & Barde, Y.-A. (2012). BDNF and its pro-peptide are stored in presynaptic dense core vesicles in brain neurons. *The Journal of Cell Biology*, *196*(6), 775–788. https://doi.org/10.1083/jcb.201201038

Dieni, S., Nestel, S., Sibbe, M., Frotscher, M., & Hellwig, S. (2015). Distinct synaptic and neurochemical changes to the granule cell-CA3 projection in Bassoon mutant mice. *Frontiers in Synaptic Neuroscience*, *7*, 18. https://doi.org/10.3389/fnsyn.2015.00018

Dityatev, A. (2010). Remodeling of extracellular matrix and epileptogenesis. *Epilepsia*, *51 Suppl 3*, 61–65. https://doi.org/10.1111/j.1528-1167.2010.02612.x

Dresbach, T., Hempelmann, A., Spilker, C., tom Dieck, S., Altrock, W. D., Zuschratter, W., Garner, C. C., & Gundelfinger, E. D. (2003). Functional regions of the presynaptic cytomatrix protein bassoon: significance for synaptic targeting and cytomatrix anchoring. *Molecular and Cellular Neuroscience*, *23*(2), 279–291. https://doi.org/10.1016/S1044-7431(03)00015-0

Elahian, B., Lado, N. E., Mankin, E., Vangala, S., Misra, A., Moxon, K., Fried, I., Sharan, A., Yeasin, M., Staba, R., Bragin, A., Avoli, M., Sperling, M. R., Engel, J., & Weiss, S. A. (2018). Low-voltage fast seizures in humans begin with increased interneuron firing. *Annals of Neurology*, *84*(4), 588–600. https://doi.org/10.1002/ana.25325

Evers, M. R., Salmen, B., Bukalo, O., Rollenhagen, A., Bösl, M. R., Morellini, F., Bartsch, U., Dityatev, A., & Schachner, M. (2002). Impairment of L-type Ca2+ channel-dependent forms of hippocampal synaptic plasticity in mice deficient in the extracellular matrix glycoprotein tenascin-C. *The Journal of Neuroscience: The Official Journal of the Society for Neuroscience*, *22*(16), 7177–7194. https://doi.org/20026735

Eyo, U. B., Murugan, M., & Wu, L.-J. (2017). Microglia-Neuron Communication in Epilepsy. *Glia*, *65*(1), 5–18. https://doi.org/10.1002/glia.23006

Favuzzi, E., Marques-Smith, A., Deogracias, R., Winterflood, C. M., Sánchez-Aguilera, A., Mantoan, L., Maeso, P., Fernandes, C., Ewers, H., & Rico, B. (2017). Activity-Dependent Gating of Parvalbumin Interneuron Function by the Perineuronal Net Protein Brevican. *Neuron*, *95*(3), 639-655.e10. https://doi.org/10.1016/j.neuron.2017.06.028

Fontanil, T., Mohamedi, Y., Espina-Casado, J., Obaya, Á. J., Cobo, T., & Cal, S. (2021). Hyalectanase Activities by the ADAMTS Metalloproteases. *International Journal of Molecular Sciences*, *22*(6). https://doi.org/10.3390/ijms22062988

Fordington, S., & Manford, M. (2020). A review of seizures and epilepsy following traumatic brain injury. *Journal of Neurology*, *267*(10), 3105–3111. https://doi.org/10.1007/s00415-020-09926-w

Frischknecht, R., Heine, M., Perrais, D., Seidenbecher, C. I., Choquet, D., & Gundelfinger, E. D. (2009). Brain extracellular matrix affects AMPA receptor lateral mobility and short-term synaptic plasticity. *Nature Neuroscience*, *12*(7), 897–904. https://doi.org/10.1038/nn.2338

Fu H, Cheng Y, Luo H, Rong Z, Li Y, Lu P, Ye X, Huang W, Qi Z, Li X, Cheng B, Wang X, Yao Y, Zhang Y, -W, Zheng W, Zheng H (2019). Silencing MicroRNA-155 Attenuates Kainic Acid-Induced Seizure by Inhibiting Microglia Activation. *Neuroimmunomodulation* 26:67-76. https://doi.org/10.1159/000496344

Gan, J., Qu, Y., Li, J., Zhao, F., & Mu, D. (2015). An evaluation of the links between microRNA, autophagy, and epilepsy. *Reviews in the Neurosciences*, *26*(2), 225–237. https://doi.org/10.1515/revneuro-2014-0062

Geissler, M., Gottschling, C., Aguado, A., Rauch, U., Wetzel, C. H., Hatt, H., & Faissner, A. (2013). Primary hippocampal neurons, which lack four crucial extracellular matrix molecules, display abnormalities of synaptic structure and function and severe deficits in perineuronal net formation. *The Journal of Neuroscience: The Official Journal of the Society for Neuroscience*, *33*(18), 7742–7755. https://doi.org/10.1523/JNEUROSCI.3275-12.2013

Ghiglieri, V., Picconi, B., Sgobio, C., Bagetta, V., Barone, I., Paillè, V., Di Filippo, M., Polli, F., Gardoni, F., Altrock, W., Gundelfinger, E. D., De Sarro, G., Bernardi, G., Ammassari-Teule, M., Di Luca, M., & Calabresi, P. (2009). Epilepsy-induced abnormal striatal plasticity in Bassoon mutant mice. *The European Journal of Neuroscience*, *29*(10), 1979–1993. https://doi.org/10.1111/j.1460-9568.2009.06733.x

Ghiglieri, V., Sgobio, C., Patassini, S., Bagetta, V., Fejtova, A., Giampà, C., Marinucci, S., Heyden, A., Gundelfinger, E. D., Fusco, F. R., Calabresi, P., & Picconi, B. (2010). TrkB/BDNF-dependent striatal plasticity and behavior in a genetic model of epilepsy: modulation by valproic acid. *Neuropsychopharmacology: Official Publication of the American College of Neuropsychopharmacology*, *35*(7), 1531–1540. https://doi.org/10.1038/npp.2010.23

Giamanco, K. A., Morawski, M., & Matthews, R. T. (2010). Perineuronal net formation and structure in aggrecan KO mice. *Neuroscience*, *170*(4), 1314–1327. https://doi.org/10.1016/j.neuroscience.2010.08.032

Gogolla, N., Caroni, P., Lüthi, A., & Herry, C. (2009). Perineuronal nets protect fear memories from erasure. *Science (New York, N.Y.)*, *325*(5945), 1258–1261. https://doi.org/10.1126/science.1174146

Gottschling, C., Wegrzyn, D., Denecke, B., & Faissner, A. (2019). Elimination of the four extracellular matrix molecules tenascin-C, tenascin-R, brevican and neurocan alters the ratio of excitatory and inhibitory synapses. *Scientific Reports*, *9*(1), 13939. https://doi.org/10.1038/s41598-019-50404-9

Gundelfinger, E. D., Reissner, C., & Garner, C. C. (2016). Role of Bassoon and Piccolo in Assembly and Molecular Organization of the Active Zone. *Frontiers in Synaptic Neuroscience*, *7*, 19. https://doi.org/10.3389/fnsyn.2015.00019

Gupta, J., Bromwich, M., Radell, J., Arshad, M. N., Gonzalez, S., Luikart, B. W., Aaron, G. B., & Naegele, J. R. (2019). Restrained Dendritic Growth of Adult-Born Granule Cells Innervated by Transplanted Fetal GABAergic Interneurons in Mice with Temporal Lobe Epilepsy. *ENeuro*, *6*(2). https://doi.org/10.1523/ENEURO.0110-18.2019

Haage, V., Elmadany, N., Roll, L., Faissner, A., Gutmann, D. H., Semtner, M., & Kettenmann, H. (2019). Tenascin C regulates multiple microglial functions involving TLR4 signaling and HDAC1. *Brain, Behavior, and Immunity*, *81*, 470–483. https://doi.org/10.1016/j.bbi.2019.06.047

Hallermann, S., Fejtova, A., Schmidt, H., Weyhersmüller, A., Silver, R. A., Gundelfinger, E. D., & Eilers, J. (2010). Bassoon speeds vesicle reloading at a central excitatory synapse. *Neuron*, *68*(4), 710–723. https://doi.org/10.1016/j.neuron.2010.10.026

Hashemi, K. (2020). *Neuroarchiver Tool - Interval Processing*. Retrieved September, 2020, from http://www.opensourceinstruments.com/Electronics/A3018/Neuroarchiver.html#Interval%20Processing

Hayashi, N., Tatsumi, K., Okuda, H., Yoshikawa, M., Ishizaka, S., Miyata, S., Manabe, T., & Wanaka, A. (2007). DACS, novel matrix structure composed of chondroitin sulfate proteoglycan in the brain. *Biochemical and Biophysical Research Communications*, *364*(2), 410–415. https://doi.org/10.1016/j.bbrc.2007.10.040

Heng, K., Haney, M. M., & Buckmaster, P. S. (2013). High-dose rapamycin blocks mossy fiber sprouting but not seizures in a mouse model of temporal lobe epilepsy. *Epilepsia*, *54*(9), 1535–1541. https://doi.org/10.1111/epi.12246

Heyden, A., Ionescu, M.-C. S., Romorini, S., Kracht, B., Ghiglieri, V., Calabresi, P., Seidenbecher, C., Angenstein, F., & Gundelfinger, E. D. (2011). Hippocampal enlargement in Bassoon-mutant mice is associated with enhanced neurogenesis, reduced apoptosis, and abnormal BDNF levels. *Cell and Tissue Research*, *346*(1), 11–26. https://doi.org/10.1007/s00441-011-1233-3

Hoffmann-Conaway, S., Brockmann, M. M., Schneider, K., Annamneedi, A., Rahman, K. A., Bruns, C., Textoris-Taube, K., Trimbuch, T., Smalla, K.-H., Rosenmund, C., Gundelfinger, E. D., Garner, C. C., & Montenegro-Venegas, C. (2020). Parkin contributes to synaptic vesicle autophagy in Bassoon-deficient mice. *ELife*, *9*. https://doi.org/10.7554/eLife.56590

Houser, C. R. (1990). Granule cell dispersion in the dentate gyrus of humans with temporal lobe epilepsy - ScienceDirect. *Brain Research*, *535*(2), 195–204. https://doi.org/10.1016/0006-8993(90)91601-C

Hughes, C. S., Foehr, S., Garfield, D. A., Furlong, E. E., Steinmetz, L. M., & Krijgsveld, J. (2014). Ultrasensitive proteome analysis using paramagnetic bead technology. *Molecular Systems Biology*, *10*(10), 757. https://doi.org/10.15252/msb.20145625

Hughes, C. S., Moggridge, S., Müller, T., Sorensen, P. H., Morin, G. B., & Krijgsveld, J. (2018). Single-pot, solid-phase-enhanced sample preparation for proteomics experiments. *Nature Protocols*, *14*(1), 68–85. https://doi.org/10.1038/s41596-018-0082-x

Huse, J. T., Snuderl, M., Jones, D. T. W., Brathwaite, C. D., Altman, N., Lavi, E., Saffery, R., Sexton-Oates, A., Blumcke, I., Capper, D., Karajannis, M. A., Benayed, R., Chavez, L., Thomas, C., Serrano, J., Borsu, L., Ladanyi, M., & Rosenblum, M. K. (2017). Polymorphous low-grade neuroepithelial tumor of the young (PLNTY): an epileptogenic neoplasm with oligodendroglioma-like components, aberrant CD34 expression, and genetic alterations involving the MAP kinase pathway. *Acta Neuropathologica*, *133*(3), 417–429. https://doi.org/10.1007/s00401-016-1639-9

ILAE (a). (2014). *The 2014 Definition of Epilepsy: A perspective for patients and caregivers // International League Against Epilepsy*. Retrieved September 24, 2020, from https://www.ilae.org/guidelines/definition-and-classification/the-2014-definition-of-epilepsy-a-perspective-for-patients-and-caregivers

ILAE (b) (2014). *In the Event of Status Epilepticus | Epilepsy Foundation*. (n.d.). Retrieved October 30, 2020, from https://www.epilepsy.com/learn/challenges-epilepsy/seizure-emergencies/status-epilepticus

Itano, N., Sawai, T., Yoshida, M., Lenas, P., Yamada, Y., Imagawa, M., Shinomura, T., Hamaguchi, M., Yoshida, Y., Ohnuki, Y., Miyauchi, S., Spicer, A. P., McDonald, J. A., & Kimata, K. (1999). Three isoforms of mammalian hyaluronan synthases have distinct enzymatic properties. *The Journal of Biological Chemistry*, *274*(35), 25085–25092. https://doi.org/10.1074/jbc.274.35.25085

Itano, Naoki, & Kimata, K. (2002). Mammalian hyaluronan synthases. *IUBMB Life*, *54*(4), 195–199. https://doi.org/10.1080/15216540214929

Jansen, S., Gottschling, C., Faissner, A., & Manahan-Vaughan, D. (2017). Intrinsic cellular and molecular properties of in vivo hippocampal synaptic plasticity are altered in the absence of key synaptic matrix molecules. *Hippocampus*, *27*(8), 920–933. https://doi.org/10.1002/hipo.22742

Jarero-Basulto, J. J., Gasca-Martínez, Y., Rivera-Cervantes, M. C., Ureña-Guerrero, M. E., Feria-Velasco, A. I., & Beas-Zarate, C. (2018). Interactions Between Epilepsy and Plasticity. *Pharmaceuticals*, *11*(1), 17. https://doi.org/10.3390/ph11010017

John, N., Krügel, H., Frischknecht, R., Smalla, K.-H., Schultz, C., Kreutz, M. R., Gundelfinger, E. D., & Seidenbecher, C. I. (2006). Brevican-containing perineuronal nets of extracellular matrix in dissociated hippocampal primary cultures. *Molecular and Cellular Neurosciences*, *31*(4), 774–784. https://doi.org/10.1016/j.mcn.2006.01.011

Johnson, M. R., & Kaminski, R. M. (2020). A systems-level framework for anti-epilepsy drug discovery. *Neuropharmacology*, *170*, 107868. https://doi.org/10.1016/j.neuropharm.2019.107868

Kakizaki, T., Ohshiro, T., Itakura, M., Konno, K., Watanabe, M., Mushiake, H., & Yanagawa, Y. (2021). Rats deficient in the GAD65 isoform exhibit epilepsy and premature lethality. *FASEB Journal: Official Publication of the Federation of American Societies for Experimental Biology*, *35*(2), e21224. https://doi.org/10.1096/fj.202001935R

Kaminski, R. M., Gillard, M., Leclercq, K., Hanon, E., Lorent, G., Dassesse, D., Matagne, A., & Klitgaard, H. (2009). Proepileptic phenotype of SV2A-deficient mice is associated with reduced anticonvulsant efficacy of levetiracetam. *Epilepsia*, *50*(7), 1729–1740. https://doi.org/10.1111/j.1528-1167.2009.02089.x

Keezer, M. R., Sisodiya, S. M., & Sander, J. W. (2016). Comorbidities of epilepsy: current concepts and future perspectives. *The Lancet Neurology*, *15*(1), 106–115. https://doi.org/10.1016/S1474-4422(15)00225-2

Kelwick, R., Desanlis, I., Wheeler, G. N., & Edwards, D. R. (2015). The ADAMTS (A Disintegrin and Metalloproteinase with Thrombospondin motifs) family. *Genome Biology*, *16*, 113. https://doi.org/10.1186/s13059-015-0676-3

Khazipov, R. (2016). GABAergic Synchronization in Epilepsy. *Cold Spring Harbor Perspectives in Medicine*, *6*(2), a022764. https://doi.org/10.1101/cshperspect.a022764

Kochlamazashvili, G., Henneberger, C., Bukalo, O., Dvoretskova, E., Senkov, O., Lievens, P. M.-J., Westenbroek, R., Engel, A. K., Catterall, W. A., Rusakov, D. A., Schachner, M., & Dityatev, A. (2010). The extracellular matrix molecule hyaluronic acid regulates hippocampal synaptic plasticity by modulating postsynaptic L-type Ca(2+) channels. *Neuron*, *67*(1), 116–128. https://doi.org/10.1016/j.neuron.2010.05.030

Köhling, R., D'Antuono, M., Benini, R., de Guzman, P., & Avoli, M. (2016). Hypersynchronous ictal onset in the perirhinal cortex results from dynamic weakening in inhibition. *Neurobiology of Disease*, *87*, 1–10. https://doi.org/10.1016/j.nbd.2015.12.002

Korotkov, A., Broekaart, D. W. M., van Scheppingen, J., Anink, J. J., Baayen, J. C., Idema, S., Gorter, J. A., Aronica, E., & van Vliet, E. A. (2018). Increased expression of matrix metalloproteinase 3 can be attenuated by inhibition of microRNA-155 in cultured human astrocytes. *Journal of Neuroinflammation*, *15*(1), 211. https://doi.org/10.1186/s12974-018-1245-y

Krishnaswamy, V. R., Benbenishty, A., Blinder, P., & Sagi, I. (2019). Demystifying the extracellular matrix and its proteolytic remodeling in the brain: structural and functional insights. *Cellular and Molecular Life Sciences: CMLS*, *76*(16), 3229–3248. https://doi.org/10.1007/s00018-019-03182-6

Kumar, S. S., & Buckmaster, P. S. (2006). Hyperexcitability, interneurons, and loss of GABAergic synapses in entorhinal cortex in a model of temporal lobe epilepsy. *The Journal of Neuroscience: The Official Journal of the Society for Neuroscience*, *26*(17), 4613–4623. https://doi.org/10.1523/JNEUROSCI.0064-06.2006

Kurazono, S., Okamoto, M., Sakiyama, J., Mori, S., Nakata, Y., Fukuoka, J., Amano, S., Oohira, A., & Matsui, H. (2001). Expression of brain specific chondroitin sulfate proteoglycans, neurocan and phosphacan, in the developing and adult hippocampus of Ihara's epileptic rats. *Brain Research*, *898*(1), 36–48. https://doi.org/10.1016/s0006-8993(01)02128-x

Lanore, F., Blanchet, C., Fejtova, A., Pinheiro, P., Richter, K., Balschun, D., Gundelfinger, E., & Mulle, C. (2010). Impaired development of hippocampal mossy fibre synapses in mouse mutants for the presynaptic scaffold protein Bassoon. *The Journal of Physiology*, *588* (Pt 12), 2133–2145. https://doi.org/10.1113/jphysiol.2009.184929

Li, L., Bragin, A., Staba, R., & Engel, J. (2019). Unit firing and oscillations at seizure onset in epileptic rodents. *Neurobiology of Disease*, *127*, 382–389. https://doi.org/10.1016/j.nbd.2019.03.027

Lighvani, S., Baik, N., Diggs, J. E., Khaldoyanidi, S., Parmer, R. J., & Miles, L. A. (2011). Regulation of macrophage migration by a novel plasminogen receptor Plg-R KT. *Blood*, *118*(20), 5622–5630. https://doi.org/10.1182/blood-2011-03-344242

Lin, T. W., Harward, S. C., Huang, Y. Z., & McNamara, J. O. (2020). Targeting BDNF/TrkB pathways for preventing or suppressing epilepsy. *Neuropharmacology*, *167*, 107734. https://doi.org/10.1016/j.neuropharm.2019.107734

Löscher, W. (2017). Animal Models of Seizures and Epilepsy: Past, Present, and Future Role for the Discovery of Antiseizure Drugs. *Neurochemical Research*, *42*(7), 1873–1888. https://doi.org/10.1007/s11064-017-2222-z

Lundell, A., Olin, A. I., Mörgelin, M., al-Karadaghi, S., Aspberg, A., & Logan, D. T. (2004). Structural basis for interactions between tenascins and lectican C-type lectin domains: evidence

for a crosslinking role for tenascins. *Structure (London, England: 1993)*, *12*(8), 1495–1506. https://doi.org/10.1016/j.str.2004.05.021

Mayer, J., Hamel, M. G., & Gottschall, P. E. (2005). Evidence for proteolytic cleavage of brevican by the ADAMTSs in the dentate gyrus after excitotoxic lesion of the mouse entorhinal cortex. *BMC Neuroscience*, *6*, 52. https://doi.org/10.1186/1471-2202-6-52

McNamara, J. O., & Scharfman, H. E. (2012). Temporal Lobe Epilepsy and the BDNF Receptor, TrkB. In J. L. Noebels, M. Avoli, M. A. Rogawski, R. W. Olsen, & A. V. Delgado-Escueta (Eds.), *Jasper's Basic Mechanisms of the Epilepsies* (4th ed.). National Center for Biotechnology Information (US). http://www.ncbi.nlm.nih.gov/books/NBK98186/

McRae, P. A., Baranov, E., Rogers, S. L., & Porter, B. E. (2012). Persistent decrease in multiple components of the perineuronal net following status epilepticus. *The European Journal of Neuroscience*, *36*(11), 3471–3482. https://doi.org/10.1111/j.1460-9568.2012.08268.x

Mendoza Schulz, A., Jing, Z., Sánchez Caro, J. M., Wetzel, F., Dresbach, T., Strenzke, N., Wichmann, C., & Moser, T. (2014). Bassoon-disruption slows vesicle replenishment and induces homeostatic plasticity at a CNS synapse. *The EMBO Journal*, *33*(5), 512–527. https://doi.org/10.1002/embj.201385887

Messaoudi, E., Bårdsen, K., Srebro, B., & Bramham, C. R. (1998). Acute Intrahippocampal Infusion of BDNF Induces Lasting Potentiation of Synaptic Transmission in the Rat Dentate Gyrus. *Journal of Neurophysiology*, *79*(1), 496–499. https://doi.org/10.1152/jn.1998.79.1.496

Meyer-Puttlitz, B., Milev, P., Junker, E., Zimmer, I., Margolis, R. U., & Margolis, R. K. (1995). Chondroitin sulfate and chondroitin/keratan sulfate proteoglycans of nervous tissue: developmental changes of neurocan and phosphacan. *Journal of Neurochemistry*, *65*(5), 2327–2337. https://doi.org/10.1046/j.1471-4159.1995.65052327.x

Mitlöhner, J., Kaushik, R., Niekisch, H., Blondiaux, A., Gee, C. E., Happel, M. F. K., Gundelfinger, E., Dityatev, A., Frischknecht, R., & Seidenbecher, C. (2020). Dopamine Receptor Activation Modulates the Integrity of the Perisynaptic Extracellular Matrix at Excitatory Synapses. *Cells*, *9*(2). https://doi.org/10.3390/cells9020260

Miyata, S., & Kitagawa, H. (2017). Formation and remodeling of the brain extracellular matrix in neural plasticity: Roles of chondroitin sulfate and hyaluronan. *Biochimica Et Biophysica Acta. General Subjects*, *1861*(10), 2420–2434. https://doi.org/10.1016/j.bbagen.2017.06.010

Miyata, S., Komatsu, Y., Yoshimura, Y., Taya, C., & Kitagawa, H. (2012). Persistent cortical plasticity by upregulation of chondroitin 6-sulfation. *Nature Neuroscience*, *15*(3), 414–422, S1-2. https://doi.org/10.1038/nn.3023

Morawski, M., Brückner, M. K., Riederer, P., Brückner, G., & Arendt, T. (2004). Perineuronal nets potentially protect against oxidative stress. *Experimental Neurology*, *188*(2), 309–315. https://doi.org/10.1016/j.expneurol.2004.04.017

Mukherjee, K., Yang, X., Gerber, S. H., Kwon, H.-B., Ho, A., Castillo, P. E., Liu, X., & Südhof, T. C. (2010). Piccolo and bassoon maintain synaptic vesicle clustering without directly participating in vesicle exocytosis. *Proceedings of the National Academy of Sciences of the United States of America*, *107*(14), 6504–6509. https://doi.org/10.1073/pnas.1002307107

Naffah-Mazzacoratti, M. G., Argañaraz, G. A., Porcionatto, M. A., Scorza, F. A., Amado, D., Silva, R., Bellissimo, M. I., Nader, H. B., & Cavalheiro, E. A. (1999). Selective alterations of glycosaminoglycans synthesis and proteoglycan expression in rat cortex and hippocampus in pilocarpine-induced epilepsy. *Brain Research Bulletin*, *50*(4), 229–239. https://doi.org/10.1016/s0361-9230(99)00195-1

Nguyen, P. T., Dorman, L. C., Pan, S., Vainchtein, I. D., Han, R. T., Nakao-Inoue, H., Taloma, S. E., Barron, J. J., Molofsky, A. B., Kheirbek, M. A., & Molofsky, A. V. (2020). Microglial Remodeling of the Extracellular Matrix Promotes Synapse Plasticity. *Cell*, *182*(2), 388-403.e15. https://doi.org/10.1016/j.cell.2020.05.050

Okazaki, M. M., Molnár, P., & Nadler, J. V. (1999). Recurrent mossy fiber pathway in rat dentate gyrus: synaptic currents evoked in presence and absence of seizure-induced growth. *Journal of Neurophysiology*, *81*(4), 1645–1660. https://doi.org/10.1152/jn.1999.81.4.1645

Okerlund, N. D., Schneider, K., Leal-Ortiz, S., Montenegro-Venegas, C., Kim, S. A., Garner, L. C., Waites, C. L., Gundelfinger, E. D., Reimer, R. J., & Garner, C. C. (2017). Bassoon Controls Presynaptic Autophagy through Atg5. *Neuron*, *93*(4), 897-913.e7. https://doi.org/10.1016/j.neuron.2017.01.026

Okuda, H. (2018). A review of functional heterogeneity among astrocytes and the CS56-specific antibody-mediated detection of a subpopulation of astrocytes in adult brains. *Anatomical Science International*, *93*(2), 161–168. https://doi.org/10.1007/s12565-017-0420-z

Oohashi, T., Hirakawa, S., Bekku, Y., Rauch, U., Zimmermann, D. R., Su, W.-D., Ohtsuka, A., Murakami, T., & Ninomiya, Y. (2002). Bral1, a brain-specific link protein, colocalizing with the versican V2 isoform at the nodes of Ranvier in developing and adult mouse central nervous systems. *Molecular and Cellular Neurosciences*, *19*(1), 43–57. https://doi.org/10.1006/mcne.2001.1061

Perosa, S. R., Porcionatto, M. A., Cukiert, A., Martins, J. R. M., Passeroti, C. C., Amado, D., Matas, S. L. A., Nader, H. B., Cavalheiro, E. A., Leite, J. P., & Naffah-Mazzacoratti, M. G. (2002). Glycosaminoglycan levels and proteoglycan expression are altered in the hippocampus of patients with mesial temporal lobe epilepsy. *Brain Research Bulletin*, *58*(5), 509–516. https://doi.org/10.1016/s0361-9230(02)00822-5

Perucca, P., Dubeau, F., & Gotman, J. (2014). Intracranial electroencephalographic seizure-onset patterns: effect of underlying pathology. *Brain: A Journal of Neurology*, *137*(Pt 1), 183–196. https://doi.org/10.1093/brain/awt299

Pizzorusso, T., Medini, P., Berardi, N., Chierzi, S., Fawcett, J. W., & Maffei, L. (2002). Reactivation of ocular dominance plasticity in the adult visual cortex. *Science (New York, N.Y.)*, *298*(5596), 1248–1251. https://doi.org/10.1126/science.1072699

Rankin-Gee, E. K., McRae, P. A., Baranov, E., Rogers, S., Wandrey, L., & Porter, B. E. (2015). Perineuronal net degradation in epilepsy. *Epilepsia*, *56*(7), 1124–1133. https://doi.org/10.1111/epi.13026

Rauch, U., Feng, K., & Zhou, X.-H. (2001). Neurocan: a brain chondroitin sulfate proteoglycan. *Cellular and Molecular Life Sciences CMLS*, *58*(12), 1842–1856. https://doi.org/10.1007/PL00000822

Reed, M. J., Damodarasamy, M., & Banks, W. A. (2019). The extracellular matrix of the blood-brain barrier: structural and functional roles in health, aging, and Alzheimer's disease. *Tissue Barriers*, *7*(4), 1651157. https://doi.org/10.1080/21688370.2019.1651157

Rempe, R. G., Hartz, A. M. S., & Bauer, B. (2016). Matrix metalloproteinases in the brain and blood-brain barrier: Versatile breakers and makers. *Journal of Cerebral Blood Flow and Metabolism: Official Journal of the International Society of Cerebral Blood Flow and Metabolism*, *36*(9), 1481–1507. https://doi.org/10.1177/0271678X16655551

Robel, S., Buckingham, S. C., Boni, J. L., Campbell, S. L., Danbolt, N. C., Riedemann, T., Sutor, B., & Sontheimer, H. (2015). Reactive astrogliosis causes the development of spontaneous seizures. *The Journal of Neuroscience: The Official Journal of the Society for Neuroscience*, *35*(8), 3330–3345. https://doi.org/10.1523/JNEUROSCI.1574-14.2015

Robel, S., & Sontheimer, H. (2016). Glia as drivers of abnormal neuronal activity. *Nature Neuroscience*, *19*(1), 28–33. https://doi.org/10.1038/nn.4184

Romberg, C., Yang, S., Melani, R., Andrews, M. R., Horner, A. E., Spillantini, M. G., Bussey, T. J., Fawcett, J. W., Pizzorusso, T., & Saksida, L. M. (2013). Depletion of perineuronal nets enhances recognition memory and long-term depression in the perirhinal cortex. *The Journal of*

Neuroscience: The Official Journal of the Society for Neuroscience, *33*(16), 7057–7065. https://doi.org/10.1523/JNEUROSCI.6267-11.2013

Roszkowska, M., Skupien, A., Wójtowicz, T., Konopka, A., Gorlewicz, A., Kisiel, M., Bekisz, M., Ruszczycki, B., Dolezyczek, H., Rejmak, E., Knapska, E., Mozrzymas, J. W., Wlodarczyk, J., Wilczynski, G. M., & Dzwonek, J. (2016). CD44: a novel synaptic cell adhesion molecule regulating structural and functional plasticity of dendritic spines. *Molecular Biology of the Cell*, *27*(25), 4055–4066. https://doi.org/10.1091/mbc.E16-06-0423

Rowlands, D., Lensjø, K. K., Dinh, T., Yang, S., Andrews, M. R., Hafting, T., Fyhn, M., Fawcett, J. W., & Dick, G. (2018). Aggrecan Directs Extracellular Matrix-Mediated Neuronal Plasticity. *The Journal of Neuroscience: The Official Journal of the Society for Neuroscience*, *38*(47), 10102–10113. https://doi.org/10.1523/JNEUROSCI.1122-18.2018

Ruoslahti, E. (1996). Brain extracellular matrix. *Glycobiology*, *6*(5), 489–492. https://doi.org/10.1093/glycob/6.5.489

Russo, I., Bonini, D., Via, L. L., Barlati, S., & Barbon, A. (2013). AMPA receptor properties are modulated in the early stages following pilocarpine-induced status epilepticus. *Neuromolecular Medicine*, *15*(2), 324–338. https://doi.org/10.1007/s12017-013-8221-6

Saghatelyan, A., de Chevigny, A., Schachner, M., & Lledo, P.-M. (2004). Tenascin-R mediates activity-dependent recruitment of neuroblasts in the adult mouse forebrain. *Nature Neuroscience*, *7*(4), 347–356. https://doi.org/10.1038/nn1211

Saghatelyan, A. K., Dityatev, A., Schmidt, S., Schuster, T., Bartsch, U., & Schachner, M. (2001). Reduced perisomatic inhibition, increased excitatory transmission, and impaired long-term potentiation in mice deficient for the extracellular matrix glycoprotein tenascin-R. *Molecular and Cellular Neurosciences*, *17*(1), 226–240. https://doi.org/10.1006/mcne.2000.0922

Scharfman, H. E., Sollas, A. L., Berger, R. E., & Goodman, J. H. (2003). Electrophysiological evidence of monosynaptic excitatory transmission between granule cells after seizure-induced mossy fiber sprouting. *Journal of Neurophysiology*, *90*(4), 2536–2547. https://doi.org/10.1152/jn.00251.2003

Scheffer, I. E., Berkovic, S., Capovilla, G., Connolly, M. B., French, J., Guilhoto, L., Hirsch, E., Jain, S., Mathern, G. W., Moshé, S. L., Nordli, D. R., Perucca, E., Tomson, T., Wiebe, S., Zhang, Y.-H., & Zuberi, S. M. (2017). ILAE classification of the epilepsies: Position paper of the ILAE Commission for Classification and Terminology. *Epilepsia*, *58*(4), 512–521. https://doi.org/10.1111/epi.13709

Schweitzer, B., Singh, J., Fejtova, A., Groc, L., Heine, M., & Frischknecht, R. (2017). Hyaluronic acid based extracellular matrix regulates surface expression of GluN2B containing NMDA receptors. *Scientific Reports*, *7*(1), 10991. https://doi.org/10.1038/s41598-017-07003-3

Seidenbecher, C. I., Richter, K., Rauch, U., Fässler, R., Garner, C. C., & Gundelfinger, E. D. (1995). Brevican, a chondroitin sulfate proteoglycan of rat brain, occurs as secreted and cell surface glycosylphosphatidylinositol-anchored isoforms. *The Journal of Biological Chemistry*, *270*(45), 27206–27212. https://doi.org/10.1074/jbc.270.45.27206

Sgobio, C., Ghiglieri, V., Costa, C., Bagetta, V., Siliquini, S., Barone, I., Di Filippo, M., Gardoni, F., Gundelfinger, E. D., Di Luca, M., Picconi, B., & Calabresi, P. (2010). Hippocampal synaptic plasticity, memory, and epilepsy: effects of long-term valproic acid treatment. *Biological Psychiatry*, *67*(6), 567–574. https://doi.org/10.1016/j.biopsych.2009.11.008

Skupien, A., Konopka, A., Trzaskoma, P., Labus, J., Gorlewicz, A., Swiech, L., Babraj, M., Dolezyczek, H., Figiel, I., Ponimaskin, E., Wlodarczyk, J., Jaworski, J., Wilczynski, G. M., & Dzwonek, J. (2014). CD44 regulates dendrite morphogenesis through Src tyrosine kinase-dependent positioning of the Golgi. *Journal of Cell Science*, *127*(Pt 23), 5038–5051. https://doi.org/10.1242/jcs.154542

Staley, K. (2015). Molecular mechanisms of epilepsy. *Nature Neuroscience*, *18*(3), 367–372. https://doi.org/10.1038/nn.3947

Stanton, H., Melrose, J., Little, C. B., & Fosang, A. J. (2011). Proteoglycan degradation by the ADAMTS family of proteinases. *Biochimica et Biophysica Acta (BBA) - Molecular Basis of Disease*, *1812*(12), 1616–1629. https://doi.org/10.1016/j.bbadis.2011.08.009

Südhof, T. C. (2012). The presynaptic active zone. *Neuron*, *75*(1), 11–25. https://doi.org/10.1016/j.neuron.2012.06.012

Sullivan, C. S., Gotthard, I., Wyatt, E. V., Bongu, S., Mohan, V., Weinberg, R. J., & Maness, P. F. (2018). Perineuronal Net Protein Neurocan Inhibits NCAM/EphA3 Repellent Signaling in GABAergic Interneurons. *Scientific Reports*, *8*. https://doi.org/10.1038/s41598-018-24272-8

Thom, M. (2014). Review: Hippocampal sclerosis in epilepsy: a neuropathology review. *Neuropathology and Applied Neurobiology*, *40*(5), 520–543. https://doi.org/10.1111/nan.12150

tom Dieck, S., Sanmartí-Vila, L., Langnaese, K., Richter, K., Kindler, S., Soyke, A., Wex, H., Smalla, K. H., Kämpf, U., Fränzer, J. T., Stumm, M., Garner, C. C., & Gundelfinger, E. D. (1998). Bassoon, a novel zinc-finger CAG/glutamine-repeat protein selectively localized at the active zone of presynaptic nerve terminals. *The Journal of Cell Biology*, *142*(2), 499–509. https://doi.org/10.1083/jcb.142.2.499

Trevelyan, A. J., Muldoon, S. F., Merricks, E. M., Racca, C., & Staley, K. J. (2015). The role of inhibition in epileptic networks. *Journal of Clinical Neurophysiology: Official Publication of the American Electroencephalographic Society*, *32*(3), 227–234. https://doi.org/10.1097/WNP.0000000000000160

Umpierre, A. D., West, P. J., White, J. A., & Wilcox, K. S. (2019). Conditional Knock-out of mGluR5 from Astrocytes during Epilepsy Development Impairs High-Frequency Glutamate Uptake. *The Journal of Neuroscience: The Official Journal of the Society for Neuroscience*, *39*(4), 727–742. https://doi.org/10.1523/JNEUROSCI.1148-18.2018

Valenzuela, J. C., Heise, C., Franken, G., Singh, J., Schweitzer, B., Seidenbecher, C. I., & Frischknecht, R. (2014). Hyaluronan-based extracellular matrix under conditions of homeostatic plasticity. *Philosophical Transactions of the Royal Society of London. Series B, Biological Sciences*, *369*(1654), 20130606. https://doi.org/10.1098/rstb.2013.0606

Vitellaro-Zuccarello, L., Meroni, A., Amadeo, A., & De Biasi, S. (2001). Chondroitin sulfate proteoglycans in the rat thalamus: expression during postnatal development and correlation with calcium-binding proteins in adults. *Cell and Tissue Research*, *306*(1), 15–26. https://doi.org/10.1007/s004410100425

Waites, C. L., Leal-Ortiz, S. A., Okerlund, N., Dalke, H., Fejtova, A., Altrock, W. D., Gundelfinger, E. D., & Garner, C. C. (2013). Bassoon and Piccolo maintain synapse integrity by regulating protein ubiquitination and degradation. *The EMBO Journal*, *32*(7), 954–969. https://doi.org/10.1038/emboj.2013.27

Wei, F., Yan, L.-M., Su, T., He, N., Lin, Z.-J., Wang, J., Shi, Y.-W., Yi, Y.-H., & Liao, W.-P. (2017). Ion Channel Genes and Epilepsy: Functional Alteration, Pathogenic Potential, and Mechanism of Epilepsy. *Neuroscience Bulletin*, *33*(4), 455–477. https://doi.org/10.1007/s12264-017-0134-1

Whelan, C. D., Altmann, A., Botía, J. A., Jahanshad, N., Hibar, D. P., Absil, J., Alhusaini, S., Alvim, M. K. M., Auvinen, P., Bartolini, E., Bergo, F. P. G., Bernardes, T., Blackmon, K., Braga, B., Caligiuri, M. E., Calvo, A., Carr, S. J., Chen, J., Chen, S., … Sisodiya, S. M. (2018). Structural brain abnormalities in the common epilepsies assessed in a worldwide ENIGMA study. *Brain: A Journal of Neurology*, *141*(2), 391–408. https://doi.org/10.1093/brain/awx341

Wlodarczyk, J., Mukhina, I., Kaczmarek, L., & Dityatev, A. (2011). Extracellular matrix molecules, their receptors, and secreted proteases in synaptic plasticity. *Developmental Neurobiology*, *71*(11), 1040–1053. https://doi.org/10.1002/dneu.20958

Xu, L., Hao, Y., Wu, X., Yu, P., Zhu, G., & Hong, Z. (2013). Tenidap, an agonist of the inwardly rectifying K+ channel Kir2.3, delays the onset of cortical epileptiform activity in a model of chronic temporal lobe epilepsy. *Neurological Research*, *35*(6), 561–567. https://doi.org/10.1179/1743132813Y.0000000157

Yamada, S. (2015). Catabolism of chondroitin sulfate. *Cellular & Molecular Biology Letters*, *20*(2), 196–212. https://doi.org/10.1515/cmble-2015-0011

Yamada, J., Nadanaka, S., Kitagawa, H., Takeuchi, K., & Jinno, S. (2018). Increased Synthesis of Chondroitin Sulfate Proteoglycan Promotes Adult Hippocampal Neurogenesis in Response to Enriched Environment. *The Journal of Neuroscience: The Official Journal of the Society for Neuroscience*, *38*(39), 8496–8513. https://doi.org/10.1523/JNEUROSCI.0632-18.2018

Yamaguchi, Y. (2000). Lecticans: organizers of the brain extracellular matrix. *Cellular and Molecular Life Sciences: CMLS*, *57*(2), 276–289. https://doi.org/10.1007/PL00000690

Yang, C.-S., Chiu, S.-C., Liu, P.-Y., Wu, S.-N., Lai, M.-C., & Huang, C.-W. (2021). Gastrodin alleviates seizure severity and neuronal excitotoxicities in the rat lithium-pilocarpine model of temporal lobe epilepsy via enhancing GABAergic transmission. *Journal of Ethnopharmacology*, *269*, 113751. https://doi.org/10.1016/j.jep.2020.113751

Yuan, W., Matthews, R. T., Sandy, J. D., & Gottschall, P. E. (2002). Association between protease-specific proteolytic cleavage of brevican and synaptic loss in the dentate gyrus of kainate-treated rats. *Neuroscience*, *114*(4), 1091–1101. https://doi.org/10.1016/s0306-4522(02)00347-0

Zhai, R., Olias, G., Chung, W. J., Lester, R. A., tom Dieck, S., Langnaese, K., Kreutz, M. R., Kindler, S., Gundelfinger, E. D., & Garner, C. C. (2000). Temporal appearance of the presynaptic cytomatrix protein bassoon during synaptogenesis. *Molecular and Cellular Neurosciences*, *15*(5), 417–428. https://doi.org/10.1006/mcne.2000.0839

Zhang, W., Yamawaki, R., Wen, X., Uhl, J., Diaz, J., Prince, D. A., & Buckmaster, P. S. (2009). Surviving hilar somatostatin interneurons enlarge, sprout axons, and form new synapses with granule cells in a mouse model of temporal lobe epilepsy. *The Journal of Neuroscience: The Official Journal of the Society for Neuroscience*, *29*(45), 14247–14256. https://doi.org/10.1523/JNEUROSCI.3842-09.2009

Zhang, Y., Chen, K., Sloan, S. A., Bennett, M. L., Scholze, A. R., O'Keeffe, S., Phatnani, H. P., Guarnieri, P., Caneda, C., Ruderisch, N., Deng, S., Liddelow, S. A., Zhang, C., Daneman, R., Maniatis, T., Barres, B. A., & Wu, J. Q. (2014). An RNA-sequencing transcriptome and splicing database of glia, neurons, and vascular cells of the cerebral cortex. *The Journal of Neuroscience: The Official Journal of the Society for Neuroscience*, *34*(36), 11929–11947. https://doi.org/10.1523/JNEUROSCI.1860-14.2014

Zhou, Q.-G., Nemes, A. D., Lee, D., Ro, E. J., Zhang, J., Nowacki, A. S., Dymecki, S. M., Najm, I. M., & Suh, H. (2019). Chemogenetic silencing of hippocampal neurons suppresses epileptic neural circuits. *The Journal of Clinical Investigation*, *129*(1), 310–323. https://doi.org/10.1172/JCI95731

Zubareva, O. E., Kovalenko, A. A., Kalemenev, S. V., Schwarz, A. P., Karyakin, V. B., & Zaitsev, A. V. (2018). Alterations in mRNA expression of glutamate receptor subunits and excitatory amino acid transporters following pilocarpine-induced seizures in rats. *Neuroscience Letters*, *686*, 94–100. https://doi.org/10.1016/j.neulet.2018.08.047

Appendix 1: Table of regulated proteins in the membrane fraction of hippocampus of the Bassoon lines

Gene Name	Protein ID	Line	Corrected P-value	log2 fold change
BSN	O88737	Bsn3	1.01E-11	-2.60
BDNF	A2AII2|H9H9S8|P21237|Q541P3	Bsn3	6.97E-05	1.64
SERPINA3N	G3X8T9|Q91WP6	Bsn3	6.97E-05	1.64
FAM129B	Q8R1F1	Bsn3	6.97E-05	0.61
SLC17A6	A0A0R4J0A6|Q8BLE7	Bsn3	1.78E-04	-0.59
IGHV1	A0A075B5Y4|A0A0A6YVW3	Bsn3	1.92E-04	-1.50
PDLIM4	P70271	Bsn3	1.92E-04	0.80
SLC25A42	Q8R0Y8	Bsn3	4.39E-04	0.66
PLXNC1	Q9QZC2	Bsn3	5.05E-04	-0.63
NPY1R	Q04573	Bsn3	5.05E-04	-0.63
SLC15A2	E9PYQ9|E9QMN8|Q9ES07	Bsn3	5.32E-04	-0.68
ALDH1L2	D3Z6B9|Q8K009	Bsn3	5.32E-04	0.83
CAV1	D3Z0J2|D3Z148|H3BKG0|P49817|P49817-2	Bsn3	5.32E-04	0.71
SCAI	B0R0E3|Q8C8N2	Bsn3	5.32E-04	-0.78
VIM	P20152|Q5FWJ3	Bsn3	5.93E-04	1.04
SCG2	Q03517|Q4W8U9	Bsn3	5.93E-04	0.93
KCNJ4	P52189|Q8R435	Bsn3	7.63E-04	-0.60
FLOT2	Q5SS83|Q60634|Q60634-2|Q60634-3	Bsn3	8.80E-04	-0.60
CD34	Q64314|Q64314-2	Bsn3	1.20E-03	-0.86
SYTL5	Q80T23|Q80T23-2	Bsn3	1.29E-03	0.60
FAM81A	Q3UXZ6	Bsn3	1.40E-03	-0.68
MSN	P26041	Bsn3	1.52E-03	0.80
PPBP	Q9EQI5	Bsn3	1.52E-03	-0.80
CA4	Q64444	Bsn3	1.53E-03	-0.79
NPTX2	O70340	Bsn3	1.55E-03	1.76
FLOT1	O08917|Q540I4	Bsn3	1.65E-03	-0.59
HSPB1	P14602|P14602-2|P14602-3	Bsn3	1.76E-03	1.50
GFAP	P03995|P03995-2	Bsn3	2.02E-03	0.99
CAPG	Q99LB4	Bsn3	2.15E-03	0.86
NPTXR	E9PZM8|F7BX42	Bsn3	2.15E-03	0.66
CRHBP	Q3UY07|Q60571	Bsn3	2.31E-03	0.60
CD44	A2APM1|A2APM2|A2APM3|A2APM4|A2APM5	Bsn3	2.31E-03	1.02
AHNAK2	E9PYB0|F7CVJ5|F7DBB3	Bsn3	2.32E-03	1.16
BEGAIN	F8WIG2	Bsn3	2.74E-03	-0.61
S100A6	P14069|Q545I9	Bsn3	3.12E-03	1.83
VGF	Q0VGU4	Bsn3	3.50E-03	1.38
SLC24A4	E9PUL6|F7B0S9|Q8CGQ8-2	Bsn3	3.70E-03	0.59
TMEM163	Q8C996	Bsn3	3.82E-03	-0.60
NEFH	P19246	Bsn3	3.84E-03	0.87
PCDH8	Q7TSK3|Q7TSK3-2	Bsn3	4.19E-03	0.73
COX7A1	A0A140LIU4|P56392|Q792A4	Bsn3	4.19E-03	0.64
REM2	E9Q4D5|Q8VEL9|Q8VEL9-2	Bsn3	4.87E-03	0.65
ANXA2	P07356|Q542G9	Bsn3	5.53E-03	0.76
PPP1R1B	Q60829|Q60829-2	Bsn3	5.58E-03	0.95
MFGE8	P21956|P21956-2	Bsn3	6.12E-03	-0.61
PDLIM1	O70400	Bsn3	6.99E-03	1.09
NEFM	A0A0R4J036	Bsn3	8.11E-03	0.74
NEFL	P08551	Bsn3	8.25E-03	0.80
THSD7A	E9PWD2|E9QNR5|Q69ZU6	Bsn3	8.51E-03	-0.62
CALB2	Q08331	Bsn3	9.37E-03	0.66
ARSA	P50428	Bsn3	1.01E-02	0.66
Q32M26	Q32M26	Bsn3	1.08E-02	0.72
CHGA	P26339	Bsn3	1.38E-02	0.71
RANBP2	Q9ERU9	Bsn3	1.41E-02	-0.75
BAG3	Q9JLV1	Bsn3	1.59E-02	0.64
DLG5	E9Q9I2|E9Q9R9	Bsn3	1.64E-02	-1.05
TGM1	A0A0R4J293	Bsn3	1.70E-02	1.43
NTNG1	F7CVQ1|F8WJ48|F8WJ50|F8WJ51|Q8R4G0	Bsn3	1.70E-02	-0.59
INA	P46660	Bsn3	1.72E-02	0.61
GPM6B	A2AEG3|A2AEG6	Bsn3	1.79E-02	-0.59
KCNT2	D3YTU6|D3Z649	Bsn3	1.81E-02	0.94
SLC7A11	A0A0B4J1P7|Q542C8|Q9WTR6	Bsn3	1.82E-02	-0.86
VWA5A	Q99KC8	Bsn3	1.91E-02	0.65
GJA1	P23242	Bsn3	2.08E-02	-0.66

SLC6A11	P31650	Bsn3	2.23E-02	-0.68
TMSB4X	P20065-2	Bsn3	2.72E-02	0.60
CNN3	A0A0G2JDV8|Q9DAW9	Bsn3	3.10E-02	0.60
OSTF1	Q62422	Bsn3	3.12E-02	0.63
GAD2	P48320|Q548L4	Bsn3	3.27E-02	0.79
ATP5E	P56382|Q545F5	Bsn3	3.74E-02	0.74
ZNFX1	Q8R151	Bsn3	3.83E-02	-0.63
2610301B20RIK|Q3UJP5	B1AV75|Q3UJP5	Bsn3	4.64E-02	0.65
UQCRH	P99028	Bsn3	5.95E-02	0.82
SLC13A5	A0A140LIC4|A0A140LIR1|Q5NBV0|Q67BT3	Bsn3	7.01E-02	-0.59
PGAM2	O70250|Q5NCI4	Bsn3	7.03E-02	0.62
CDH20	Q9Z0M3	Bsn3	7.34E-02	-0.59
EFHD2	Q8C845	Bsn3	9.29E-02	0.66
IGKC|P01837	A0A075B5P2|P01837	Bsn3	9.30E-02	-0.82
ARHGDIB	Q61599	Bsn3	1.53E-01	1.15
CMC2	Q8K199	Bsn3	1.70E-01	-1.56
TBC1D7	Q9D0K0	Bsn3	1.92E-01	0.62
KDELR1|KDELR2	Q99JH8|Q9CQM2	Bsn3	1.99E-01	0.83
BSN	O88737	B2E	3.58E-10	-1.94
IGHV1	A0A075B5Y4|A0A0A6YVW3	B2E	6.90E-02	-0.83
SLC4A2	A0A0R4J101|A0A0R4J1K4|A0A0R4J1K9|P13808	B2E	1.93E-01	0.69
ALDH1L2	D3Z6B9|Q8K009	B2I	1.20E-03	0.99
INMT	P40936	B2I	1.20E-03	0.66
BBS4	A6H669|Q8C1Z7	B2I	1.20E-03	-1.05
IGHV1	A0A075B5Y4|A0A0A6YVW3	B2I	1.20E-03	-1.27
SLC25A42	Q8R0Y8	B2I	1.20E-03	0.61
CD44	A2APM1|A2APM2|A2APM3|A2APM4|A2APM5	B2I	1.20E-03	1.32
GLIPR2	Q9CYL5	B2I	2.61E-03	0.65
BDNF	A2AII2|H9H9S8|P21237|Q541P3	B2I	2.70E-03	1.02
CYB5R1	Q9DB73	B2I	2.92E-03	0.70
RANBP2	Q9ERU9	B2I	3.01E-03	-1.20
SF3B1	G5E866|Q99NB9	B2I	4.81E-03	-0.82
MSN	P26041	B2I	9.02E-03	0.65
PLGRKT	Q9D3P8	B2I	9.98E-03	0.62
H2AFV|H2AFZ	B2RVP5|P0C0S6|Q3THW5|Q3UA95	B2I	1.00E-02	-0.68
COX7A1	A0A140LIU4|P56392|Q792A4	B2I	1.00E-02	0.63
S100A6	P14069|Q545I9	B2I	1.13E-02	1.63
CD34	Q64314|Q64314-2	B2I	1.13E-02	-0.62
CAPG	Q99LB4	B2I	1.17E-02	0.69
OCIAD2	A0A0J9YU93|Q9D8W7	B2I	1.20E-02	0.64
HSPB1	P14602|P14602-2|P14602-3	B2I	1.32E-02	1.12
VIM	P20152|Q5FWJ3	B2I	1.56E-02	0.62
TMSB4X	P20065-2	B2I	1.91E-02	0.75
TMLHE	Q91ZE0	B2I	2.06E-02	0.62
FDFT1	P53798	B2I	2.08E-02	-0.66
SERPINA3N	G3X8T9|Q91WP6	B2I	2.27E-02	0.64
TGM1	A0A0R4J293	B2I	2.46E-02	1.49
ANXA2	P07356|Q542G9	B2I	3.17E-02	0.59
SLC4A2	A0A0R4J101|A0A0R4J1K4|A0A0R4J1K9|P13808	B2I	3.65E-02	0.71
ATP5J	P97450	B2I	3.72E-02	0.72
APOA1	Q00623	B2I	3.81E-02	0.78
LMNB2	P21619	B2I	5.00E-02	-1.36
THBS4	B2RTL6|Q9Z1T2	B2I	9.06E-02	0.67
NPTX2	O70340	B2I	9.21E-02	0.76
RAD23B	P54728	B2I	9.91E-02	-0.72
LMNA	P48678|P48678-2	B2I	1.11E-01	-1.05
LMNB1	P14733	B2I	1.15E-01	-1.19
UQCRH	P99028	B2I	1.25E-01	0.72
ANXA11	P97384	B2I	1.27E-01	0.60
DYNLRB1	P62627	B2I	1.34E-01	-0.70
VGF	Q0VGU4	B2I	1.34E-01	0.62
SLC4A1	P04919|P04919-2	B2I	1.39E-01	-0.72
CHN2	Q3V2R3	B2I	1.59E-01	-0.71
IGKC|P01837	A0A075B5P2|P01837	B2I	1.63E-01	-0.73
CENPF	E9Q3P4	B2I	1.98E-01	-0.93

Declaration of Honour

Ich versichere hiermit, dass ich die vorliegende Arbeit ohne unzulässige Hilfe Dritter und ohne Benutzung anderer als der angegebenen Hilfsmittel angefertigt habe; verwendete fremde und eigene Quellen sind als solche kenntlich gemacht.

Ich habe insbesondere nicht wissentlich:

- Ergebnisse erfunden oder widersprüchlich Ergebnisse verschwiegen,
- statistiche Verfahren absichtlich missbraucht, um Daten in ungerechtfertigter Weise zu interpretieren,
- fremde Ergebnisse oder Veröffentlichungen plagiiert,
- fremde Forschungsergebnisse verzerrt wiedergegeben.

Mir ist bekannt, dass Verstöße gegen das Urheberrecht Unterlassungs- und Schadensersatz- ansprüche des Urhebers sowie eine strafrechtliche Ahndung durch die Strafverfolgungsbe- hörden begründen kann.

Ich erkläre mich damit einverstanden, dass die Arbeit ggf. mit Mitteln der elektronischen Datenverarbeitung auf Plagiate überprüft werden kann.

Die Arbeit wurde bisher weder im Inland noch im Ausland in gleicher oder ähnlicher Form als Dissertation eingereicht und ist als Ganzes auch noch nicht veröffentlicht.

Magdeburg, 26th May 2021